The Graduate University for Advanced Studies, SOKENDAI

Doctoral Thesis

Study on thermal and mechanical stability of the superconducting coil with liquid helium permeable structure

Author:
AOKI Manabu

Supervisor:
Prof. SASAKI Ken-ichi

in the

Department of Accelerator Science

June 2021

The Graduate University for Advanced Studies, SOKENDAI

Abstract

School of High Energy Accelerator Science

Doctor of Philosophy

Study on thermal and mechanical stability of the superconducting coil with liquid helium permeable structure

by AOKI Manabu

Some superconducting magnets for particle accelerators have the liquid helium cooling channels within the coil windings to improve the thermal stability. On the other hand, a closely wound coil using the monolithic superconducting wires can not have similar cooling channels due to structural constraints, but the coil using the self-bonding wires can have voids into which liquid helium can permeate (hereafter referred to as "helium-permeable structure"). However, the larger helium-permeable structures could make the coil windings fragile and lose the mechanical stability of superconducting coils. Therefore, we developed a three-point bending test stand working at a cryogenic temperature of 4.2 K within a magnet field, which can evaluate a strain for the magnet quench (hereafter referred to as "quench strain") as the mechanical stability including statistical variation. Besides, we evaluated a minimum heater energy for the quench as the thermal stability to verify the cooling effect of this structure.

The test coils were racetrack-shaped (200 mm×50 mm), and two straight sections were bent with the three-point bending test stand. Superconducting wires were NbTi multifilament monolithic wire coated with polyvinyl formal and a self-bonding resin. The helium-permeable structures existed in the area surrounded by three wires and occupied about 2 % of the cross-section. For comparison, the test coils without the helium-permeable structure were made by putting additional self-bonding resin during the winding process. The test coils were energized from 150 A to 250 A in the magnetic field of 5.8 T, and the critical current margin defined as the ratio of operation current to the conductor critical current was from 32.0 % to 53.3 %.

The minimum heater energy for the quench of the test coils with the helium-permeable structure were 5.6 mJ to 22 mJ, which were about 2.3 to 3.1 times higher than the test coils without the helium-permeable structure. These results indicated that the helium permeable structure improved the thermal stability of the superconducting coil. However, the differences of the

minimum heater energy for the quench between both types of the test coils tended to decrease when the current of the test coil became larger.

The quench strains of the test coils with helium-permeable structure were about 1.6 times larger compared to the test coils without the helium-permeable structure when the current of the test coil was 150 A (the critical current margin 32.0 %). On the other hand, there were almost no differences of the quench strains between both types of the test coils when the current of the test coil was 185 A or more (the critical current margin 39.4 % or more). Although the quench strains depended on the current of the test coil, the helium permeable structure had the effect to improve the mechanical stability of the superconducting coil.

The frequency of the voltage spikes, which indicate that mechanical disturbance occurred in the coil winding, were almost the same regardless of the presence or absence of the helium-permeable structure. The presence of the helium-permeable structure did not increase the number of mechanical disturbances. We consider that this is because the phenoxy resin applied as the self-bonding resin has three times larger fracture toughness than that of the epoxy resin. The higher fracture toughness restrained crack growth in the resin; therefore, the test coils with the helium-permeable structure seemed not to lose the quench stability.

The cooling mechanism of helium-permeable structure was investigated by a transient thermal analysis of the coil windings. It was found that the helium-permeable structure functions as a type of temperature fixed point and enhances thermal stability. However, it was also found that there is almost no difference in the initial temperature rise from 4.2 K to 5.7 K regardless of the presence or absence of the helium-permeable structure. This result shows that the cooling effect of the helium-permeable structure can not be expected under the condition of the high critical current margin where the current sharing temperature is low.

From the above results, we had three design guidelines of the superconducting coil with the helium-permeable structure: 1) Expansion of the helium-permeable structure is expected to improve the quench stability, since the mechanical stability was not impaired even if the helium-permeable structure that occupies 2 % of the coil cross-sectional area was applied. Furthermore, past studies of magnets for LHC (Large Hadron Collider) revealed that the expansion of the cooling perimeter of the superconducting strand increases MQE (Minimum Quench Energy). When the helium-permeable structure is expanded to a cross-sectional area ratio of 6 %, the cooling perimeter is expanded from 22 % to 47 %, and further

improvement of the quench stability is expected. 2) The number of training quenches can be reduced under the condition of the low critical current margin without expanding the helium permeation structure, since the quench stability was improved under the critical current margin of 32.0 % or less in the three-point bending test. 3) The Young's modulus of the self-bonded coil tended to be lower than that of the prepreg coil. Therefore, when a self-bonded coil is applied, it is necessary to reinforce a support structure according to the magnitude of the electromagnetic force in order to suppress the deformation of the coil winding.

Acknowledgement

Special thanks to Mr. NAKAGAWA Ryoji, who helped with the detail design of the three bending test stand when he was a member of Hitachi. Ltd.

The author's heartful appreciation goes to Mr. WADA Satoshi, who made a lot of test coils and cross-sectional observation sample. His study would not have been possible without his support.

The author would like to heartful thank to Dr. MIYAZOE Akihisa, who provided helpful comment and suggestion for non-impregnation molding method.

The author would also like to express his gratitude to Dr. ABE Mitsushi and Dr. ANDO Ryuuya for their considered comment and feedback in the design of the three-point bending test.

Finally, the author is deeply grateful to Prof. SASAKI Ken-ichi, Associate Prof. IIO Masami, Mr. IIDA Masahisa and member of the cryogenic section, this thesis is the result of many fertile discussions and supports from them.

Contents

List of Figures

List of Tables

1. Introduction

1.1 Superconducting Coil

Superconducting coils can be energized with a several hundred times higher current density than normal conducting coils and can generate a strong magnetic field. Therefore, superconducting coils have various applications such as MRI machine, NMR spectrometer, particle accelerator, magnetic levitation train, and so on.

Among these applications, the most commercialized one is MRI machine that acquire tomographic images of the human body using the nuclear magnetic resonance phenomenon. The superconducting coils are indispensable to generate a strong magnetic field with a large space to accommodate the patient [1]. The NMR spectrometer is a device that analyzes the molecular structure of a substance by utilizing the nuclear magnetic resonance phenomenon. Although the NMR spectrometer does not need to generate the magnetic field in a space as large as the MRI machines, a strong magnetic field of 9.4 T or more is required for recent products because the resolution and sensitivity improve as the magnetic field applied to the sample becomes stronger [2]. Particle accelerators are devices used for particle physics research and cancer therapy. Superconducting coils are used to change the orbit of charged particles that move at high speed and to converge the charged particle beams. In case of accelerators for particle physics research, charged particle beams with kinetic energy on the order of hundreds of GeV to several TeV require the strong magnetic field generated by superconducting coils [3]. In case of the accelerators for cancer therapy, superconducting coils are used for the purpose of making the orbital radius of charged particle beams as small as possible and miniaturizing the accelerators [4]. The magnetic levitation train is a high-speed railway that moves while levitating using electromagnetic force. Some magnetic levitation trains use a normal conducting coil, but using superconducting coils has the advantage of ensuring safety against disturbances such as earthquakes because it can levitate higher [5].

Superconducting wires applied to the above applications are classified into low-temperature superconducting wires and high-temperature superconducting wires according to their critical temperature. Low-temperature superconducting wires have a critical temperature of 25 K or less, and niobium-titanium alloys and niobium-tin compounds have been put into practical use. Of these, the niobium-titanium alloy has many applications due to its high strain resistance and is used in most of the MRI

machines currently on the market [6] The niobium-tin compound has a larger critical temperature and critical magnetic field than the niobium-titanium alloy [7]. However, its strain resistance is inferior to that of niobium-titanium alloys, and it is difficult to manufacture a coil. Therefore, its usage is currently limited to NMR spectrometers and accelerator magnets that require a strong magnetic field of 10 T or more. In addition, superconducting joint technology has been established for low-temperature superconducting wires, and it is possible to construct a closed circuit consisting of all superconducting materials. Then, a persistent current operation is possible in which the current is hardly attenuated even if it is separated from the power supply. In a persistent current operation, it is possible to generate a time-stable magnetic field without being affected by noise from the power supply. It is applied to MRI machines and NMR spectrometers that require a stable magnetic field with a change rate of 0.1 ppm/hr.

High-temperature superconducting wires have a critical temperature of 25 K or higher, and bismuth-based, yttrium-based, and magnesium diboride (MgB2) have been put into practical use. There are two types of bismuth-based wire: Bi-2212 and Bi-2223. Among these, Bi-2223 is becoming popular because it can be mass-produced [8]. Since bismuth-based wires have a critical magnetic field that surpasses that of low-temperature superconducting wires at low temperatures of 20 K or less, they are applied to ultra-high magnetic field magnets [9]. On the other hand, in the temperature range of 20 K or higher, the critical temperature of bismuth-based wires decreases significantly with a small magnetic field, so they are used as a power cable or power lead with a small empirical magnetic field [10]. In addition, bismuth-based wires tend to be more expensive than niobium-titanium wire rods because silver is used for their production, which is an obstacle to their widespread use. Yttrium-based wires have the highest critical current density in a magnetic field among the superconducting wires that have been put into practical use, and they are applied to ultra-high magnetic field magnets with a magnetic field strength of over 30 T [11]. However, its production requires a relatively time-consuming process of depositing a thin film of superconductor on a metal tape [12]. The critical temperature of MgB_2 wire is as low as 39 K compared to bismuth and yttrium wire, but the wire price is relatively low because the cost of the manufacturing method (PIT method) and materials used for its production are low [13]. However, it is positioned as a low magnetic field application material at a temperature of 20 K or less because its critical current density is lower than that of bismuth-based wires and yttrium-based wires. It is expected to be

applied to power cables [14] and low magnetic field MRI machines with a magnetic field strength of about 0.5 T [15,16].

1.2 The Superconducting Coils Targeted in This Study

The superconducting coils targeted in this study are immersed in liquid helium and cooled to 4.2 K, which is mainly used in MRI magnets. In the manufacturing process as shown in Fig. 1-1, the superconducting wire is wound without gaps (Closely winding), and then a molding is performed to fix the superconducting wire with resin. The closely winding can maximize the space factor and increase the ampere-turns per coil, and it has an advantage that the cross-sectional dimension of the coil can be accurately controlled. The superconducting wire is a monolithic conductor with NbTi filaments embedded in an oxygen-free copper matrix [17], and its surface is insulated with PVF, enamel, etc.

Fig. 1-2 shows the general manufacturing process of the superconducting coil using the monolithic conductor. The manufacturing process differs depending on the molding method. There are three typical molding methods: (a)impregnation method, (b)wet-winding method, and (c)non-impregnation method. (a)The impregnation method submerges the coil winding in the resin before curing, and the resin is permeated into the coil winding and then cured [18]. There is an advantage that the resin can be filled without voids by evacuating when the resin permeates into the coil winding, but a mold release work for removing the resin remaining around the coil winding is required later. (b)The wet winding method is a method of winding while applying the resin before curing to the surface of the superconducting wire [19]. There is an advantage that the mold release work is not necessary, but there is a possibility that air bubbles (hereinafter, void) are generated inside the coil winding. (c)The non-impregnation method has two kinds of method depending on the type of resin: prepreg molding method and self-bonded molding method. The prepreg molding method inserts glass-fiber sheets impregnated with a semi-cured epoxy resin (hereinafter, prepreg) inside the coil winding, and then the prepreg is heated and cured [20]. The prepreg molding method also contains a lot of voids, but it is expected that the prepreg becomes fiber reinforced plastic (FRP) and the strength of the coil winding increase. In addition, there is an example in which the prepreg molding method is applied when a resin that has high radiation resistance, although it is unsuitable for impregnation method due to its high viscosity [21]. The self-bonded molding method is a method in which a thermoplastic resin that melts at high

temperature is previously applied to the surface of a superconducting wire. After winding, the thermoplastic resin is heated and melted, and then cooled and cured [22]. This also has the advantage of eliminating mold release work, but there is a possibility that voids will be generated inside the coil winding similar to the prepreg molding method.

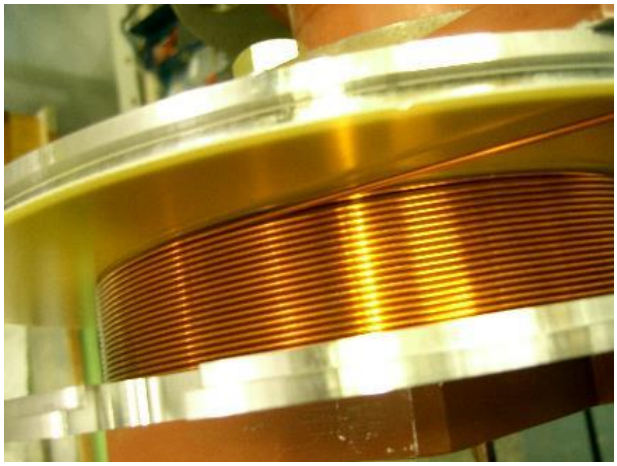

(a) Winding

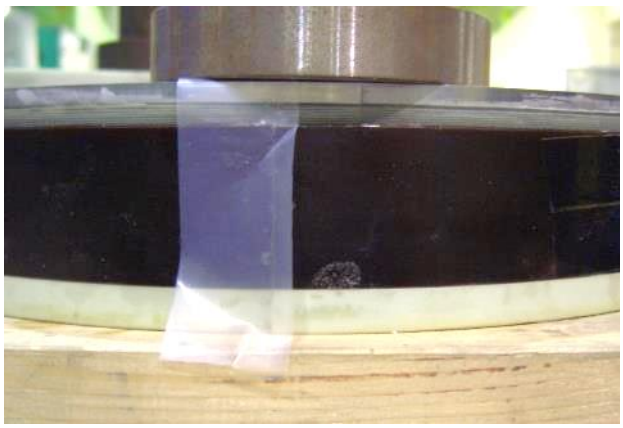

(b) Molded coil

Fig. 1-1 A superconducting coil using monolithic wire. Superconducting wire with a round cross section is closely wounded without any gap between wires. After winding, a molding is performed to fix the superconducting wire with resin.

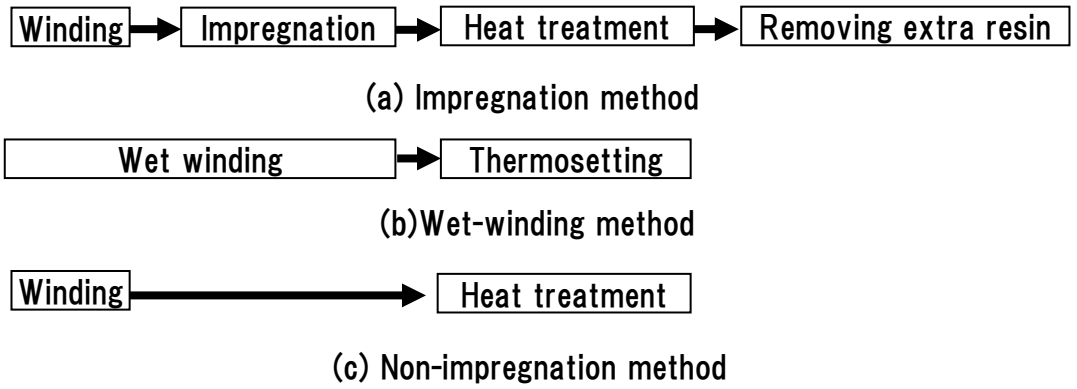

Fig. 1-2 The general manufacturing process of the closely winding coil using the monolithic conductor. The manufacturing process differs depending on the molding method.

1.3 Background and Issues for The Superconducting Coils

One of the issues of superconducting coils is a magnet quench. The magnet quench is a phenomenon in which a superconducting coil undergoes the superconducting-to-normal transition, and stored energy is consumed by Joule heat generation, and the magnetic field disappears unintentionally. At that time, the liquid helium used for cooling the superconducting coil is vaporized and discharged to the outside of the magnet. Since it is necessary to refill liquid helium in order to resume operation, it is a problem for large superconducting magnets to stop operation for several days to several weeks. In the excitation test after the magnet is fabricated, it may experience multiple magnet quenches called “training quench” before energizing to the rated current [23]. Reducing the number of training quenches is also an issue.

Furthermore, the supply and demand of helium has become tight due to its resource depletion in recent years, and it has become an issue to reduce its consumption. As shown in Fig. 1-3, the usage of helium in Japan is 18.6 % for MRI machines and 4.4 % for the cryogenics represented by particle accelerators. In other words, superconducting magnets consume the most helium in Japan [24]. In addition, as shown in Fig. 1-4, the helium price has more than doubled in the 20 years since 2000, and it is estimated that the helium price will rise further due to the increase in demand for MRI machines in emerging countries [25]. Therefore, in order to reduce the consumption of helium, it is essential to improve the quench stability of superconducting magnets for MRI machines among other superconducting magnets.

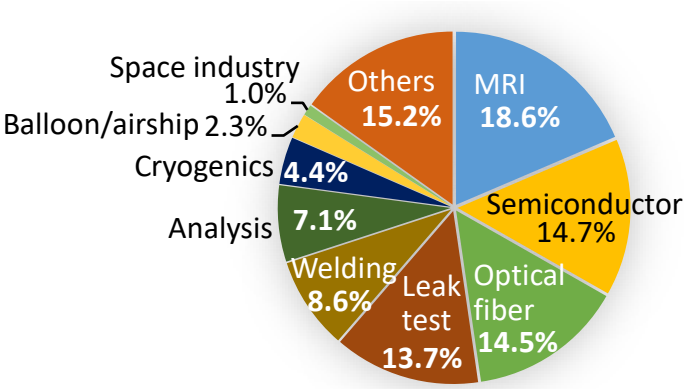

Fig. 1-3 Usage of helium in Japan [24]

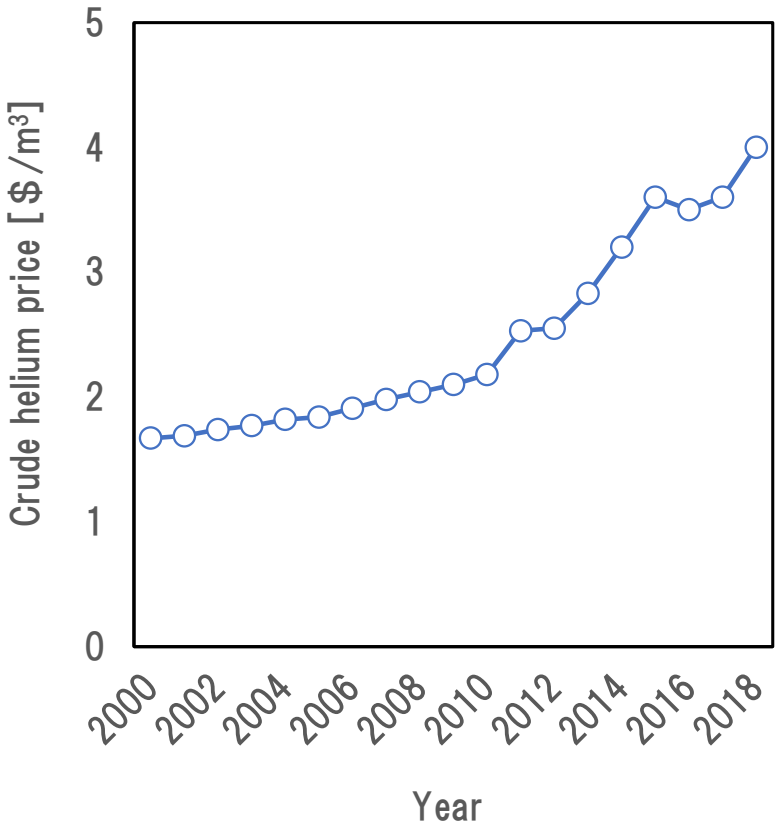

Fig. 1-4 Bureau of Land Management crude helium price [25]

1.4 Causes of Magnet Quench and Countermeasures

Magnet quenches are triggered by slight heat input into the coil winding. The minimum heat input for the quench is called as Minimum Quench Energy (hereafter referred to as "MQE"). In the case of a superconducting coil using NbTi superconducting wire, MQE is quantitatively evaluated analytically or experimentally to be on the order of several μJ to several mJ [26,27,28,29,30].

The causes of magnet quench are divided into two types: thermal disturbance and mechanical disturbance. As a cause of magnet quench due to thermal disturbance, it is conceivable that the temperature of the superconducting wire rises above the critical temperature due to insufficient supply of liquid helium due to heat generation of the superconducting wire such as AC loss [31]. As causes of magnet quench due to mechanical disturbance, they are conceivable: "wire movement" in which the superconducting wire is displaced by electromagnetic force and generate heat, "frictional heat" in which the coil winding is displaced by electromagnetic force and generates heat, "resin crack" in which the molding resin is destroyed by electromagnetic force and generates heat. In particular, mechanical disturbance due to "resin crack" is considered to be the main cause of magnet quenches in superconducting coils using monolithic conductors [32].

As a general countermeasure against magnet quenches, the operating point of current I_{op}, magnetic field B_{op}, and temperature T_{op} are chosen with proper margins. Fig.1-5 schematically shows operating margins [33,34,35]. The typical value used for operating margins are:

a) Critical current margin i

The ratio of the operating current I_{op} to the critical current at B_{op} and T_{op}

$$i = I_{op}/I_c(B_{op},T_{op}).$$

The critical current margin of superconducting coils using commercially available superconducting wires is designed to be 55% or less to ensure sufficient quench stability [36].

b) Current load factor f

The current load factor is margin along the load line, expressed as the ratio of the operating current I_{op} to the maximum current of the superconducting coil I_{max} which is evaluated at the intersection of the load line and the critical current at B_{max} and T_{op}

$$f = I_{op}/I_{max}(B_{max},T_{op}).$$

Where, B_{max} is maximum magnetic field of the coil winding at I_{max}.

The practical current load factor of superconducting magnets is designed to be from 50 % to 70 % to ensure the sufficient quench stability [33,37].

On the other hand, in research applications such as particle accelerators, there are cases where the current load factor is designed around 80 % or more [38].

In order to achieve high quench stability, superconducting coils are designed so that the operating current I_{op} is low, but a longer superconducting wire is required, which increases the manufacturing cost. In addition, long superconducting wire increases the size of coil winding, and superconducting coil may not be installed in a vacuum vessel. Therefor, the following additional countermeasures are adopted in order to obtain high quench stability in some cases.

Countermeasures against thermal instability include strengthening the cooling of the coil windings and reducing heat generation in superconducting wires. As strengthening the cooling of the coil winding, there is a method of providing a flow path of liquid helium inside the conductor like a CICC conductor [39]. There is also a method of providing a gap between conductors with a spacer like an accelerator magnet for LHC (Large Hadron Collider) and allowing superfluid helium to permeate into the gap [40]. As reducing heat generation, there is method of a shortening of the twist pitch of the superconducting filament [41]. There is also reduction in AC loss due to the high resistance of the matrix in the monolithic wire [42]. The superconducting coil targeted in this paper is operated by DC mode, and countermeasures against magnet quench due to AC loss are not considered.

As a countermeasure against mechanical disturbance, there is an improvement in mechanical strength of coil components. There is also a method of improving the coil design by identifying the type and position of the mechanical disturbance that caused the magnet quenches with various sensors.

One of the improvements in mechanical strength is adding a filler to the molding resin to prevent the resin crack [43]. However, when a filler is added, the viscosity of the resin increases, and impregnation molding may become difficult. It is also known that the cause of resin crack is stress concentration on voids in the resin, and that the larger the void size provides the smaller stress at which resin cracking occurs [44]. Therefore, there is an example that vacuum pressure impregnation is adopted, in which the pressure of the vacuum vessel during cure is made higher than the atmospheric pressure to reduce the size of the void [45].

As a method of identifying the type of mechanical disturbance, there is a

method of discriminating from the duration and waveform of ultrasonic waves generated by the mechanical disturbance using an acoustic emission sensor [46.47]. There is also a method of detecting the displacement of the coil winding using a magnetic sensor represented by a search coil [48]. A method has also been developed to analyze the frequency of mechanical disturbances with an acoustic emission sensor and predict the occurrence of mechanical disturbances leading to the magnet quenches [46]. It is also known that voltage spikes are generated in the superconducting coil when mechanical disturbances occur. There are methods to analyze the cause of quenching by analyzing the pattern and frequency of voltage spike [49-51].

As a method of identifying the position where the mechanical disturbance occurs, there are methods of measuring the change of the current distribution in the conductor caused by the superconducting-to-normal transition using a search coil [52-53]. There are also methods of measuring ultrasonic waves generated from mechanical disturbance with multiple sensors and calculating the position of mechanical disturbance from the detection time difference of each sensor [46,54].

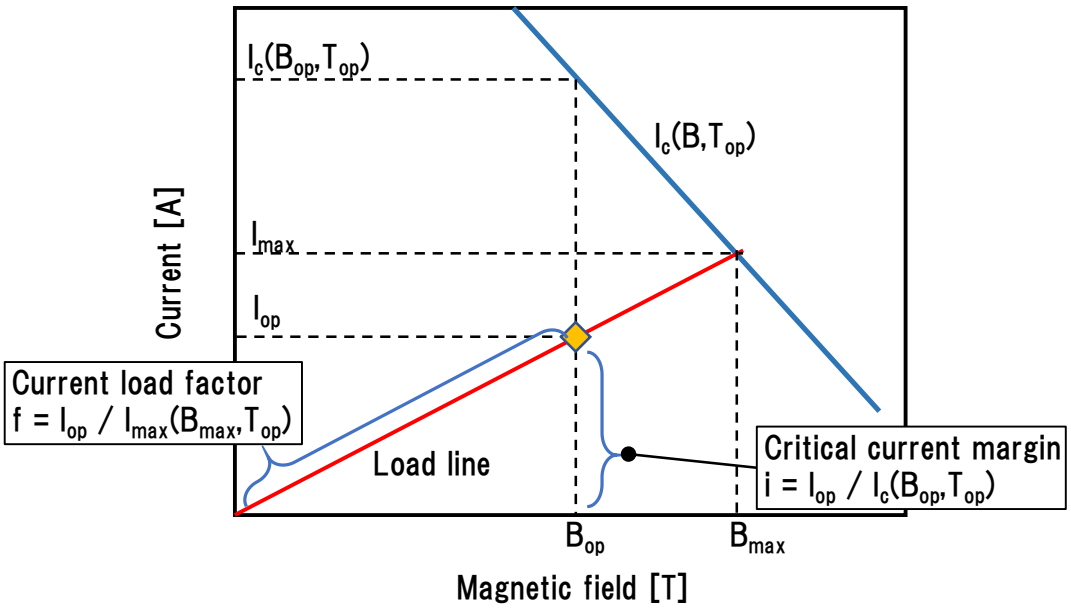

Fig. 1-5 Operation margins of a superconducting coil [33,34,35]. The critical current margin i is defined as a ratio of the operating current I_{op} to the critical current at B_{op} and T_{op}. The current load factor f is margin along the load line, expressed as the ratio of the operating current I_{op} to the maximum current of the superconducting coil I_{max}

1.5 Motivation and Objective

As described above, it is necessary to reduce the consumption of helium by preventing magnet quench. For that purpose, it is effective to improve the thermal stability by providing channels through which liquid helium permeates into the conductor or the coil winding [39,40]. In addition to reducing the consumption of helium, it will be possible to further increase the magnetic field and performance of superconducting magnets. However, in the case of superconducting coils using monolithic conductors, such channels cannot be provided within the conductor due to structural restrictions. Further, a gap through which helium permeates is not positively provided in the coil winding, since the coil using the monolithic conductor is wound closely in order to increase the current density.

On the other hand, even in the coils using the monolithic wires, voids can be provided inside the coil winding by applying the non-impregnation method as described in Section 1-2. Then, the thermal stability can be improved if liquid helium permeates into these voids (hereinafter, these voids are referred to as helium-permeable structure). Fig. 1-6 shows a cross section of the prepreg molded coil. There is a void that is not filled with resin at the point where the corners of the four rectangle wires meet. It is expected that the cooling performance of the superconducting coil will be improved by the permeation of liquid helium into these voids. It can also be expected that the heat capacity of the coil winding will increase due to the liquid helium that has permeated into the voids. As shown in Fig. 1-7, the heat capacity of liquid helium is about 200 times higher than that of epoxy resin and about 600 times higher than that of copper [55]. For example, in the case of a rectangle wire shown in Fig. 1-6, the heat capacity of liquid helium that has permeated into a void is equivalent to the heat capacity of about 12 rectangle wires.

As an example of evaluating the cooling effect of the liquid helium permeated into the winding, there is an example of evaluating the amount of heat input for the quench by the heater put on the superconducting wire [56] or transient heat analysis [57]. In each case, the improvement of the cooling effect is quantitatively evaluated. On the other hand, stress is concentrated on the voids and resin cracks occur, which may cause magnet quench. In past studies, it has been reported that the fracture stress is reduced by about 40% when a void with a diameter of about 0.2 mm is generated in the resin [44]. In other words, there is a concern that the quench stability may be lowered by providing the helium-permeable structure. Therefore, the objective of this study is to evaluate the effect of the helium-permeable structure in terms of both mechanical stability and thermal stability. Then, the design guideline for

the superconducting coil with the helium-permeable structure will be clarified.

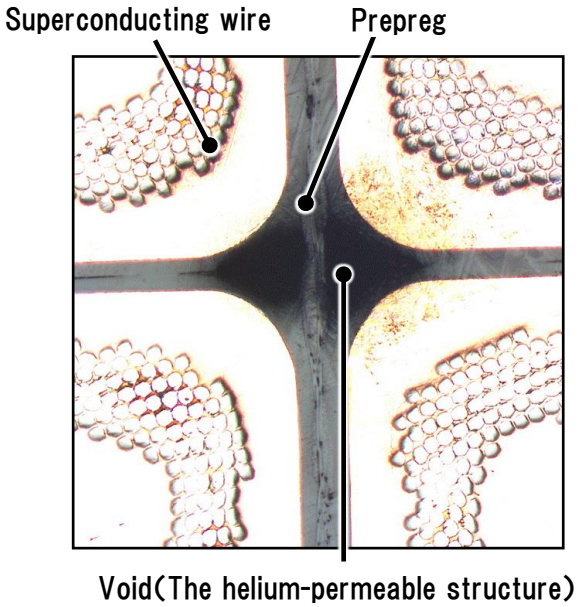

Fig. 1-6 Photo of cross section of a prepreg molding coil, which using rectangle wires with dimensions of 2.2 x 1.7 mm, 0.3 mm radius of the corner

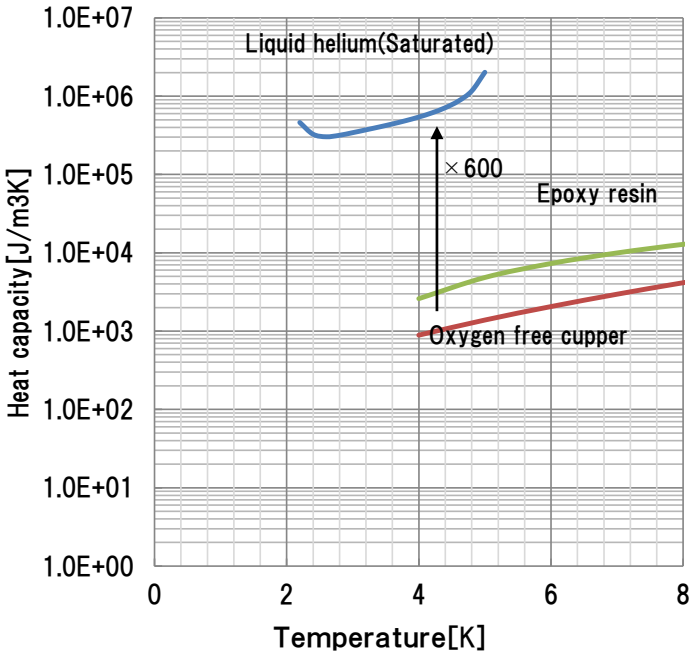

Fig. 1-7 Heat capacity of the helium and materials for superconducting coil [55]

1.6 Composition of The Thesis

In this chapter, the application of the superconducting coils and the types of superconducting coils targeted in this study were described. As one of the issues of the superconducting coils, the magnet quench and its countermeasures done by previous works were described. Then, as a method to improve the quench stability, the helium-permeable structure was described. Finally, the objective of this study was described.

In Chapter 2, the design concept of the three-point bending stand developed to evaluate the quench stability is described. Two kind of test coils prepared to verify the feasibility of the three-point bending test stand are also described. The test procedure using the three-point bending test stand is described, and the installation of sensors and data recording system are described.

In Chapter 3, the operation test results of the three-point bending test stand are described. The results of the three-point bending test performed on the test coils prepared in Chapter 2 are described. The results of evaluating the frequency of mechanical disturbance by analyzing the voltage spikes generated during three-point bending test are described.

In Chapter 4, two kind of test coils created to evaluate the effect of helium-permeable structure on the quench stability are described.

In Chapter 5, the results of the heater quench test conducted to evaluate the thermal stability of the superconducting coil with the helium-permeable structure are described. The results of three-point bending test conducted to evaluate mechanical stability of the superconducting coils with the helium-permeable structure are also described.

In Chapter 6, the characteristics of mechanical disturbance caused by the presence or absence of the helium-permeable structure are described by analyzing the frequency of the voltage spike detected during the three-point bending test in Chapter 5. The cooling mechanism of the helium-permeable structure analyzed by transient thermal analysis is also described. The design guidelines for the superconducting coils with a helium-permeable structure are described.

In Chapter 7, this thesis is summarized.

2. Development of Three-point Bending Test Stand

In this chapter, the design concept of the three-point bending stand developed to evaluate the quench stability is described. The details of the test coils prepared to verify the feasibility of the three-point bending test stand are also described.

2.1 Three-point bending test stand

In this study, in order to evaluate the mechanical and thermal stability of a superconducting coil with the helium-permeable structure, we have developed a test stand that can measure the strain at the point of the quench (hereafter referred to as "quench strain") by applying a load to the superconducting coil energized in a magnetic field. The method of applying the load is three-point bending. Three-point bending is used in various material strength tests [58]. In addition, it is difficult to precisely control the size and shape of the helium-permeable structure produced by non-impregnation molding; thus, the quench strains should be evaluated including statistical variations. Therefor, we designed the three-point bending stand with a configuration that can evaluate multiple test coils under the same condition.

As shown in Fig. 2-1, the test stand consists of a sample holder, magnetic field coils that applies a magnetic field to the test coil, and a bending-load coil that applies a three-point bending load to the test coil. The sample holder has a structure that allows it to be pulled out from the cryostat and evaluates multiple test coils under the same conditions. This configuration makes it possible to evaluate the quench strains including statistical variations.

The magnetic field coils are composed of two superconducting coils, and a racetrack-shaped test coil is installed between each coil. As shown in Fig. 2-2, the magnetic field at the test coil is 5.8 T when the magnetic field coils are energized to 550 A. Since the empirical magnetic field of the superconducting coil in the 1.5T-MRI machines is 5 T or more [59], sufficient magnetic field strength can be generated to evaluate the quench stability of the superconducting coil. Fig. 2-3 shows the magnetic flux flow of the three-point bending test stand when the magnetic filed coils is energized to 550 A. The direction of the magnetic field is along the center axis of the test coil.

Fig. 2-4 shows the circuit diagram of the three-point bending test stand. The test coil, the magnetic field coil, and bending-load coil can be energized independently. In the conventional test in which the energizing current to the superconducting coil is increased until the quench occurs, the critical current margin and the current load factor change as the energizing current increases.

On the other hand, this test stand makes it possible to induce the quench of the test coils with arbitrary critical current margin and current load factor.

An excessive load of 100 kg/cm or more is applied to the superconducting coil used in a strong magnetic field by electromagnetic force. Since it is difficult to apply such stress manually, the method of applying the load using electromagnetic force was also adopted in this test stand. When the bending-load coil is energized, the bending-load coil is attracted to the magnetic field coils by electromagnetic force. Then, as shown in Fig. 2-5, the FRP plate attached to the bending-load coil pushes the test coil, and a straight section with a length of 100 mm is bent. The bending-load coil is a superconducting coil using an NbTi superconducting wire. Its diameter is 330 mm, and the number of turns is 20 turns. The bending-load coil can be energized up to 10 A, and a bending load of up to 2668 N can be applied to the test coil. The shape of the indenter is a semicircle with a radius of 5 mm for the purpose of avoiding local stress concentration [60].

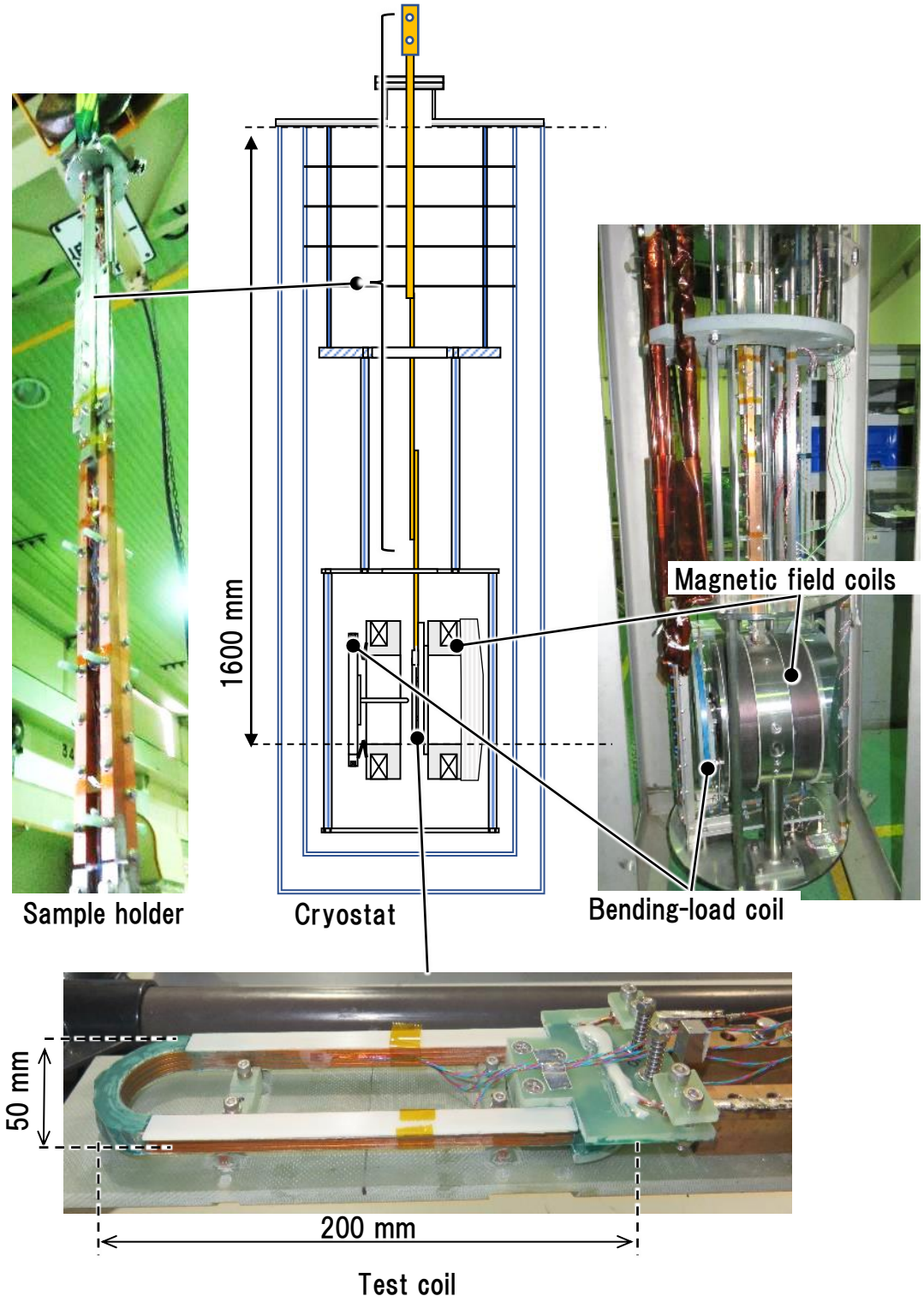

Fig. 2-1 Three-point bending test stand. This test stand consists of a sample holder, magnetic field coils that applies a magnetic field to the test coil, and a bending-load coil that applies a three-point bending load to the test coil.

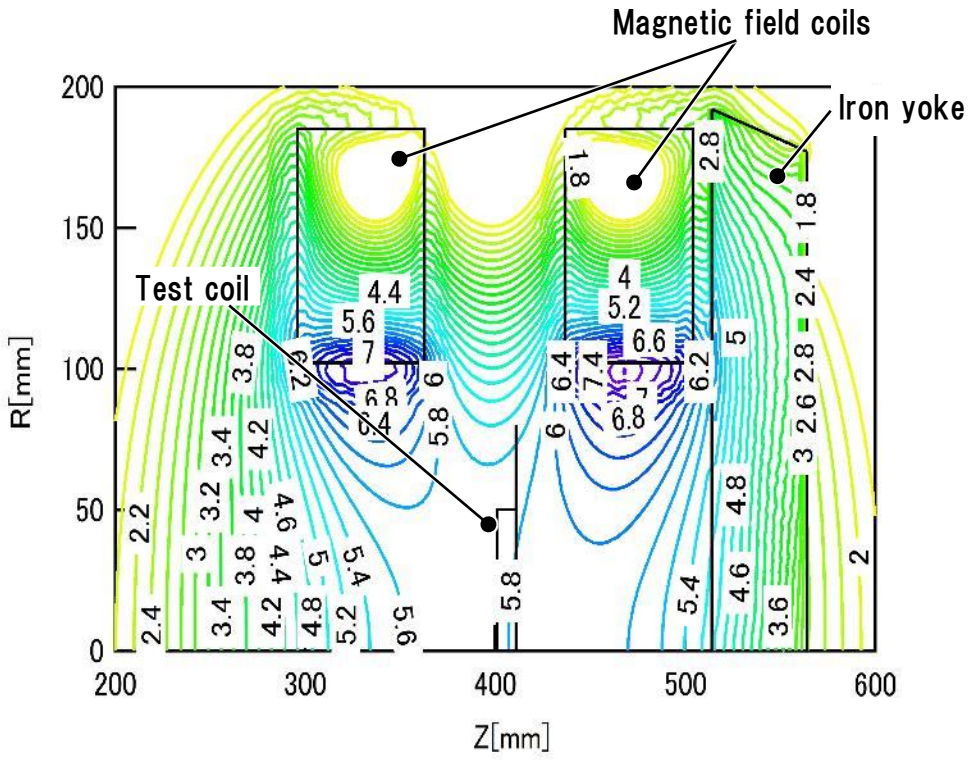

Fig. 2-2 The magnetic field of the three-point bending test stand. The empirical magnetic field of the test coil is 5.8 T when the magnetic field coils is energized to 550 A.

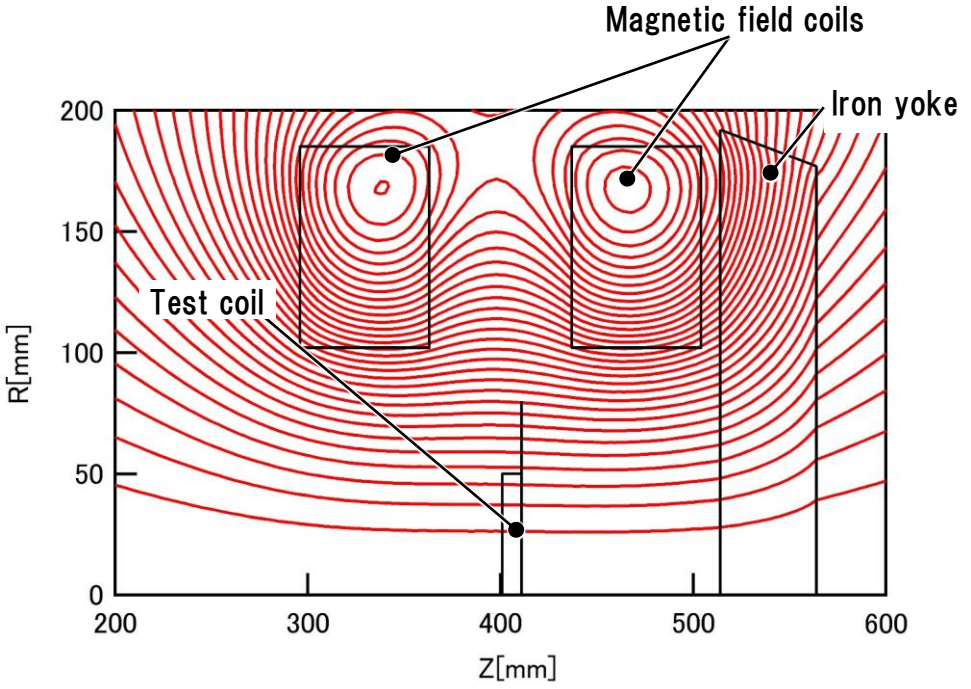

Fig. 2-3 The magnetic flux flow of the three-point bending test stand when the magnetic filed coils is energized to 550 A. The direction of the magnetic field is along the center axis of the test coil.

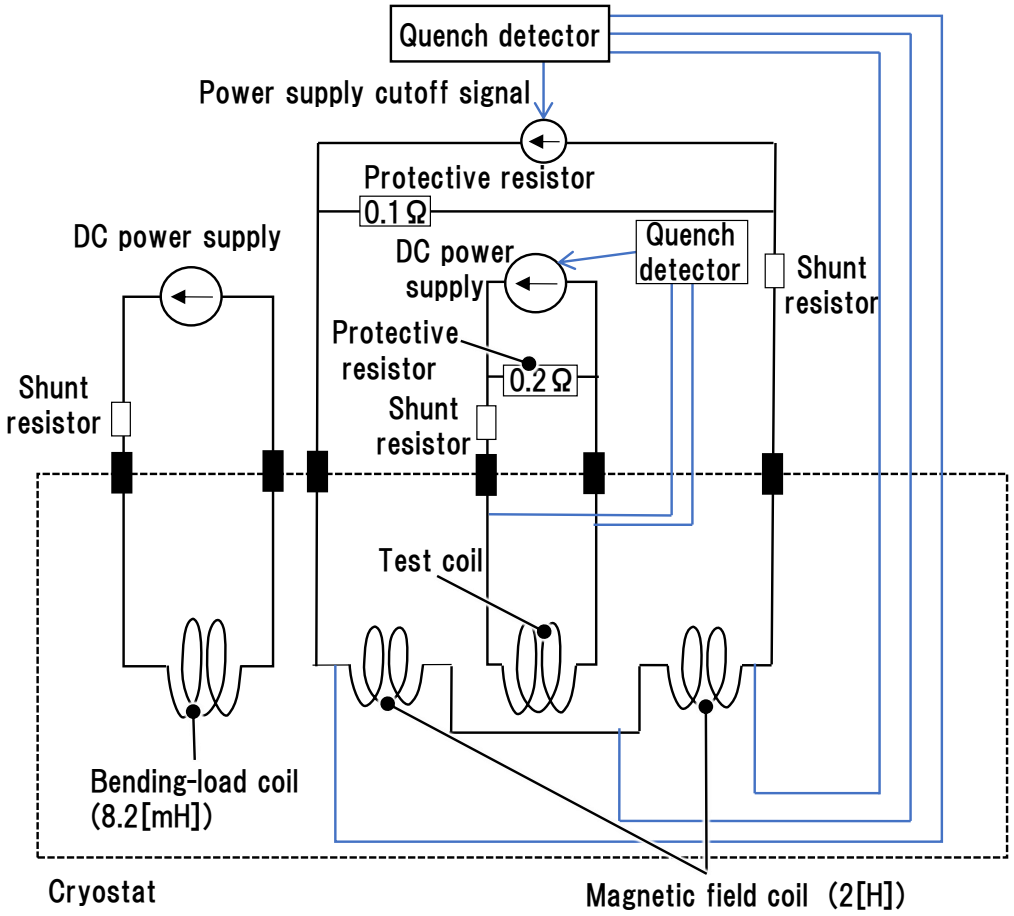

Fig. 2-4 The circuit diagram of the three-point bending test stand. The test coil, the magnetic field coil, and bending-load coil can be energized independently.

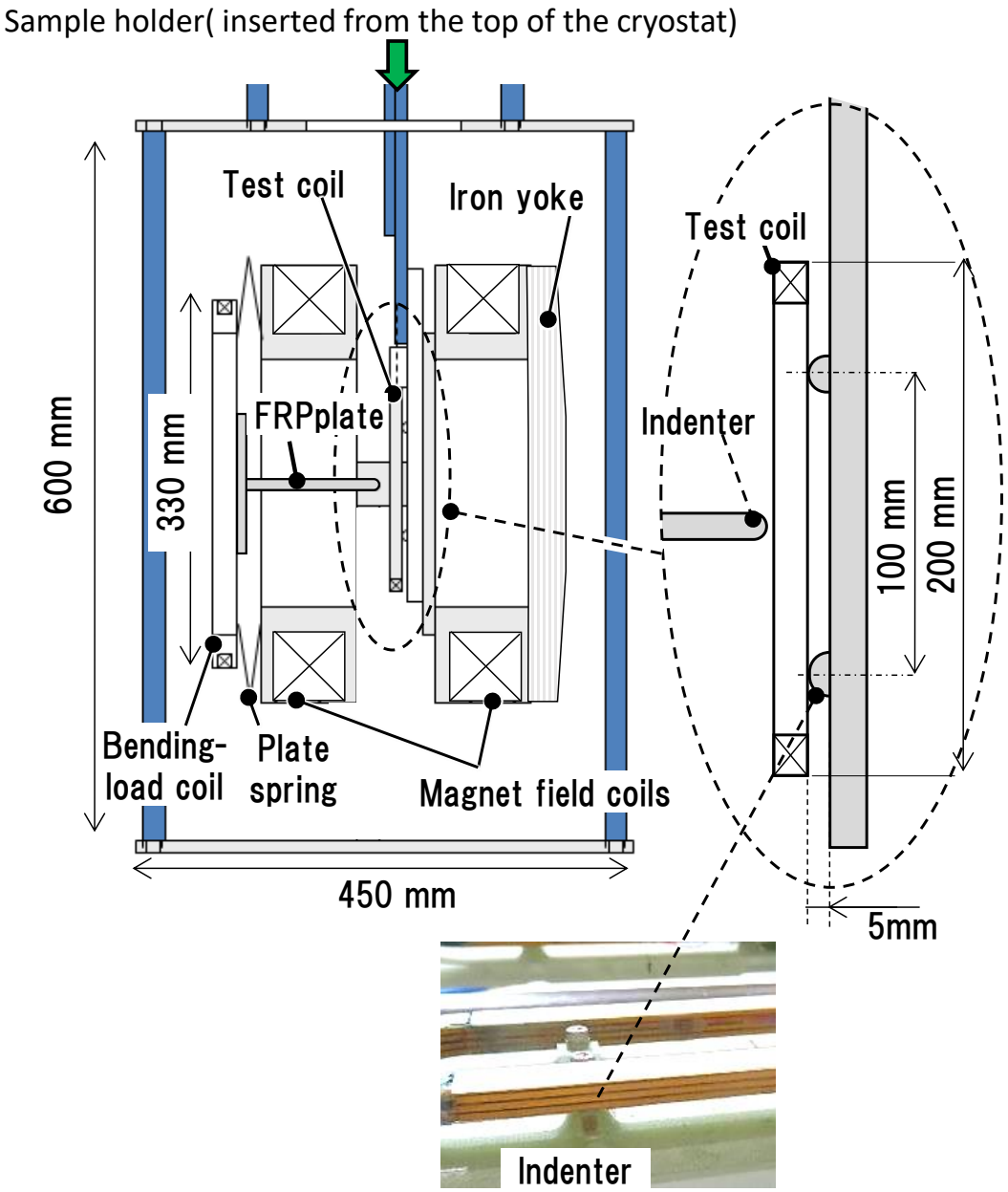

Fig. 2-5 Schematic diagram of cross section of three-point bending test stand. The test coil was replaceable. The magnetic field coils applied a magnetic field of about 5.8 T to the test coil. The bending-load was generated by the electromagnetic force attracting the bending-load coil and the magnetic field coils to each other. The direction of the bending-load was parallel to the stacking direction of the superconducting wire. The maximum bending-load was 2668 N.

2.2 Test Coils to Verify The Feasibility of The Three-Point Bending Test Stand

In this study, two types of test coils with different molding methods were manufactured for the purpose to verify the feasibility of the three-point bending test stand. In the test, it was verified whether three-point bending is possible with bending-load and magnetic field as designed. It was also verified whether the three-point bending test stand can evaluate the mechanical stability of the superconducting coil with the reproducibility for multiple samples. In addition, we examined which molding method is suitable as the superconducting coil with the helium-permeable structure.

Table 2-1 shows the specifications of the test coil for verification test. The test coil was a racetrack-shaped coil, and a superconducting wire with a rectangular cross section of 1.7 mm x 1.1 mm was wound in 4 rows and 6 layers. Non-induction winding was adopted so that the test coil was not deformed by the electromagnetic force generated by itself. By using non-inductive winding, the current directions of adjacent superconducting wires were opposite to each other. The directions of the electromagnetic force were also opposite to each other, and the electromagnetic force were canceled out; therefore, the test coil had a turning back point as shown in Fig. 2-6. The plastic insulation plates were glued to the two straight sections with molding resin in order to avoid a quench due to the frictional heat between the test coil and the fiber-reinforced plastic (FRP) plate that bent the test coils.

As the molding method, prepreg molding and self-bonded molding were adopted. Fig. 2-7 schematically shows the cross-sectional structure of the test coil. In the prepreg molding method, the prepreg sheets were inserted between the coil layers during the winding. Then, they were heated and cured after the winding process. The resin used in the prepreg was a thermosetting epoxy resin that cures at 130 ℃.

In the self-bonded molding method, a thermoplastic resin was previously applied to the surface of a superconducting wire. After the winding process, the thermoplastic resin is heated and melted, and then cooled and cured. The thermoplastic resin was a phenoxy resin composed of bisphenol A and epichlorohydrin. The glass transition temperature at which the phenoxy resin softens is 102 ℃.

Fig. 2-8 shows the coil winding jig used for coil winding and molding. The coil winding jig can pressurize the straight section of the coil up to 4.0 MPa in each of the coil axial direction and the radial direction by using a spring or a countersunk spring. The pressure was determined according to prior adhesion tests and manufacturer recommendations. The pressure was 0.5 MPa for both

molding methods. In addition, the arc sections of the test coils were molded by applying a room temperature curable epoxy adhesive SK-229 into the coil winding. There was no problem with this molding method, since bending stress was not generated in the arc section during the three-point bending test.

Table 2-1 The specifications of the test coil for verification test

		Prepreg molding	Self-bonding molding
Coil size	Whole	200 mm×50 mm	
	Straight part	Length 150 mm	
	Arc part	Radius 25 mm	
Number of turns		24(6layers, 4turns/layer)	
Size of coil cross section		7.2 mm×7.2 mm	
Superconducting wire	Copper ratio	2	
	RRR	100	
	Cross section (bare wire)	Rectangle 1.7 mm×1.1 mm	
	Thickness of PVF* layer	50 μm	
	Thickness of self-bonding layer	-	20 μm
Number of samples		6	6

*Polyvinyl Formal

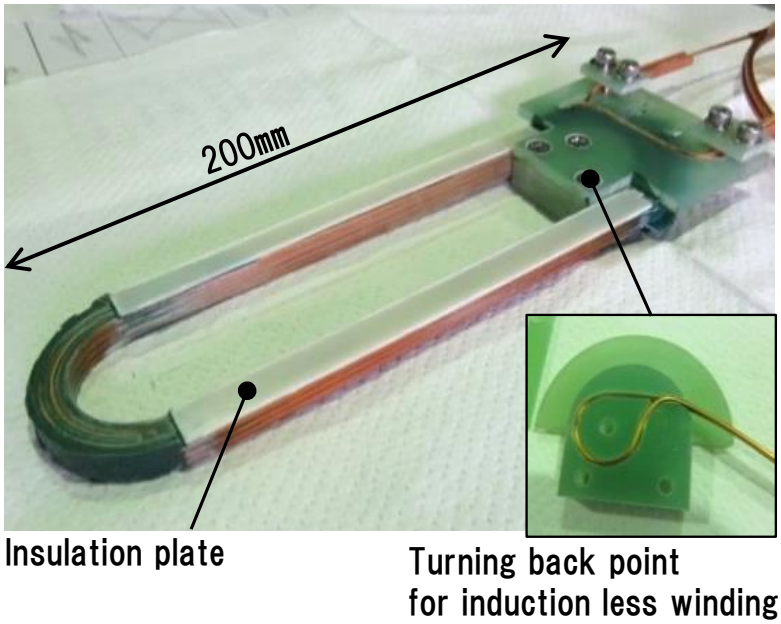

Fig. 2-6 Turning back point for non-inductive winding

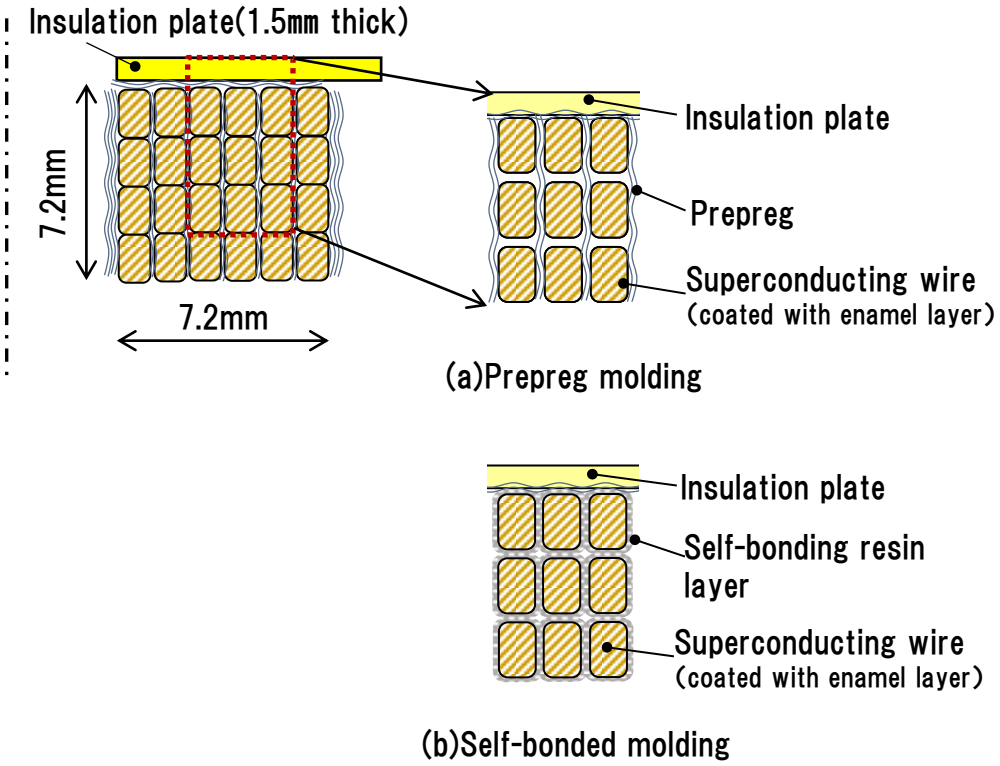

Fig. 2-7 Schematical diagram of the cross-sectional structure of the test coil. Superconducting wire with a rectangular cross section of 1.7 mm x 1.1 mm was wound in 4 rows and 6 layers. In the prepreg molding method, the prepreg sheets were inserted between the coil layers during the winding. In the self-bonded molding method, a thermoplastic resin was previously applied to the surface of a superconducting wire.

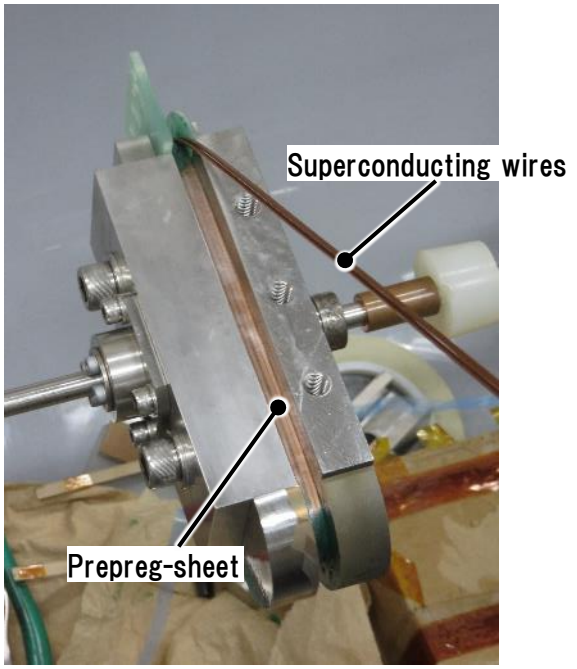

(a)Winding

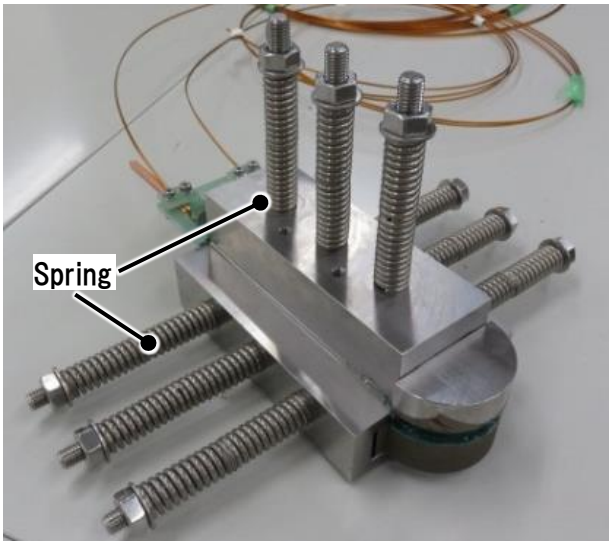

(b)Jig to apply the molding pressure

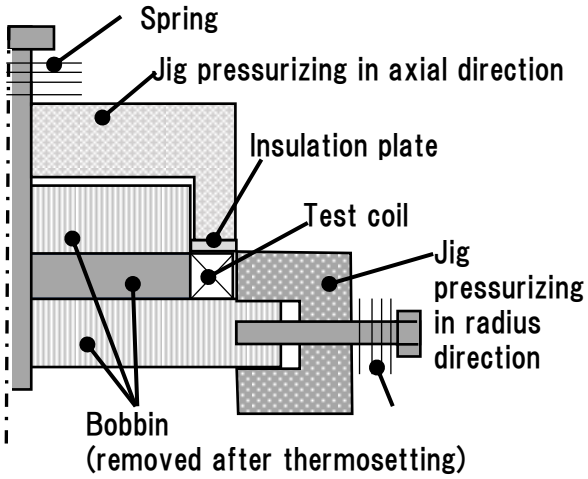

(c) Cross-sectional view on the short axis side

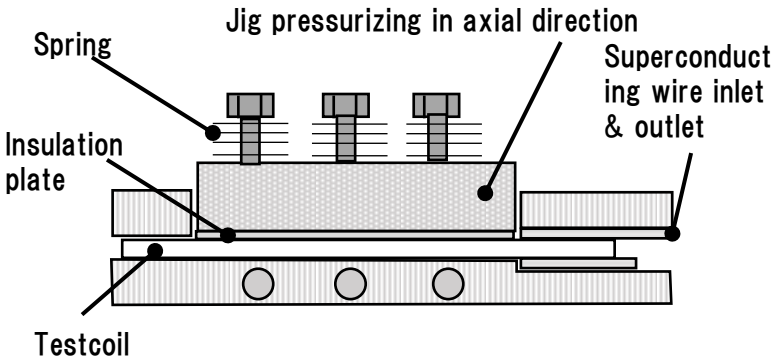

(d) Cross-sectional view on the long axis side

Fig. 2-8 The coil winding jig used for coil winding and molding. The coil

winding jig can pressurize the straight section of the coil up to 4.0 MPa in each of the coil axial direction and the radial direction using a spring or a countersunk spring.

2.3 Procedure of Three-Point Bending Test

Fig. 2-9 schematically shows the test procedure. First, the magnetic field coils are energized up to 550 A, and a magnetic field of 5.8 T was applied to the test coil. Next, the test coil was energized up to 500 A. Finally, the test coil was bent at three points. In the test when the bending-load coil was energized, the current increase rate of the bending-load coil was set so that the strain increase rate of the test coil complied with the JIS standard of the three-point bending test [61]. By setting the current increase rate of the bending-load coil to 0.04 A / s, the strain increase rate became about 10000 με/min [57].

Fig. 2-10 shows the maximum bending stress calculated by the equations (1) and (2), which are the stress formula for three-point bending [57]. When the bending-load coil is energized at 10 A, the maximum bending stress is 536MPa. The stress generated in the superconducting coil for general MRI machines is several hundred MPa [62], and a sufficiently large stress can be generated by the three-point bending test stand.

$$\sigma = (W \cdot l \cdot h/2)/4I \qquad (1)$$
$$I = 1/12 \cdot b \cdot h^3 \qquad (2)$$

Where, σ : Maximum bending stress [Pa]、W:Bending-load [N]、l : Length of the test sample [m]、h: Thickness of the test sample [m]、b:Width of the test sample [m]、I: Moment of inertia of rectangle [m^4]

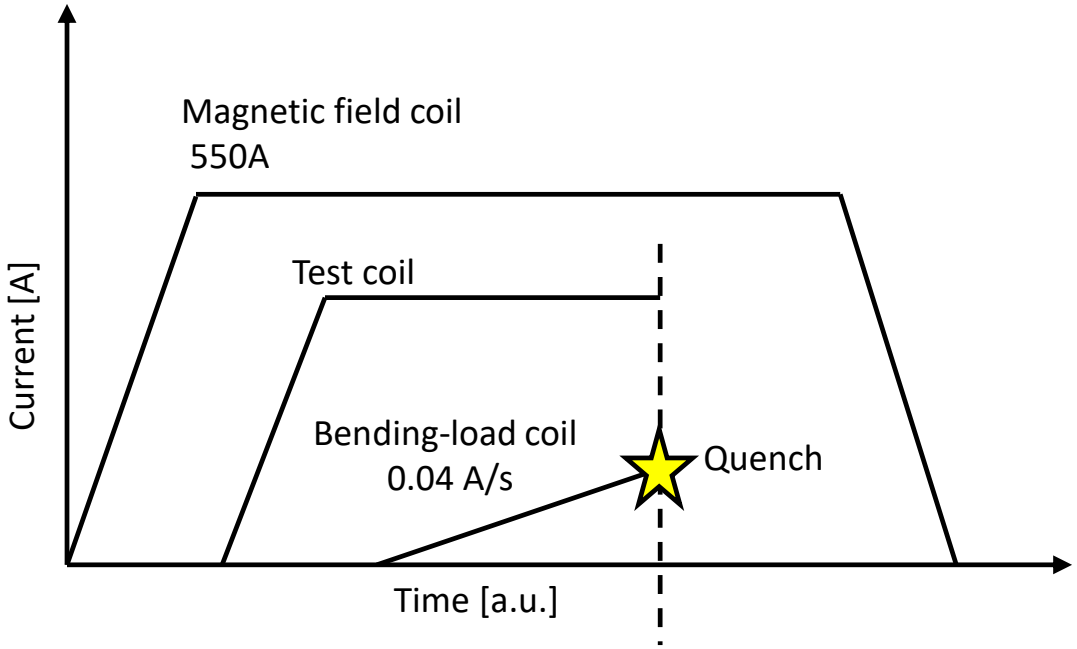

Fig. 2-9 Procedure of the three-point bending test.

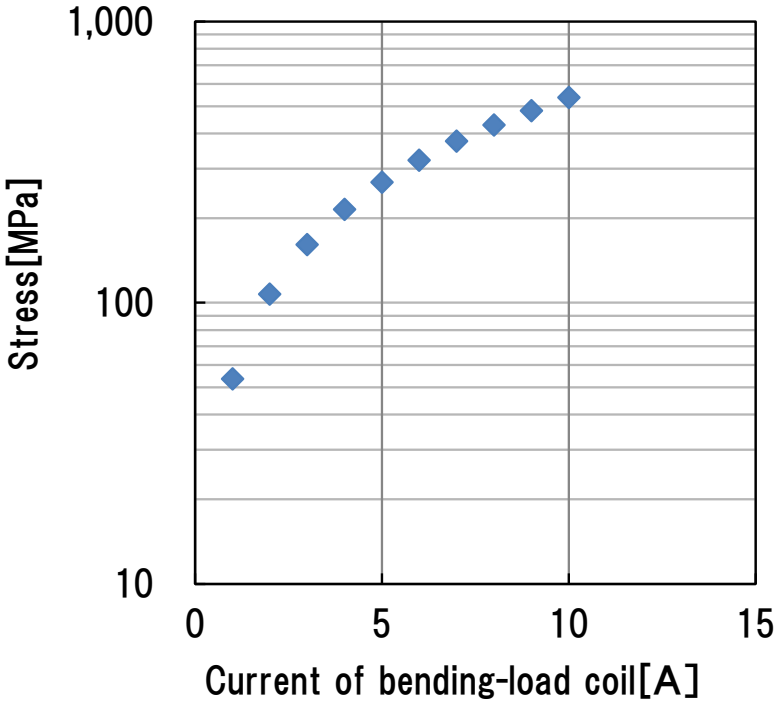

Fig. 2-10 Bending stress depending on the current of bending-load coil in the magnetic field of 5.8 T.

2.4 Sensor and Data Recording System

Fig. 2-11 shows the sensors installed on the test coil. Strain gauges were installed at the midpoint of the straight section, and the maximum bending strain due to three-point bending test was measured. The strain gauge was a low temperature strain gauge with a resistance value of 350 Ω. Two voltage taps were installed on the test coil to detect the voltage due to the superconducting-to-normal transition. In addition, the voltage spikes generated during the three-point bending were measured, and the frequency of mechanical disturbances was also analyzed. Then, as shown in Fig. 2-12, a Hall probe was set on the sample holder, and measured the magnetic field applied to the test coil.

Fig. 2-13 schematically shows the wiring diagram of the data recording system. The wires of the sensors installed in the cryostat were pulled out via the hermetic seal connector. Then, each signal except the strain gauge signal was amplified by an isolation amplifier (NF-P64) and AD-converted by an AD converter (NI-9215). Then, measurement data were recorded by a data recording PC. The signals of strain gauges were AD-converted by an AD converter (NI-9236) that also served as a bridge box, and then recorded on the data recording PC. The sampling frequency was set to 2 kHz, which is sufficient for recording the voltage spike having the fastest frequency among the recorded data.

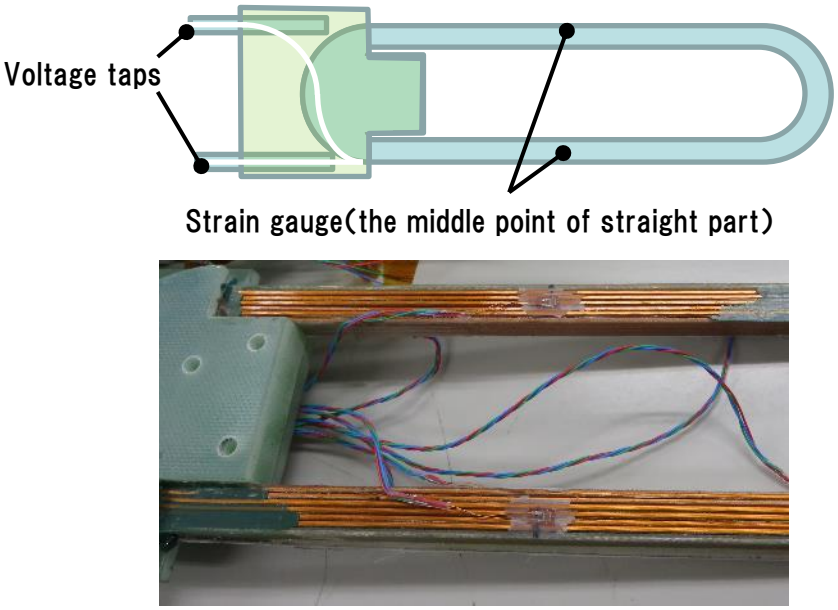

Fig. 2-11 The sensor installed on the test coil. Strain gauges were installed at the midpoint of the straight section. Two voltage taps were installed on the test coil.

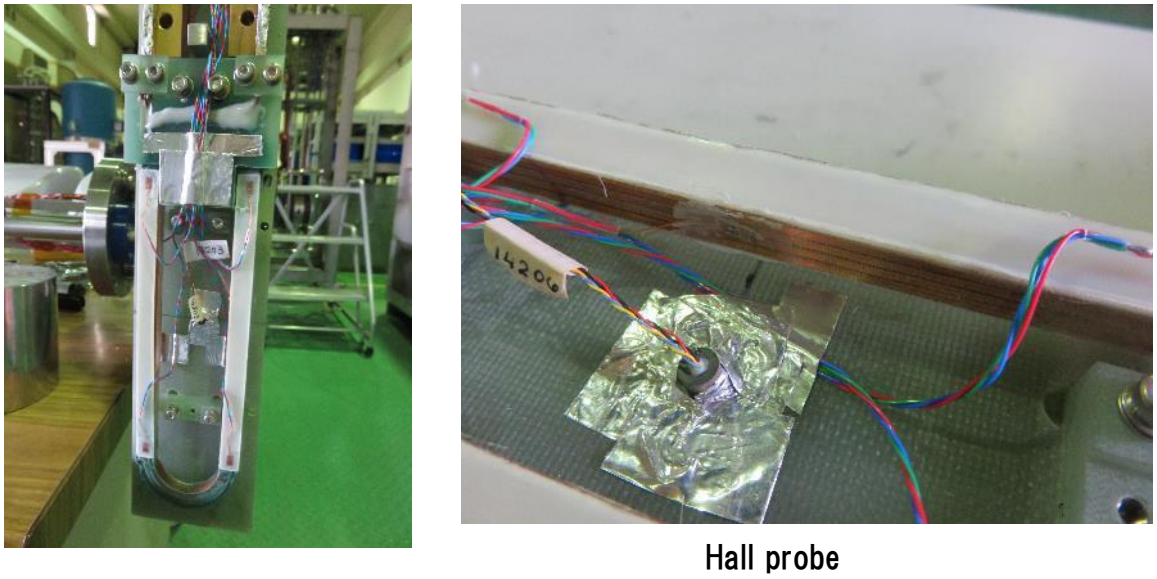

Fig. 2-12 Hall probe installed on the sample holder.

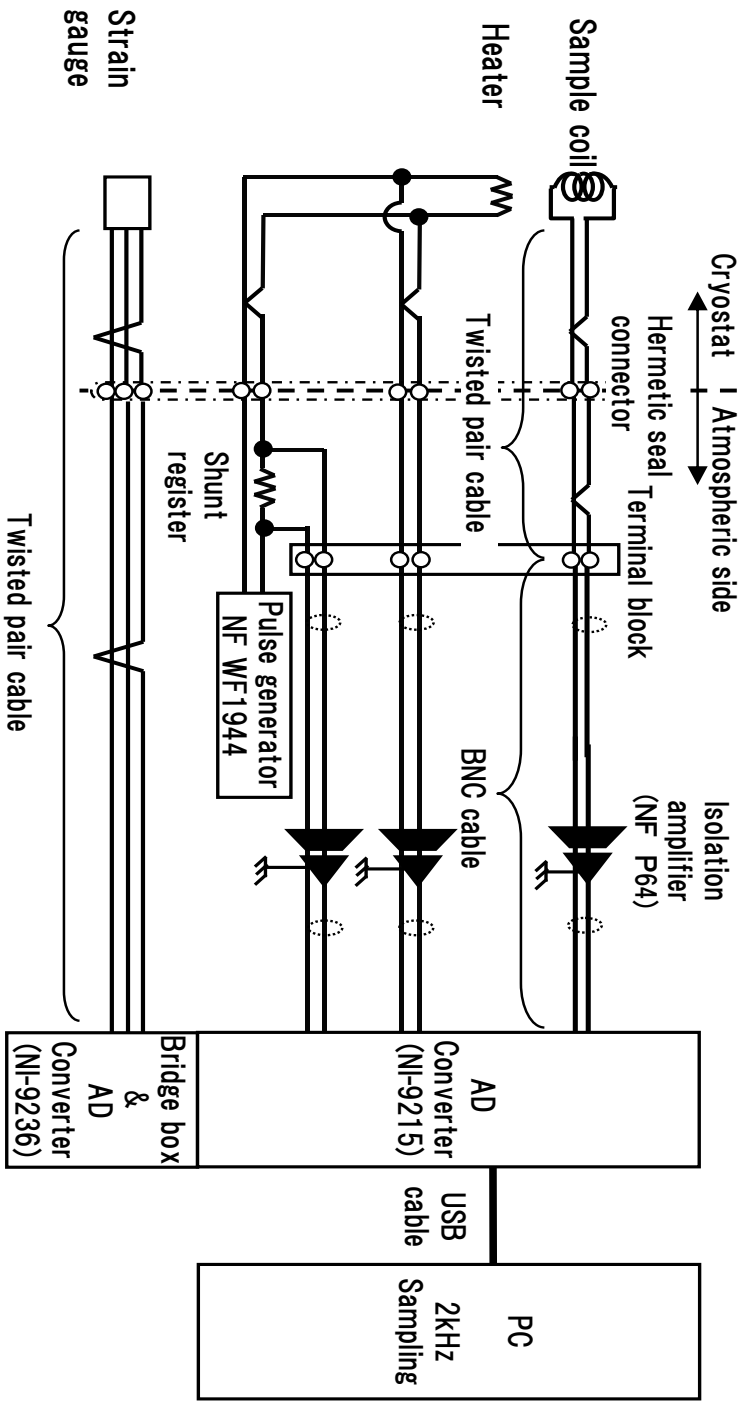

Fig. 2-13 Wiring diagram of the data recording system. The wiring of the sensor installed in the cryostat was pulled out via the hermetic seal connector. The sampling frequency was set to 2 kHz, which is sufficient for recording the voltage spike having the fastest frequency among the recorded data.

3. Verification Test of The Three-point Bending Test Stand

In this chapter, the operation test results of the three-point bending test stand are described. The results of the three-point bending test performed on the test coils prepared in Chapter 2 are described.

3.1 The Operation Test Results of The Three-point Test Stand

In order to verify that the three-point test stand is able to apply the magnetic field and the bending-load as designed, the operation test was performed. Fig. 3-1 shows the magnetic field measurement results at the position of the test coil. The magnetic field was 5.8 T when the current value of the magnetic field coils reached 550 A, and the magnetic field could be generated at the position of the test coil as designed. Incidentally, the magnetic field coils were energized by changing the current sweep rate in two steps. The current sweep rate was 1 A/s up to 300 A and 0.5 A/s up to 550 A. In order to avoid the magnet quench of the magnetic field coils due to AC loss, the current sweep rate was slowed down in the region where the current load factor was high.

Fig. 3-2 shows the typical bending strain measured during the three-point bending test. The dashed lines represent the strain calculated on the assumption that the coil is made from a bulk of copper with the same cross-sectional area. Most of the coil windings are made of copper, and its Young's modulus is about 30 times higher than that of the molding resin. Therefore, if the designed bending-load is applied, the measured strain should be in good agreement with the calculated value. The strain of the prepreg molding coil was almost the same as the calculated value, and it was confirmed that the designed bending-load could be applied by the three-point bending test stand. On the other hand, in the self-bonded molding coil, the bending strain was about 3 times larger than the calculated value. One possible cause for this disparity is that the self-bonded molding coils reached the limit of adhesive strength inside the coil winding earlier than the prepreg molding coils, so the separation of the superconducting wires from each other reduced the Young's modulus of the self-bonded molding coils.

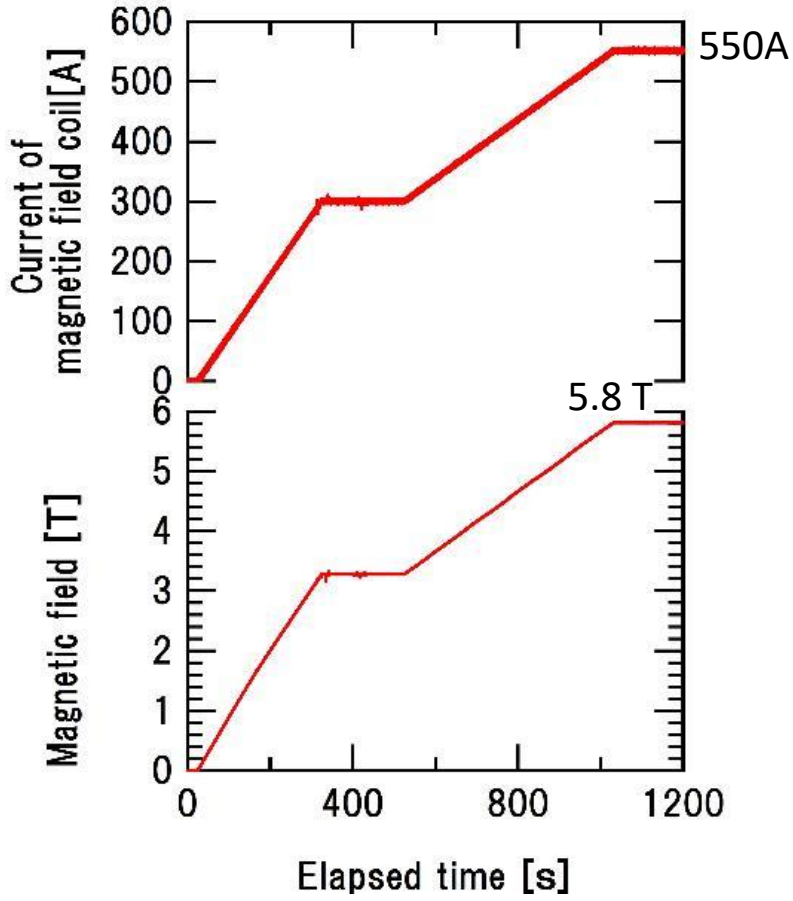

Fig. 3-1 The magnetic field measurement results at the position of the test coil. The magnetic field was 5.8 T when the current value of the magnetic field coils reached 550 A, and the magnetic field could be generated at the position of the test coil as designed.

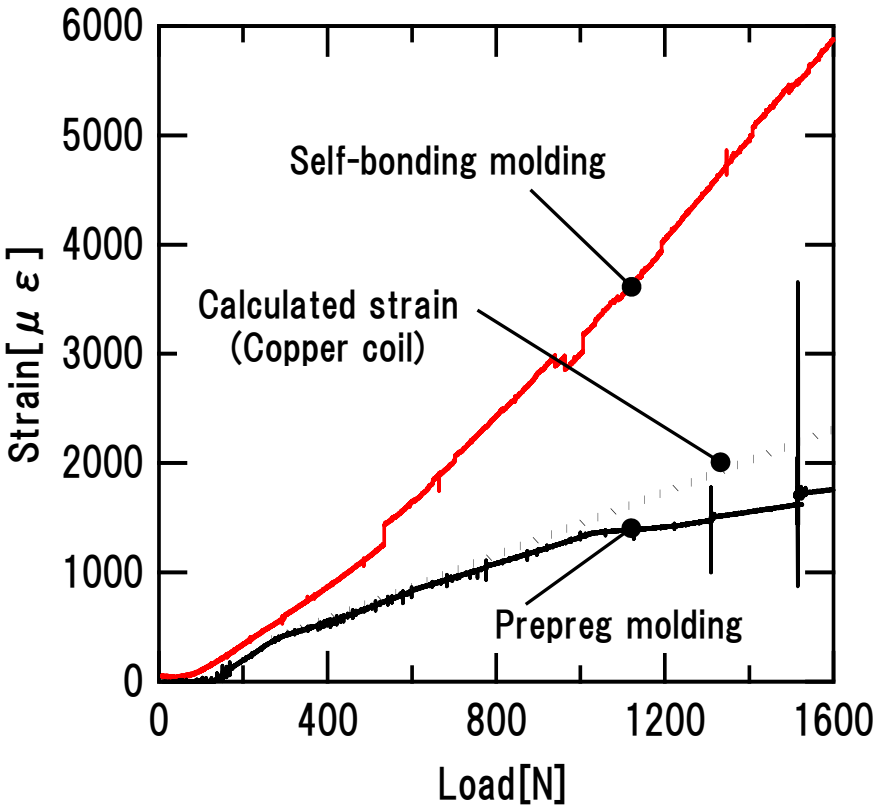

Fig. 3-2 the typical bending strain measured during the three-point bending test. The dashed lines represent the strain calculated on the assumption that the coil is made from a bulk of copper with the same cross-sectional area.

3.2 The Quench Test by Three-point Bending.

The quench test by three-point bending was performed on 6 prepreg molding coils and 6 self-bonded molding coils. Fig. 3-3 shows the load line of the three-point bending test. The critical current I_c at the maximum magnetic field of 5.8 T is 1300 A. In the test, the test coil was energized with I_{op} 500 A, which is the maximum current of the power supply, and the critical current margin defined as $I_{op}/I_c(B_{op},T_{op})$ in Section 1.4 was 38.5 % [33,34,35]. In addition, Fig.3-4 shows the load line of a superconducting coil designed with I_{op} 500A and maximum magnetic field of the coil winding B_{op} 5.8 T. The current load factor defined as $I_{op}/I_{max}(B_{max},T_{op})$ in Section 1.4 was 73 %. Since the practical current load factor of superconducting magnets is designed to be from 50 % to 70 % to ensure the sufficient quench stability [33,37], the verification test of the three-point bending test stand could be performed under practical load condition.

Fig. 3-5 shows the current sharing temperature calculated by Equation (3) [63]. By changing the current of the test coil in the range of 400 A to 1000 A, the current sharing temperature can be controlled in the range of 4.8 to 6.0 K. In the case of the test condition of 500 A, the current sharing temperature is 5.8 K. In other words, if mechanical disturbance during the three-point bending test raises the temperature of the superconducting wire to 5.8 K or higher, the quench of the test coil is induced.

$$T_{cs} = T_c(B) - (T_c(B) - T_b) \cdot I/I_c\,(B, T_b) \qquad (3)$$

Where, Tc (B) [K]: the critical temperature in the magnetic field B, Tb [K]: the liquid helium temperature, Ic (B, Tb) [A]: the critical current under the conditions of the magnetic field B and the temperature Tb.

Fig. 3-6 shows a typical example of the measurement waveform of the three-point bending test. The test object was a prepreg molding coil. The waveform is the result of repeating the three-point bending test twice on the same test coil. In both cases, the bending strain started to increase after the bending-load coil was energized, and the superconducting-to-normal transition occurred when the bending strain reached 1000 με or more. Further, as shown in the enlarged display of Fig. 3-7, the spike signal of the strain gauge was detected about 20 ms before the coil voltage increase due to the superconducting-to-normal transition; therefore, mechanical disturbances triggered the coil quenches as intended.

The quench strain was 1080 με in the first time and increased to 1197 με in the second time. This increase of the quench strain indicates a training

phenomenon that allows the superconducting coil to withstand greater electromagnetic forces and strain after undergoing the quench. In addition, the spike signals of the test coil voltage (hereafter referred to as “voltage spike”) were detected during the three point-bending tests. In the second three-point bending test, the number of the voltage spikes decreased. This decrease of the voltage spikes may indicate the Kaiser effect [64]. In the future, it will be possible to evaluate the quench strain of superconducting coils including the training phenomenon.

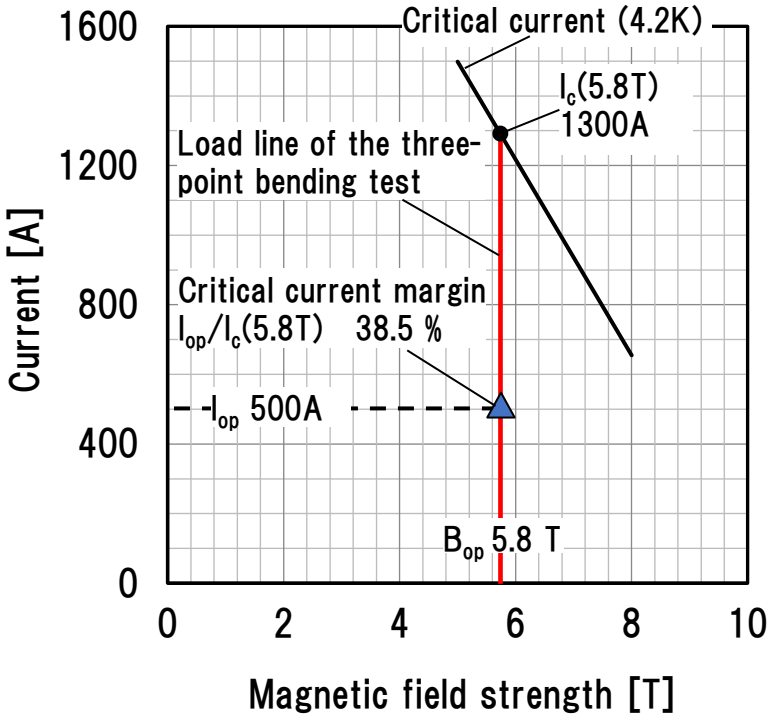

Fig. 3-3 The load line of the three-point bending test. The critical current at the magnetic field of 5.8 T was 1300 A. The critical current margin defined as $I_{op}/I_c(B_{op},T_{op})$ in Section 1.4 was 38.5 %.

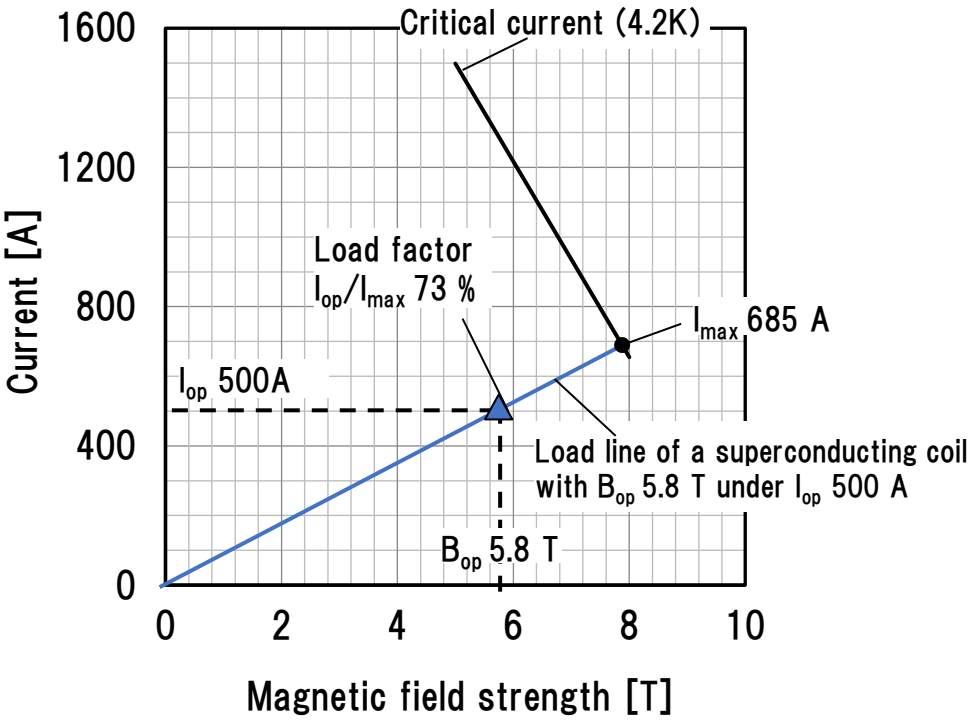

Fig. 3-4 Load line of a superconducting coil designed with maximum magnetic field of the coil winding B_{op} 5.8 T at I_{op} 500 A. The current load factor defined as $I_{op}/I_{max}(B_{max},T_{op})$ in Section 1.4 was 73 %. The practical current load factor of superconducting magnets is designed to be from 50 % to 70 % [33, 37].

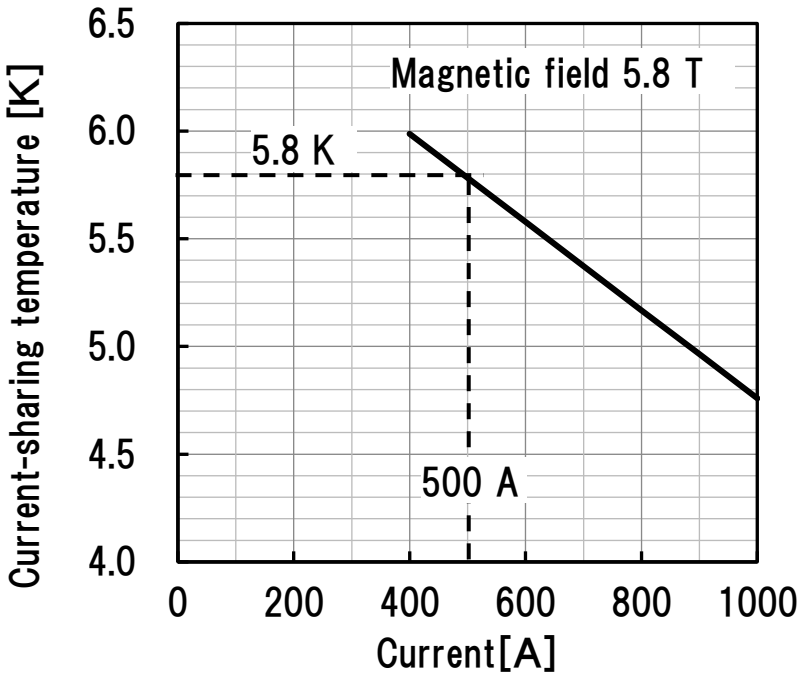

Fig. 3-5 The current sharing temperature of the test coil [59]. Magnetic field is 5.8 T. By changing the current value of the test coil in the range of 400A to 1000A, the current sharing temperature can be controlled in the range of 4.8 to 6.0 K.

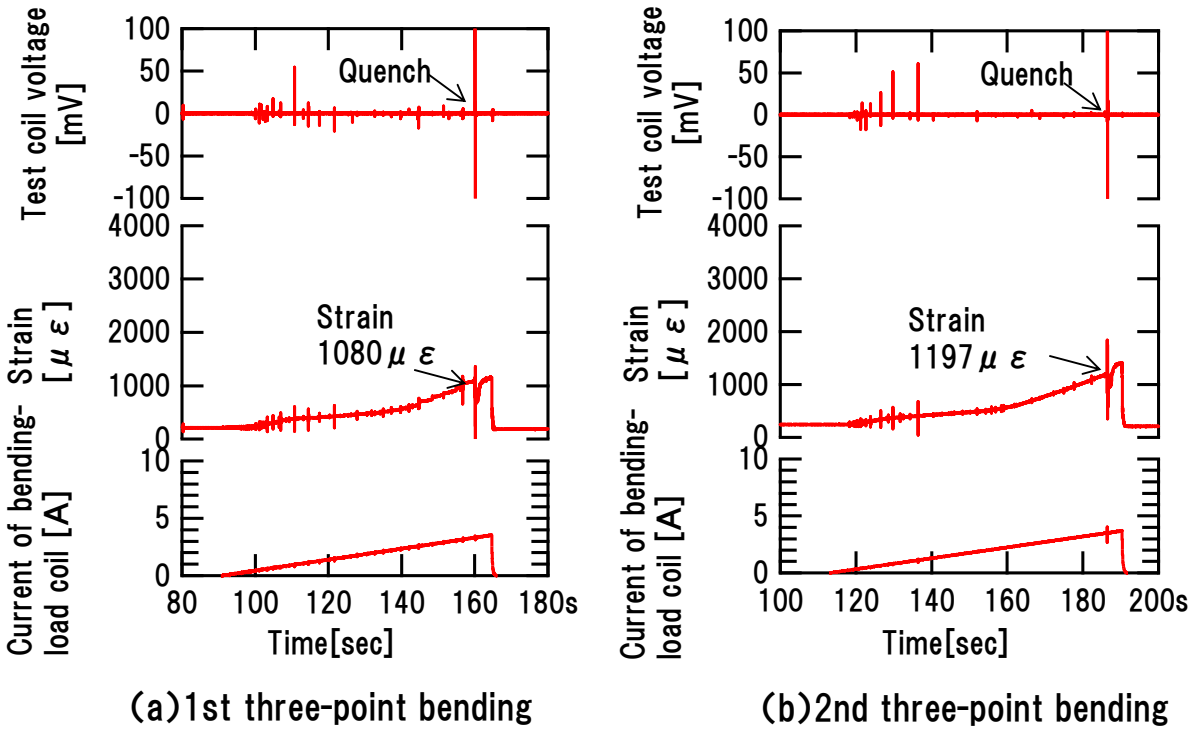

Fig. 3-6 Typical example of the measurement waveform of the three-point bending test. The test object was a prepreg molding coil.

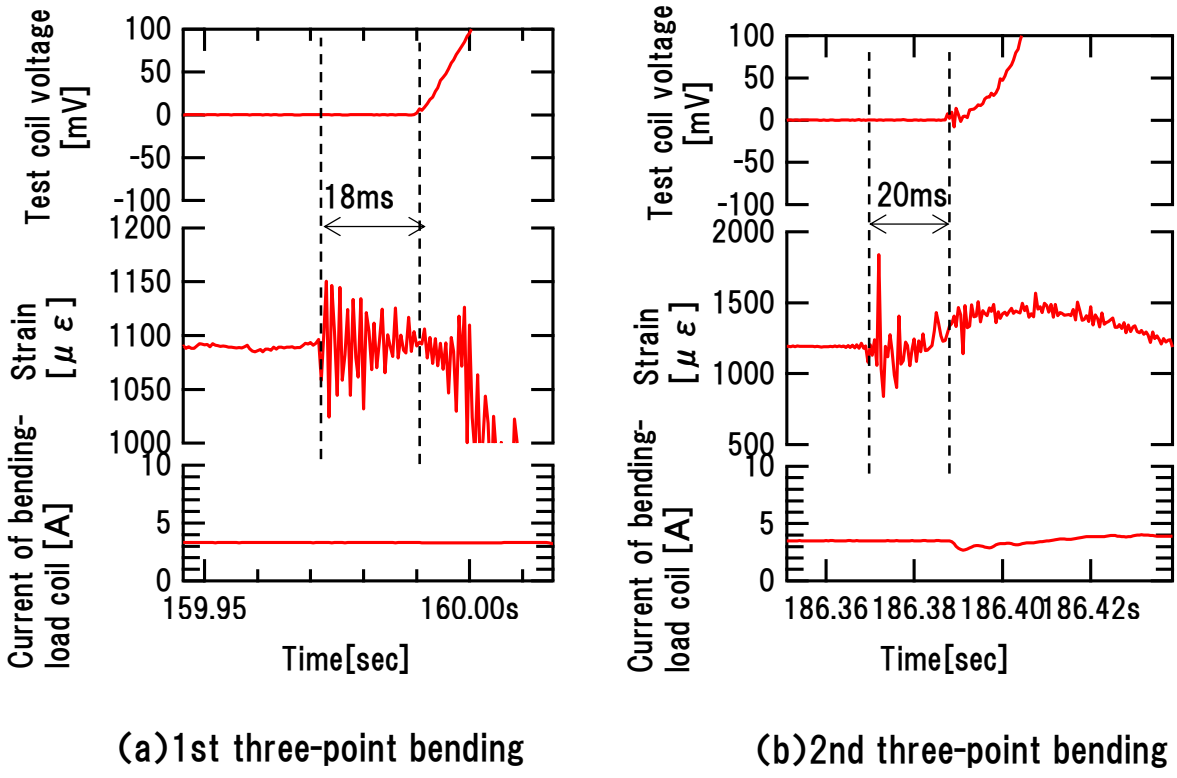

Fig. 3-7 Typical example of the measurement waveform at the event of the quench. The test object was a prepreg molding coil.

3.3 Comparison of the quench strain

Fig.3-8 shows the quench strains and the bending-load at the point of the first quench of each test coil (hereafter referred to as “quench bending-load”). The average quench bending-load of the self-bonded molding coils was 1.6 times higher than that of the prepreg molding coils. The self-bonded molding coils had a higher quench strain. The average quench strain of the self-bonded molding coils was 6441 με (about 2.5 times higher than the prepreg molding coils). The standard deviation of the quench strains was 954 με for the self-bonded molding coil and 966 με for the prepreg molding coil. Statistical variations were comparable.

From the above results, it was verified that the three-point bending test stand can evaluate the mechanical stability of the superconducting coil with the reproducibility for multiple samples.

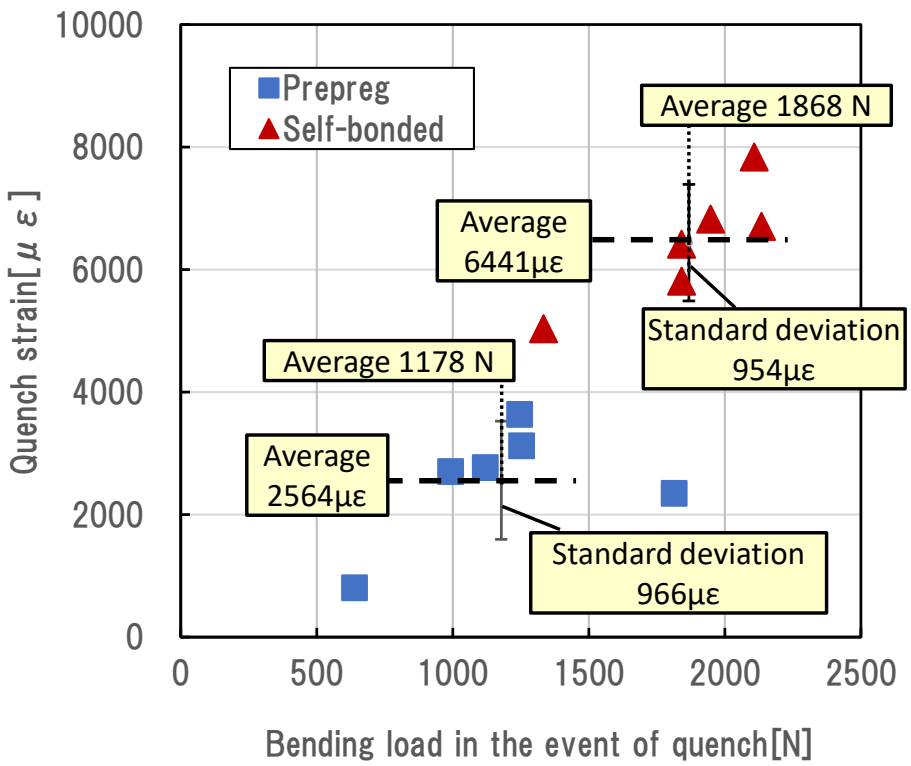

Fig. 3-8 The quench strains and the quench bending-load. The average quench bending-load of the self-bonded molding coils was 1.6 times higher than that of the prepreg molding coils.

3.4 Frequency Analysis of Mechanical Disturbances

Fig.3-9 shows typical waveforms of the prepreg molding coil and the self-bonded molding coil during the three-point bending test. Both waveforms are the measurement results of the test coil with the maximum quench load. Comparing the waveforms, more voltage spikes were detected in the prepreg molding coil, which had a smaller quench strain in the previous section. The voltage spike indicates that mechanical disturbance occurred in the coil winding. Therefore, we analyzed the correlation between the frequency of mechanical disturbance and the quench strains.

In the waveform analysis, the detection threshold was ± 0.6 mV, which is about three times the noise level to prevent false detection. A dead time of 60 ms was set after the detection of a voltage spike to prevent double counting of the voltage spike. For the above waveform analysis, the waveform analysis software "IGOR ver6.1" was used.

Fig.3-10 shows the results of the voltage spike frequency analysis. The voltage spike frequency is expressed as the number of voltage spikes generated per 1 kN load. The voltage spike frequency was higher in the prepreg molding coil, which was about 20 times that of the self-bonded molding coil. In other words, it means that the coil with the smaller quench strain generated more mechanical disturbance.

As described above, the three-point bending test stand could not only evaluate the quench strain but also could analyze the characteristics of the mechanical disturbance generated in each test coil by analyzing the voltage spike.

Incidentally, it was presumed that the voltage spike frequency of the self-bonding molded coil decreased because the voltage spike intensity fell below the detection limit due to the following two factors. The first factor is that the adhesive strength of the self-bonding resin was low, so the strain release energy in one mechanical disturbance became small. The second factor is that the phenoxy resin in the self-bonded molding coils had about two times more fracture toughness than that of epoxy resin [65,66]. The higher fracture toughness restrained crack growth in the resin; thus, energy release for the wire motion could be low.

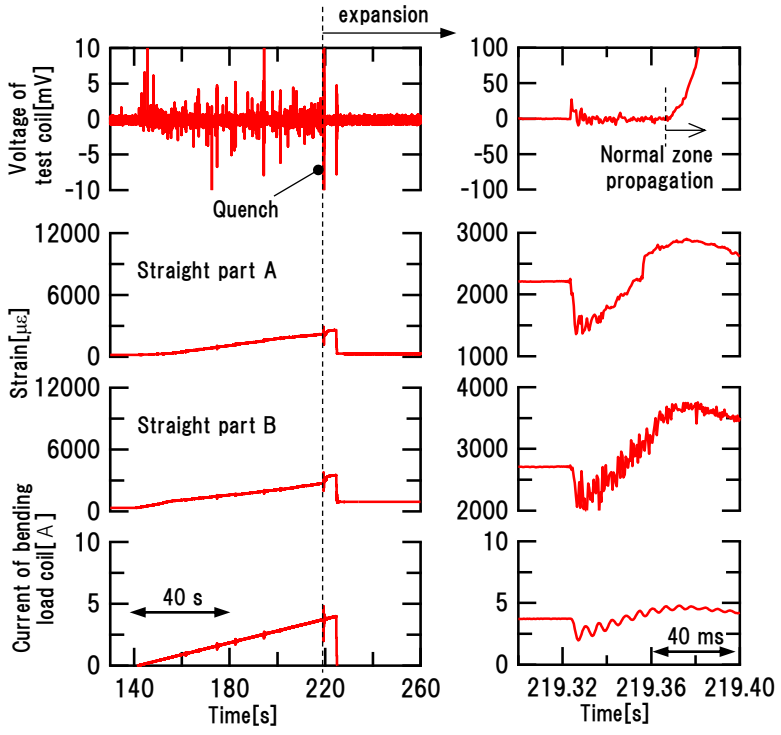

(a) prepreg molding coil

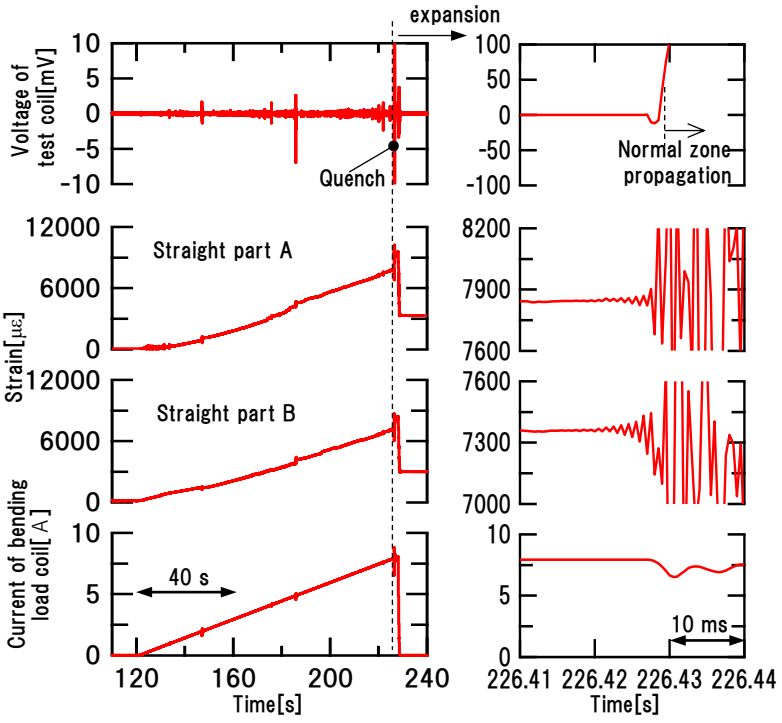

(b) self-bonded molding coil

Fig. 3-9 Typical waveforms of the prepreg molding coil and the self-bonded molding coil during the three-point bending test. The voltage spike indicates that mechanical disturbance occurred in the coil winding. More voltage spikes

were detected in the prepreg molding coil, which had a smaller quench strain in the Section 3-3.

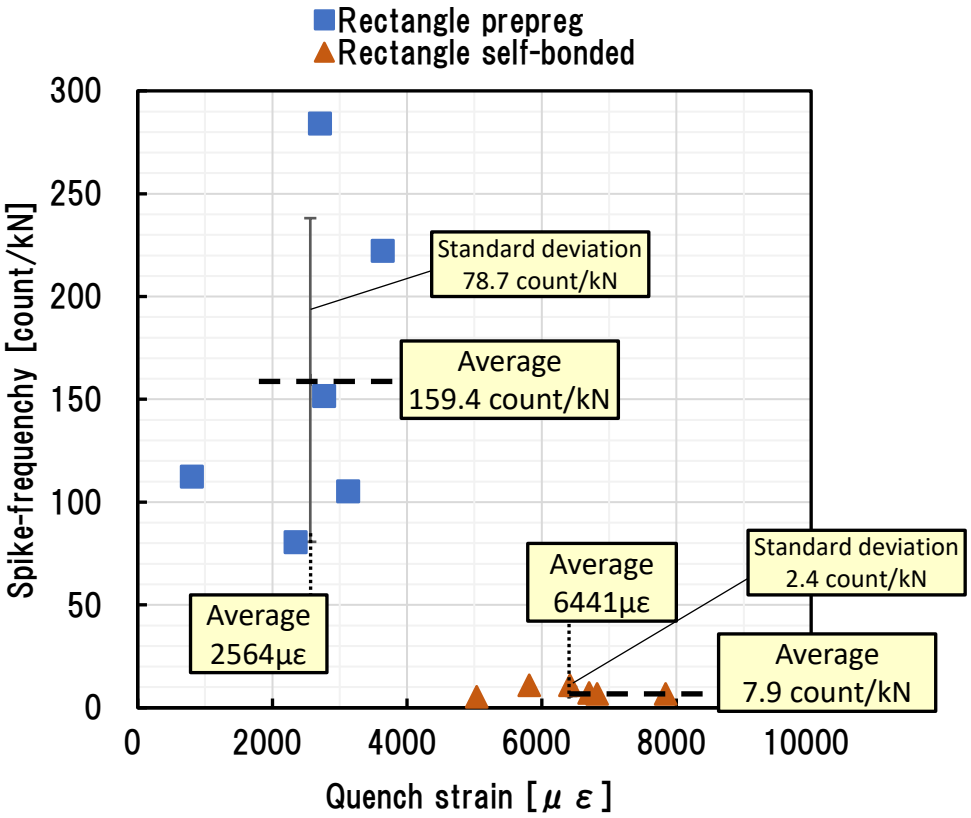

Fig. 3-10 Results of the voltage spike frequency analysis. The voltage spike frequency is expressed as the number of voltage spikes generated per 1 kN load. The voltage spike frequency was higher in the prepreg molding coil, which was about 20 times that of the self-bonded molding coil.

3.5 Summary of Verification Test of The Three-point Bending Test Stand

We obtained the following results of the verification test in this chapter.

1) The three-point bending test stand operated correctly at the cryogenic temperature of 4.2 K within a magnetic field. The magnetic field could be generated at the position of the test coil as designed. The bending-load could be applied by the three-point bending test stand as designed.

2) The racetrack-shaped test coils were quenched by the three-point bending test. The three-point bending test stand could evaluate the mechanical stability of the superconducting coil with the reproducibility for multiple samples.

3) The average quench strain of the self-bonded molding coils was about 2.5 times higher than the prepreg molding coils. The voltage spike frequency, which indicate that mechanical disturbance occurred in the coil winding, was higher in the prepreg molding coil and was about 20 times that of the self-bonded molding coil. Therefore, we considered the self-bonded molding method is suitable as the molding method for the superconducting coil with the helium-permeable structure.

4. The test coils to evaluate the effect of the helium-permeable structure on the quench stability

In this chapter, the test coils manufactured to evaluate the effect of the helium-permeable structure on the quench stability are described. As the test coil, following two type of test coils were created: (a)test coil with the helium-permeable structure and (b)test coil without the helium-permeable structure.

4.1 Selection of the superconducting wire and molding method

A superconducting wire with a circular cross section (hereinafter referred to as "round wire ") was selected for the test coils with the helium-permeable structure. The space factor of the round wire is reduced to about 90% [67], but conversely, it is possible to provide a large number of the helium permeable structures. Another merit of using a round wire is to reduce the manufacturing cost by shortening the winding process. As shown in Fig. 4-1 (a), the round wire can be wound at high speed by following the groove formed between the wires of the layer that has already been wound (hereinafter referred to as "orthocyclic winding"). On the other hand, since it is necessary to wind the rectangular wire while paying attention to the twist of the wire and actively closing the gap between the wires as shown in Fig.4-1(b), the winding tends to be slow.

A self-bonded molding method was adopted as the molding method. According to the results of the three-point bending test in Section 3-3, the self-bonded molding method tends to have the larger quench strain; therefore, a superconducting coil with high quench stability can be expected.

Table 4-1 shows the specifications of the superconducting wire. The superconducting wire was NbTi superconducting wire with a diameter of 1.0 mm. This diameter dimension was almost the same as the short side dimension of 1.1 mm of the rectangular wire adopted in Chapter 3. The copper ratio, which is the volume ratio of superconductor and stabilized copper, was 2.4. The superconducting wire was coated with electrical insulation (material PVF: Polyvinyl Formal) with a thickness of 25 μm and a self-bonding resin with a thickness of 20 μm. The self-bonding resin was a phenoxy resin composed of bisphenol A and epichlorohydrin. The glass transition temperature at which the phenoxy resin softens is 102 ℃.

Fig. 4-2 shows the load line of three-point bending test. The critical current is 469 A at 5.8 T, which is the maximum magnetic field of this test stand. In the test, the current of the test coil was changed from 150 A to 250 A to

evaluate the current dependence of thermal stability and mechanical stability. The critical current margin was from 32 % to 52 %. In addition, the current load factor when superconducting coils are designed under these load conditions was from 71.0 % to 80.1 % as shown in Fig.4-3. Practical current load factor of superconducting magnets is designed to be from 50 % to 70 % to ensure the sufficient quench stability [28,32]; thus, the three-point bending test can evaluate the effect of the helium-permeable structure under not only practical load conditions but also load conditions aiming at high performance of superconducting magnets.

Fig. 4-4 shows the current sharing temperature calculated by equation (3) in Section 3-2. By changing the current value of the test coil in the range of 150 A to 250 A, the current sharing temperature can be controlled in the range of 5.4 K to 6.0 K.

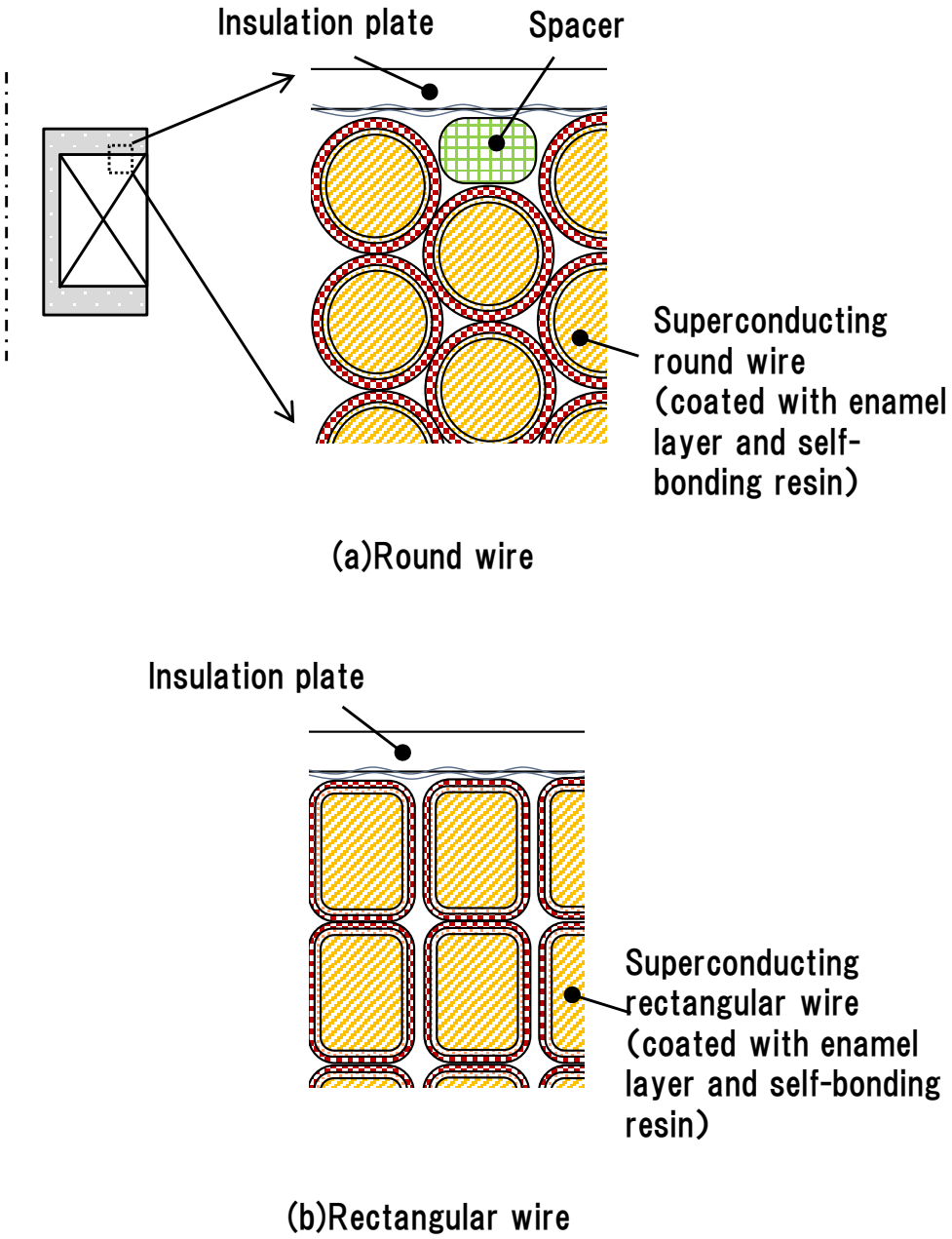

Fig. 4-1 Comparison of cross-section of the test coil using the self-bonded molding method.

Table 4-1 Specification of the superconducting wire

Copper ratio		2.4
RRR		>100
Cross section(bare wire)		Round φ1.0 mm
Thickness of PVF* layer		25 μm
Thickness of self-bonding layer		20 μm
Self-bonding resin	Material	Bisphenol-A phenoxy
	Glass-transition temperature	102℃

*Polyvinyl formal

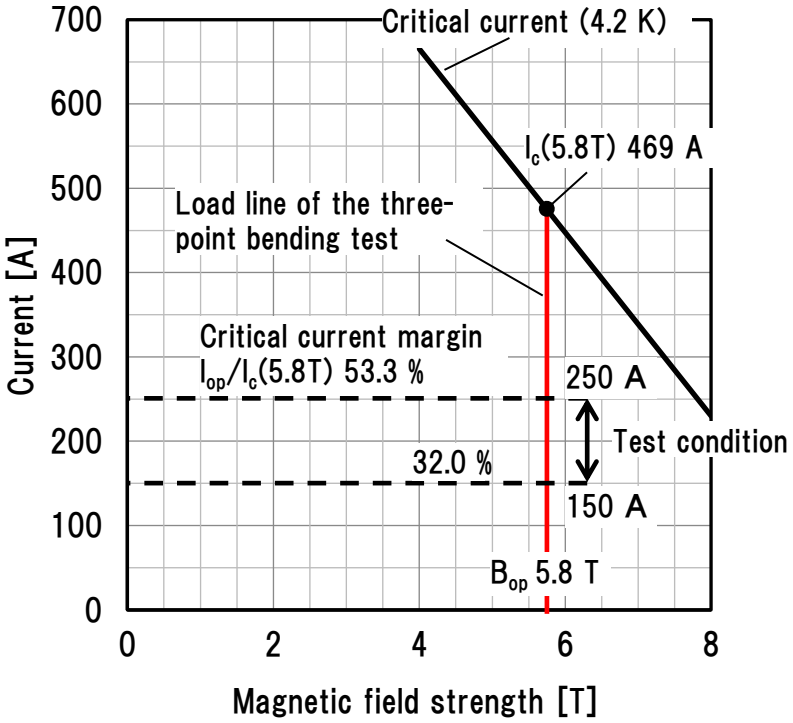

Fig. 4-2 The load line of the three-point bending test. The critical current value is 469 A at 5.8 T, which is the maximum magnetic field of this test stand. The critical current margin defined as $I_{op}/I_c(B_{op},T_{op})$ in Section 1.4 was from 32 % to 52 %.

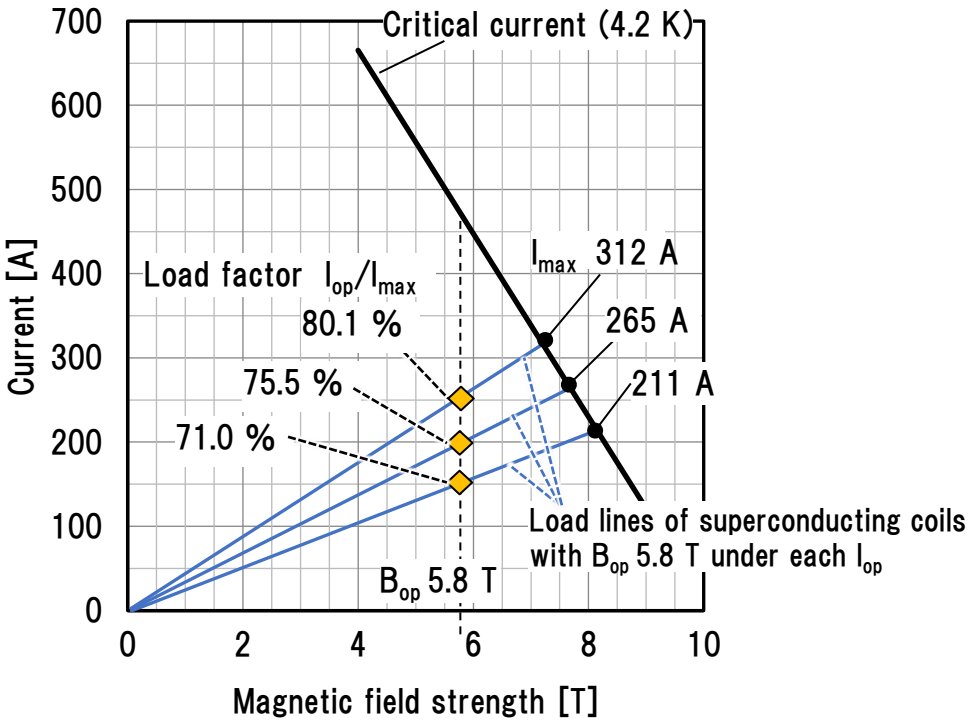

Fig. 4-3 Load lines of superconducting coils designed under load conditions of the three-point bending test. The current load factor defined as $I_{op}/I_{max}(B_{max},T_{op})$ in Section 1.4 was from 71.0 to 80.1 %. The practical current load factor of superconducting magnets is designed to be from 50 % to 70 % [28,32]; thus, the three-point bending test can evaluate the effect of the helium-permeable structure under not only practical load conditions but also load conditions aiming at high performance of superconducting magnets.

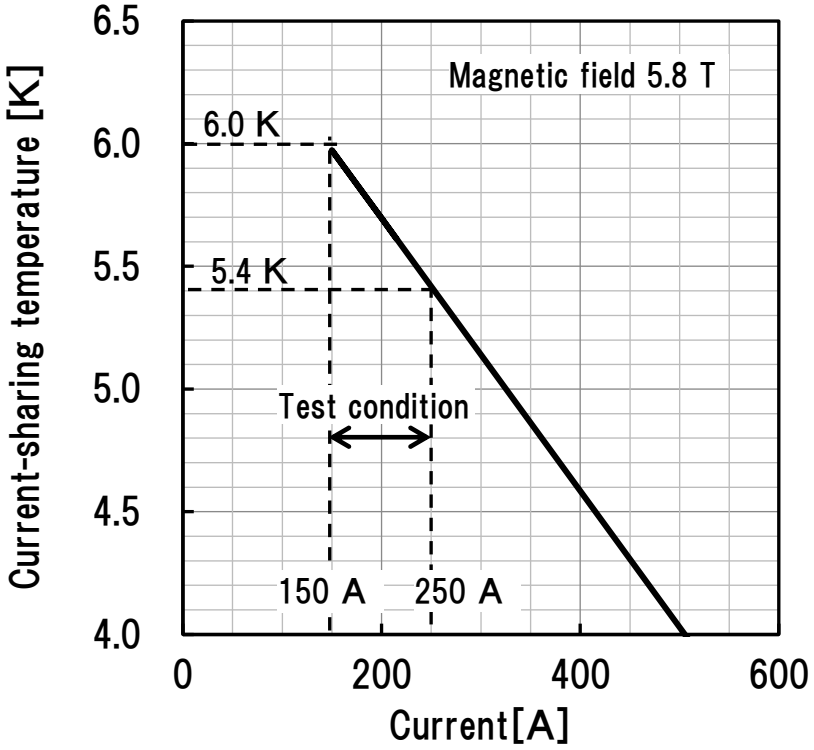

Fig. 4-4 Current-sharing temperature depending on the current of the test coil in the magnetic field of 5.8 T. By changing the current value of the test coil in the range of 150 A to 250A, the current sharing temperature can be controlled in the range of 5.4 K to 6.0 K.

4.2 Making of The Test Coil with The Helium-permeable Structure

In this section, a method for manufacturing a test coil with the helium-permeable structure are described. For manufacturing the test coil, we investigated the molding pressure to achieve sufficient adhesive strength while generating a helium permeation structure.

4.2.1 The Molding Pressure to Achieve Sufficient Adhesive Strength

When using a round wire, there is a concern that the adhesive strength will decrease due to the decrease in the adhesive area between the wires. Therefore, in this section, the molding pressure for achieving sufficient adhesive strength was investigated.

In order to investigate the adhesive strength, a tensile shear strength test was conducted. Fig. 4-5 shows the test sample for the tensile shear strength test. The test sample was made by stacking and adhering two superconducting wires and three superconducting wires and had the same

structure as a coil winding using a round wire.

Fig. 4-6 shows a pressure jig to prepare test samples. As shown in Fig. 4-6 (a), the Pressure jig was composed of a base plate and a pressure member. As shown in Fig. 4-6 (b), 3 test samples can be manufactured by stacking 13 wires on the upper side and 12 wires on the lower side and heating while pressurizing. Some wires were made of copper wires that were not coated with self-bonding resin. By disassembling with the copper wires as the boundary, it was possible to manufacture three test samples at a time. The pressure force during heating was controlled using a jig as shown in Fig. 4-6 (c). The pressure can be controlled by changing the length of the pressure spring with the pressure control screw.

Table 4-2 shows the manufacturing conditions of the test sample. The heat treatment temperature and heat treatment time were fixed at 130 ℃ and 3 hours, which achieved sufficient adhesive strength with the rectangular wire described in Chapter 2. On the other hand, the pressure force was changed in the range of 0.1 MPa to 1.0 MPa, and the effect on the adhesive strength was investigated. Six test samples were prepared under the same conditions, and the pressure dependence of the adhesive strength was measured, including statistical variations.

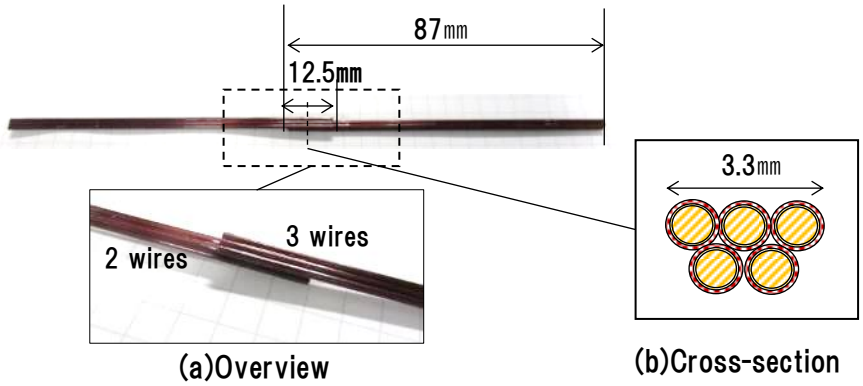

Fig. 4-5 Test sample for the tensile shear strength test

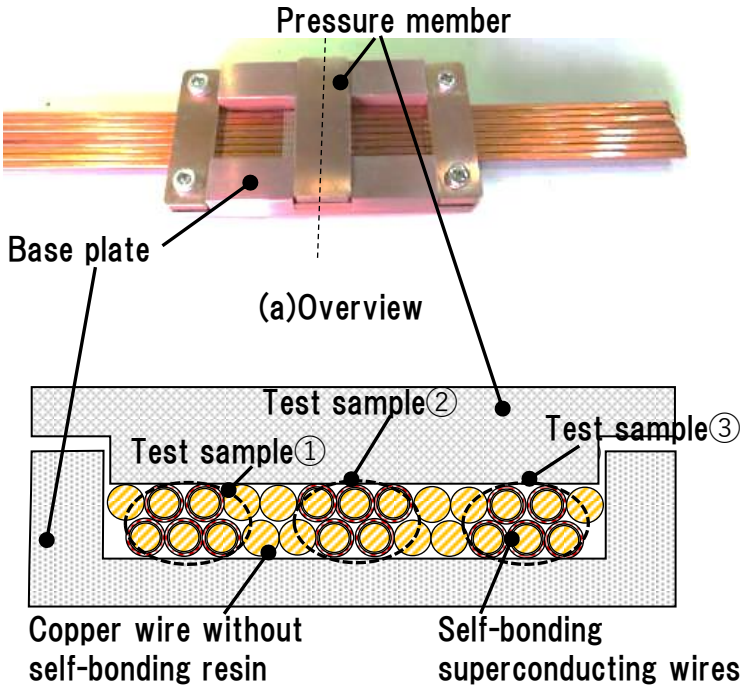

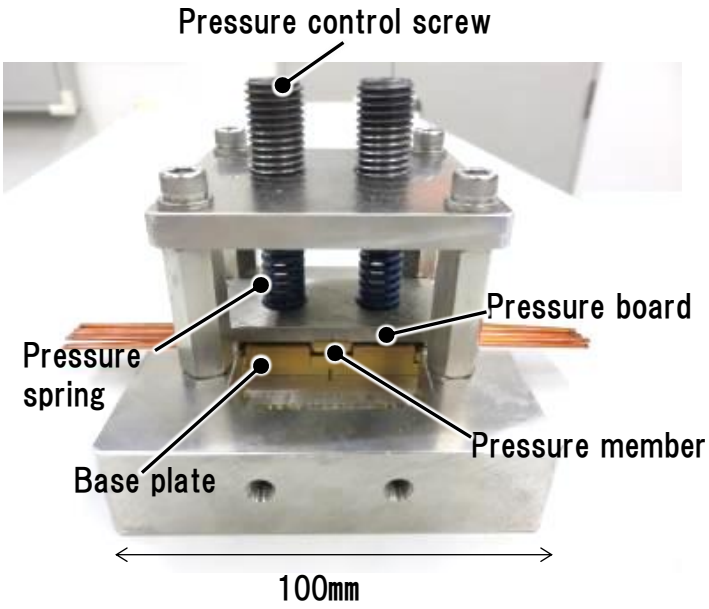

Fig. 4-6 Pressure jig to prepare test samples. 3 test samples can be manufactured by stacking 13 wires on the upper side and 12 wires on the lower side and heating while pressurizing. The pressure can be controlled by changing the length of the pressure spring with the pressure control screw.

Table 4-2 Manufacturing conditions of the test sample

Heat treatment temperature [℃]	Heat treatment time [hr.]	Molding pressure [MPa]
130	3	0.1 0.5 1.0

Fig. 4-7 shows a photograph of the tensile testing machine used for the tensile shear strength test, and Fig. 4-8 shows a schematic diagram of the measurement system. The tensile testing machine was the Autograph AG10TC manufactured by Shimadzu Corporation. The tensile load was measured with a load cell, and the displacement was measured with a displacement sensor. Each measurement signal was converted to a digital signal with a dynamic strainmeter and then recorded with a personal computer at a sampling frequency of 10 Hz. In the test, both ends of the sample are pulled at a constant speed, but if the tension speed is too high, the adhesive strength tends to be overestimated [68]. Therefor, the tensile speed was set to 0.5 mm/min so that the time until peeling was 65 seconds ± 20 seconds or more specified in JIS K 6850 [69].

Fig. 4-7 The tensile testing machine.
(The Autograph AG10TC manufactured by Shimadzu Corporation)

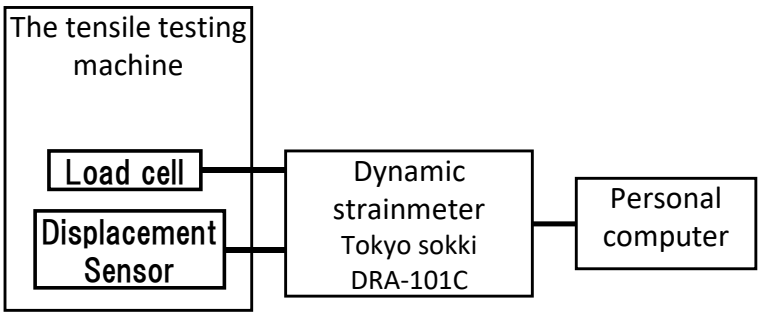

Fig. 4-8 Schematic diagram of the measurement system. Each measurement signal was converted to a digital signal with a dynamic strainmeter and then recorded with a personal computer at a sampling frequency of 10 Hz.

Fig. 4-9 shows the molding pressure dependence of the tensile shear strength. The tensile shear strength σt [MPa] was calculated by dividing the tensile load W [N] by the bonded area S [m^2]. However, since the bonded area S [m^2] was not clear, it was assumed that half surface of the wire was bonded. The error bar is the standard deviation of the measurement results for 6 test samples. The tensile shear strength increases as the molding pressure increases. Then, when the molding pressure was 0.5 MPa or more, it became constant at about 20 MPa.

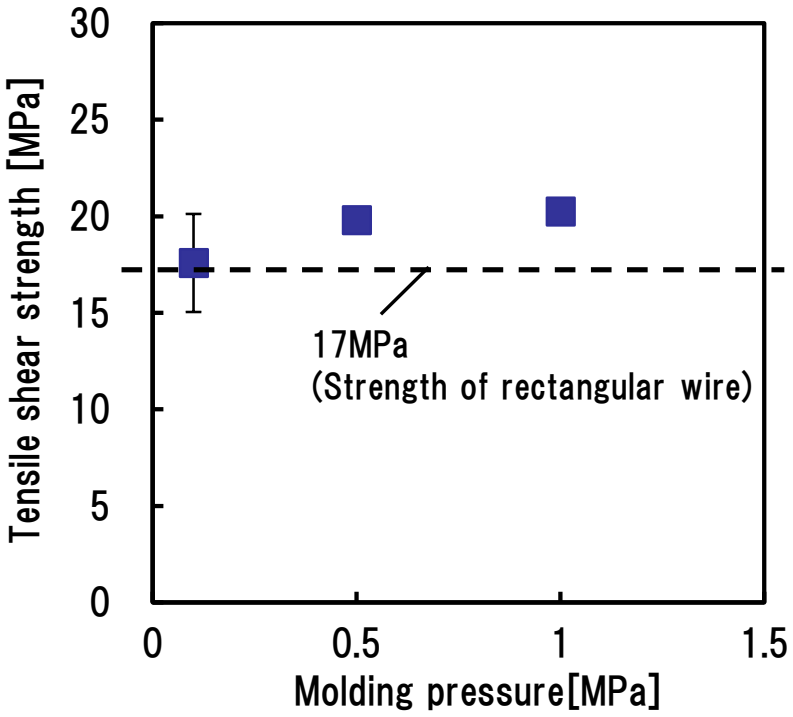

Fig. 4-9 Molding pressure dependence of the tensile shear strength between

wires. The error bar is the standard deviation of the measurement results for 6 test samples.

4.2.2 The Molding Pressure to Form The Helium-permeable Structure

Fig. 4-10 shows the cross-sectional observation results of the test sample. The bonding conditions were compared between a mold pressure of 0.1 MPa in which the adhesive strength was unsaturated and a mold pressure of 0.7 MPa in which the adhesive strength was saturated. When the molding pressure was increased, the self-bonding resin between the wires was deformed and extruded, and the joint surface was expanded. At 0.1 MPa, 53 % of the wire surface was joint surface, whereas at 0.7 MPa, 78 % of the wire surface was joint surface. This expansion of the joint surface seems to be a factor of the increase in adhesive strength.

Voids exist in the space surrounded by three wires. These voids are the helium-permeable structures. The ratio of the area occupied by each helium-permeable structure to the coil cross section was calculated to be about 6 % at 0.1 MPa and about 2 % at 0.7 MPa. Molding pressure of 0.1 MPa, which has large helium-permeable structures, should be selected in order to obtain a greater cooling effect, but molding pressure of 0.7 MPa should be selected in order to obtain sufficient adhesive strength.

As shown in Fig. 4-10 (b), the self-bonding resin was completely deformed, and the wires were closest to each other at molding pressure 0.7 MPa. In this state, the self-bonding resin will not be deformed any more, so it is possible to provide a helium permeation structure with a stable shape and area. Therefore, a molding pressure of 0.7 MPa was selected for the test coil in this study.

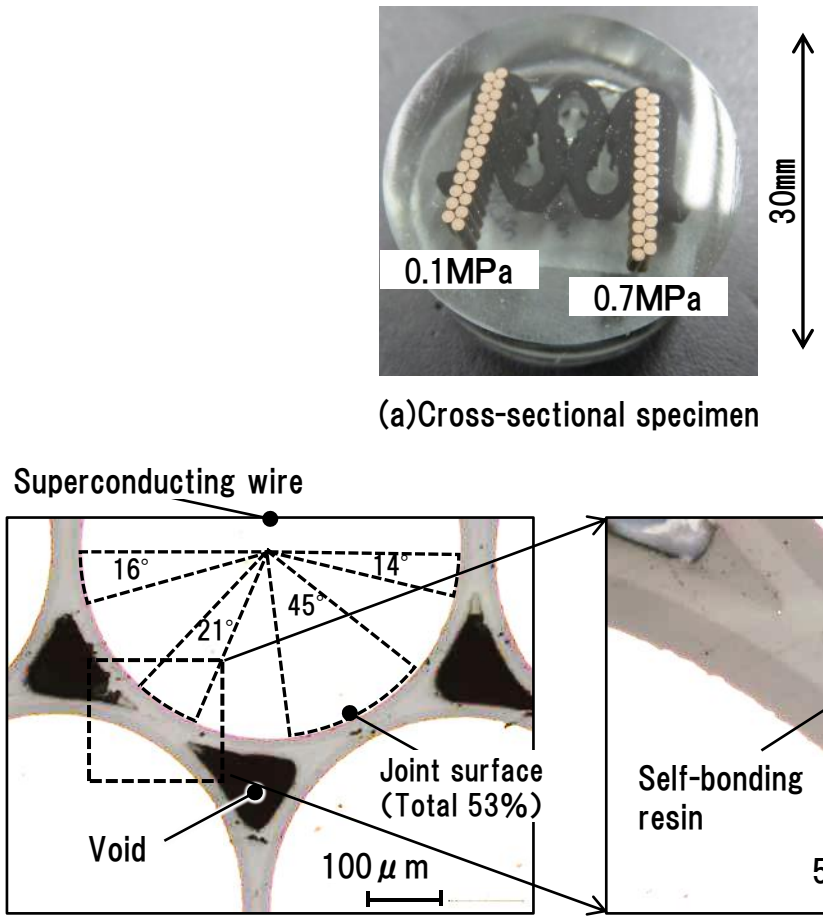

Fig. 4-10 The cross-sectional observation results of the test sample. The bonding conditions were compared between a mold pressure of 0.1 MPa in which the adhesive strength was unsaturated and a mold pressure of 0.7 MPa in which the adhesive strength was saturated.

4.2.3 Making of The Test Coil with The Helium-permeable Structure

Table 4-3 shows the specifications of the test coil with the helium-permeable structure, and Fig. 4-11 shows an overview photograph of the test coil. The test coil was a racetrack-shaped coil with dimensions of 20 mm x 50 mm, similar to the one described in Section 2-2. Non-induction winding was adopted so that it will not be deformed by the electromagnetic force generated in the test coil. By using non-inductive winding, the current directions of adjacent superconducting wires are opposite to each other. The directions of the electromagnetic force are also opposite to each other, and the electromagnetic force is canceled out.

Fig. 4-12 shows a schematic diagram of the coil cross section. Superconducting wire with a round cross section was wound in 6 rows and 6 layers. The cross-sectional dimensions of the coil were 7.4 mm x 6.1 mm, which were almost the same as the test coil manufactured in Section 2-2. Since the test coils applied the orthocyclic winding, there were gaps at the upper and lower ends of the coil cross section. Spacers were inserted in these gaps to prevent the superconducting wire from slipping into these gaps and collapsing. The spacer was a glass fiber yarn.

Fig. 4-13 shows the cross-sectional observation results of the test coil. As intended, there was a void with a diameter of about 100 μm in the area surrounded by the three superconducting wires. The helium-permeable structures with a cross-sectional area ratio of about 2 % could also be provided in the test coil.

Table 4-3 Specifications of the test coil with the helium-permeable structure

Coil size	Whole	200 mm×50 mm
	Straight part	Length 150 mm
	Arc part	Radius 25 mm
Number of turns		36(6layers, 6turns/layer)
Size of coil cross section		7.4 mm×6.1 mm

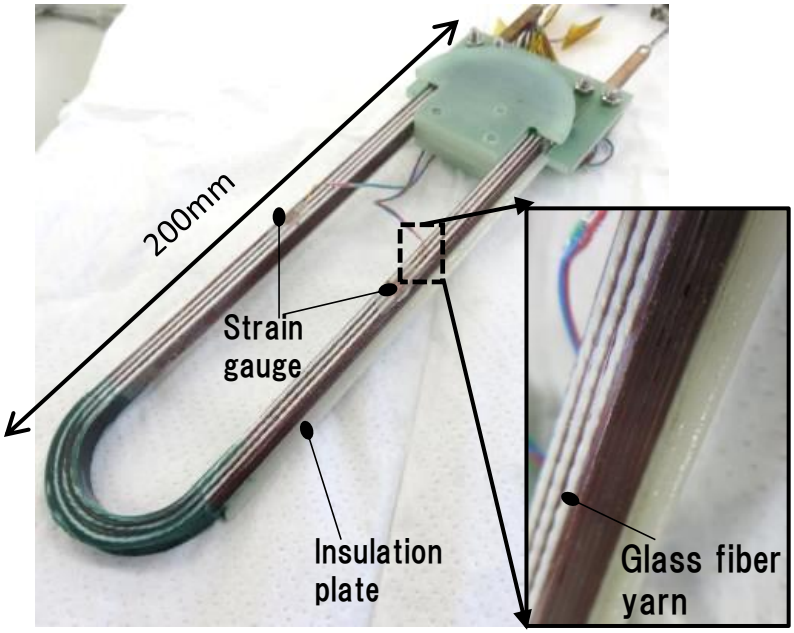

Fig. 4-11 Overview photograph of the test coil with the helium-permeable structure

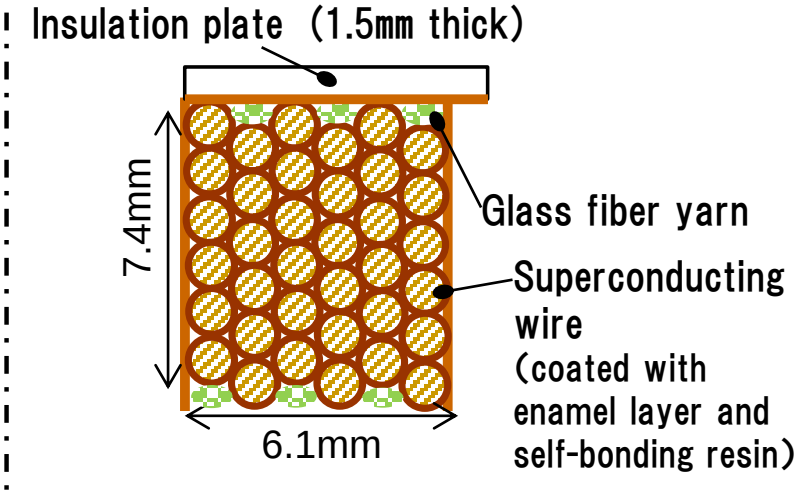

Fig. 4-12 Schematic diagram of the coil cross section. Superconducting wire with a round cross section was wound in 6 rows and 6 layers.

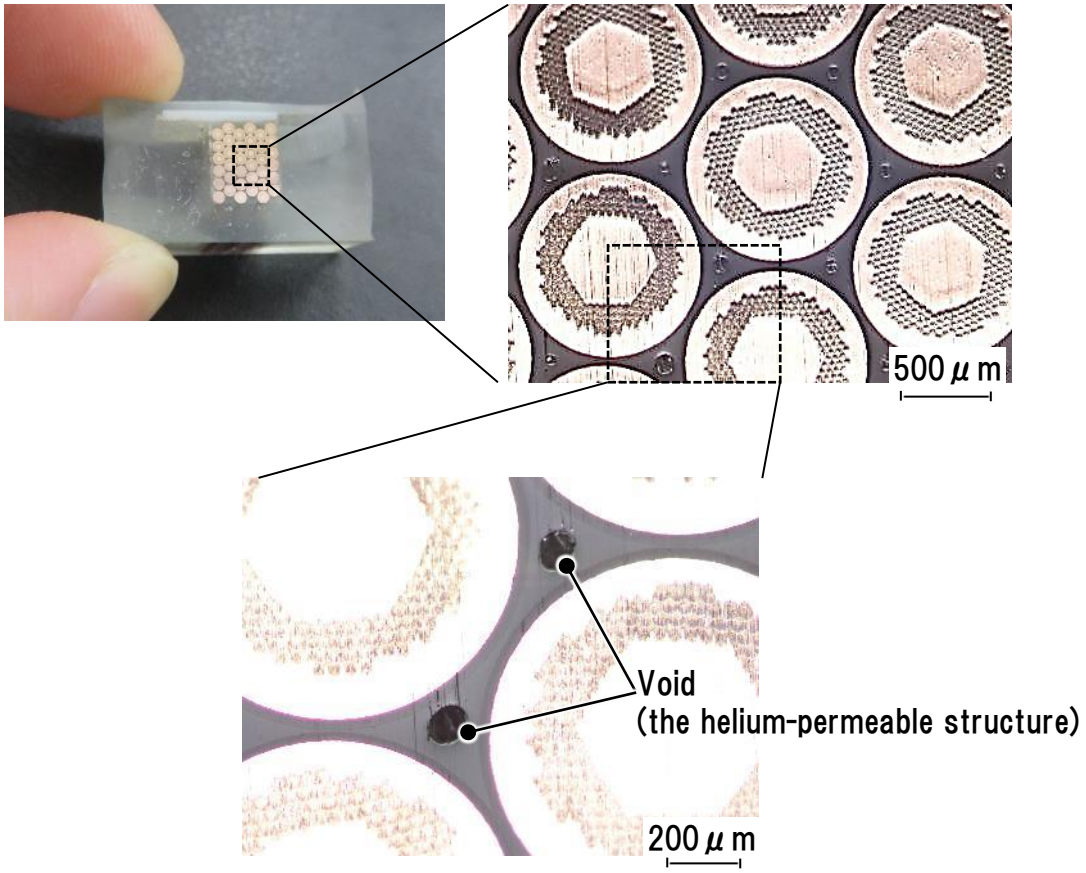

Fig. 4-13 Cross-sectional observation results of the test coil. There was a void with a diameter of about 100 μm in the area surrounded by the three superconducting wires.

4.3 Making of The Test Coil Without The Helium-permeable Structure

In order to evaluate the effect of the helium-permeable structure on the quench stability, the test coils without the helium-permeable structure were also manufactured.

The helium-permeable structures are generated because there is not enough resin to fill the gaps between the wires. Therefor, the test coils without the Helium-permeable structure could be made by putting additional self-bonding resin during the coil windings.

As the method for adding the self-bonding resin, different methods were adopted for the quench test using a heater and the three-point bending test. For the test coil used in the quench test using a heater, as shown in Fig. 4-14, wet-winding method was adopted. An organic solvent (cyclohexanone) was added to the self-bonding resin to reduce the viscosity. Although the organic solvent volatilizes in the heating process after winding, it cannot be completely removed, so there is a concern that the Young's modulus and adhesive strength of the resin may decrease. Therefore, the test coils made by wet-winding method were not applied to the three-point bending test, but they were applied only to the quench test using a heater.

On the other hand, for the test coils applied to the three-point bending test, a method of inserting a phenoxy resin film between layers was adopted as shown in Fig. 4-15. During the heat treatment after winding, the phenoxy resin film melts and integrates with the self-bonding resin coating the superconducting wire. Fig. 4-16 shows an overview of t the phenoxy resin film, and Table 4-3 shows the specifications of the phenoxy resin film. As a result of investigating the manufacturers of phenoxy resins, only Gabriel Performance Products of the United States manufactures thin films that can be inserted between layers. The thickness of the film is 127 μm. The resin of the film is bisphenol A type phenoxy similar to the resin coating the superconducting wire.

Fig. 4-17 shows a photograph of the cross-sectional observation results of the test sample. As intended, it could be confirmed that there was no helium-permeable structure in the area surrounded by the three superconducting wires in either manufacturing method.

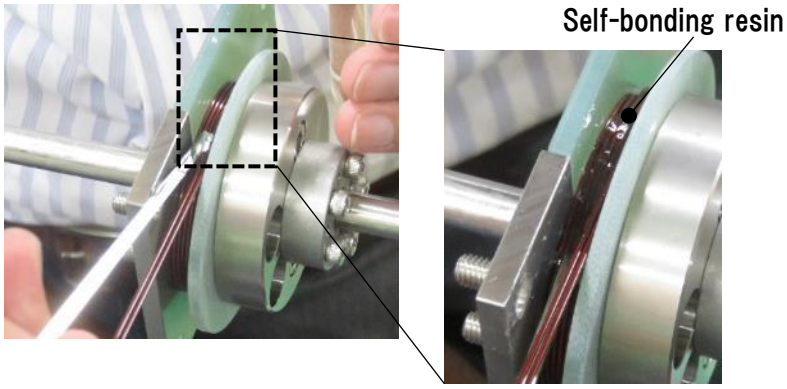

Fig. 4-14 Method of adding the self-bonding resin during the winding by wet-winding. An organic solvent (cyclohexanone) was added to the self-bonding resin to reduce the viscosity.

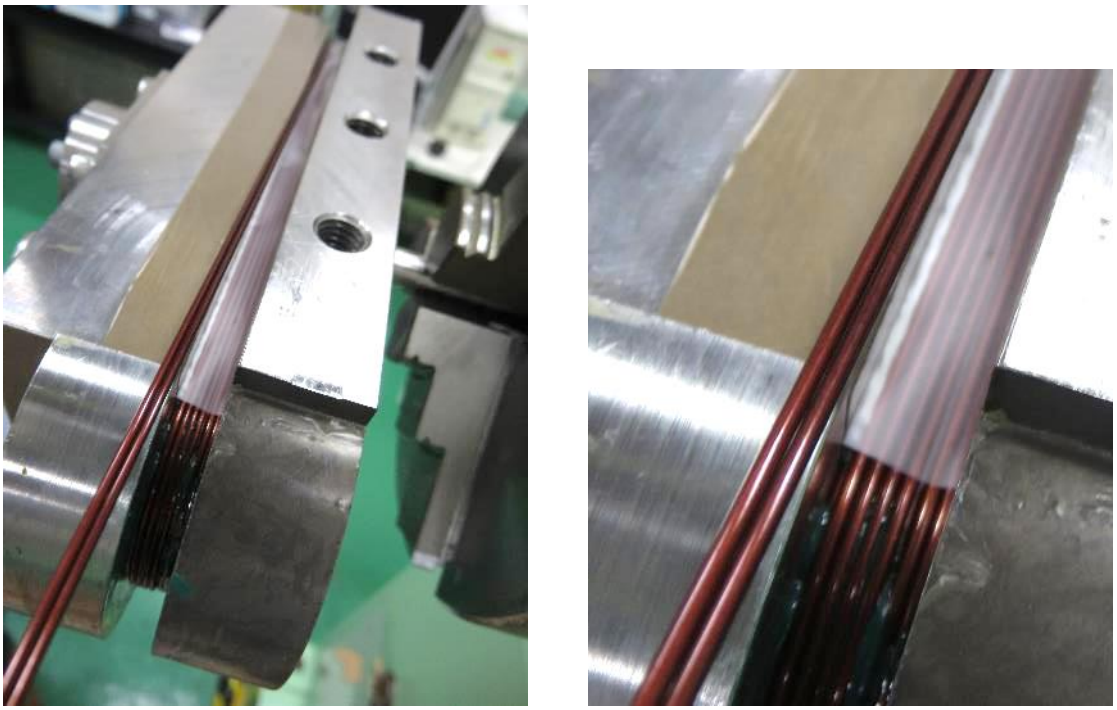

Fig. 4-15 Method of adding the self-bonding resin during the winding by inserting a phenoxy resin film between layers.

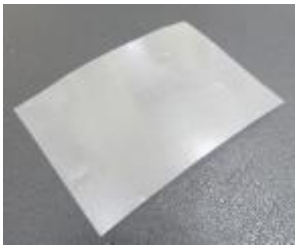

Fig. 4-16 Overview of t the phenoxy resin film

Table 4-3 Specifications of the phenoxy resin film manufactured by Gabriel Performance Products of the United States

Material (supplier, product name)	Bisphenol-A phenoxy (Gabriel,PKHH)
Glass-transition temperature	92 ℃
Thickness	127 μm

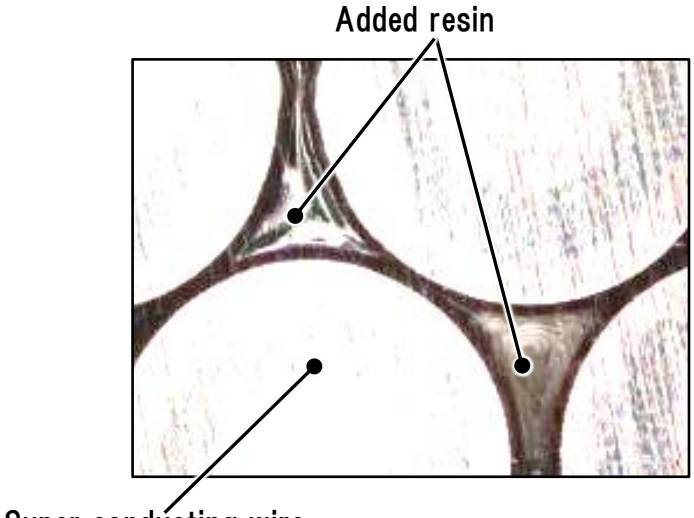

(a)Wet-winding

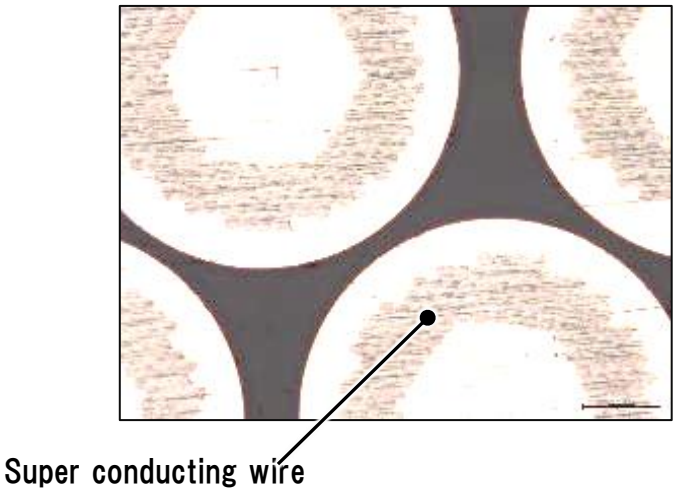

(b)Inserting the phenoxy resin film between the layers

Fig. 4-17 Cross-sectional observation results of the test sample to add the self-bonding resin during the winding. There was no helium-permeable structure in the area surrounded by the three superconducting wires in either manufacturing method.

4.4 Heater to Evaluate The Thermal Stability of The Test Coil

The developed three-point bending test stand can also evaluate the thermal stability of the test coil by heating the test coil energized in a magnetic field with a heater. The heater applied to the test and the test procedure thereof are described below.

Fig. 4-18 shows the heater installed in the test coil. The heater is required to have the same dimensions as the superconducting wire and to have sufficient electrical resistance to be used as a heater. A strain gauge for low temperature (Tokyo Sokki, CF series) was applied as an element that satisfies these conditions. The resistance value of the applied strain gauge is 350 Ω, and the dimensions are 1.7 mm x 1.0 mm. When installing the heater, the resin on the surface of the test coil and the insulation of the superconducting wire were removed so that the contact state between the superconducting wire and the heater would not vary in each test coil. The heater was fixed using a room temperature curable epoxy adhesive SK-229. A 1 mm thick FRP plate was installed on the heater for the purpose of thermal insulation with the liquid helium.

Fig. 4-19 shows MPZ (Minimum Propagation Zone) and MQE (Minimum Quench Energy) [27], both of which are calculated values. Assuming that all the heat input is supplied to the superconducting wire without diffusing to the liquid helium, MPZ is from 10.2 mm to 17.0 mm under the test conditions with the coil current of 150 A to 250 A in the magnetic field of 5.8 T. Therefore, the length of the thermal insulation plate was set to 25 mm, which is sufficiently larger than MPZ. In addition, MQE is from 48 μJ to 80 μJ under the test conditions.

The procedure of the heater quench test is as follows. First, the magnetic field coils are energized up to 550 A, and a magnetic field of 5.8 T is applied to the test coil. Next, the test coil is energized up to a targeted current. Finally, when the heater is energized, the test coil is heated.

The amount of heat input to the test coil was controlled by fixing the heater power at a constant value and changing its duration. In the test, as shown in the schematic diagram shown in Fig. 4-20, the duration of pulsed heat input was gradually increased, and the amount of heat input for the quench was evaluated. The difference between the maximum and minimum MQE values under the test conditions is 32 μJ as shown in Fig. 4-18(b); therefore, it was necessary to control the amount of heat input with a resolution of at least 32 μJ or less in order to accurately evaluate the amount of heat input for the quench. The amount of heat input was controlled with a resolution of 14 μJ by

keeping the heater power at 0.14 W and controlling its duration in units of 0.1 ms. A pulse generator (NF-WF1944) capable of generating a square wave with a time resolution of 0.1 ms was used as the heater power supply.

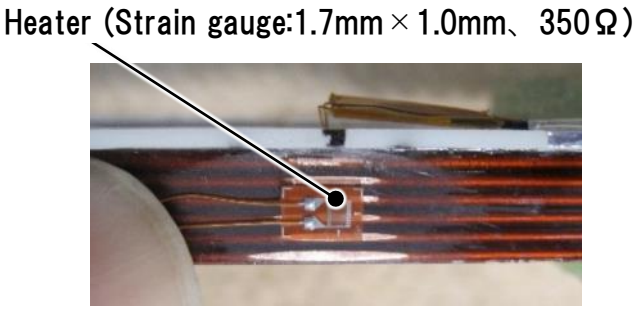

(a)Heater

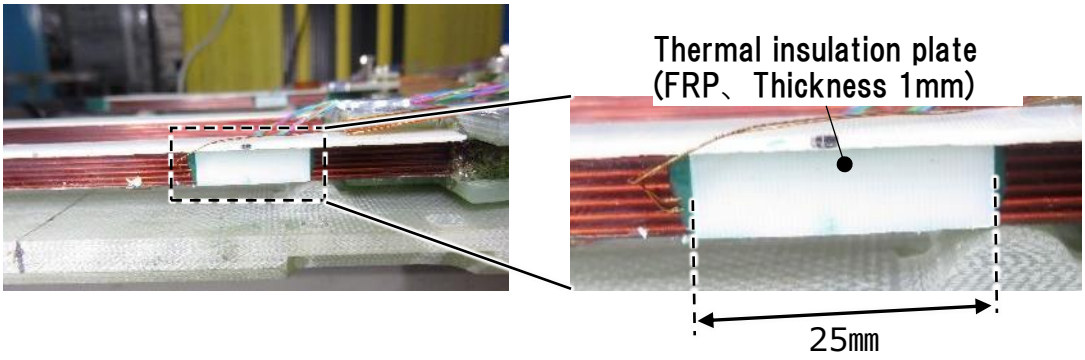

(b)Thermal insulation plate

Fig. 4-18 Installation of the heater. A strain gauge for low temperature (Tokyo Sokki, CF series) was applied as a heater. The resistance value of the applied strain gauge is 350 Ω, and the dimensions are 1.7 mm x 1.0 mm.

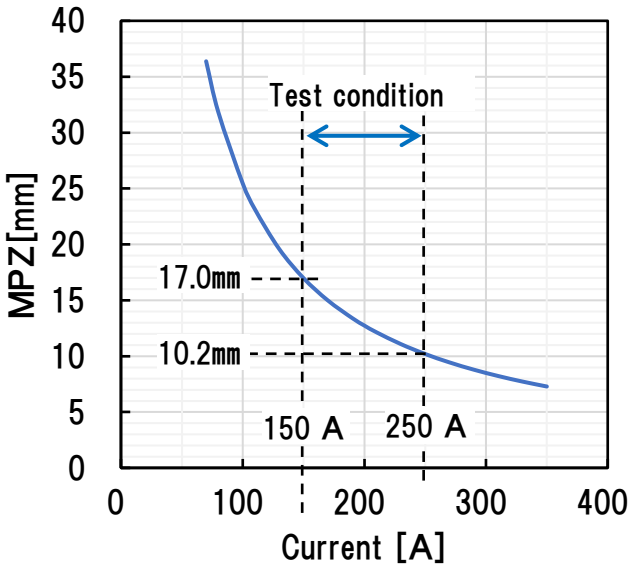

(a)MPZ (Calculated value)

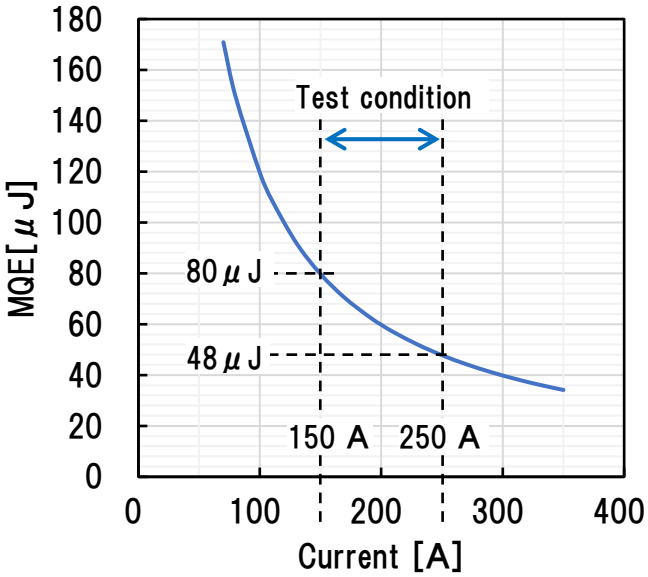

(b)MQE (Calculated value)

Fig. 4-19 Calculated MPZ and MQE under the test condition. Strength of the magnetic field is 5.8 T. MPZ is a calculated normal zone which is longer than this will grow because heat generation exceeds cooling [27]. Assuming an adiabatic state, the amount of heat input required to raise the temperature of the superconducting wire corresponding to the length of MPZ to the critical temperature was calculated as MQE.

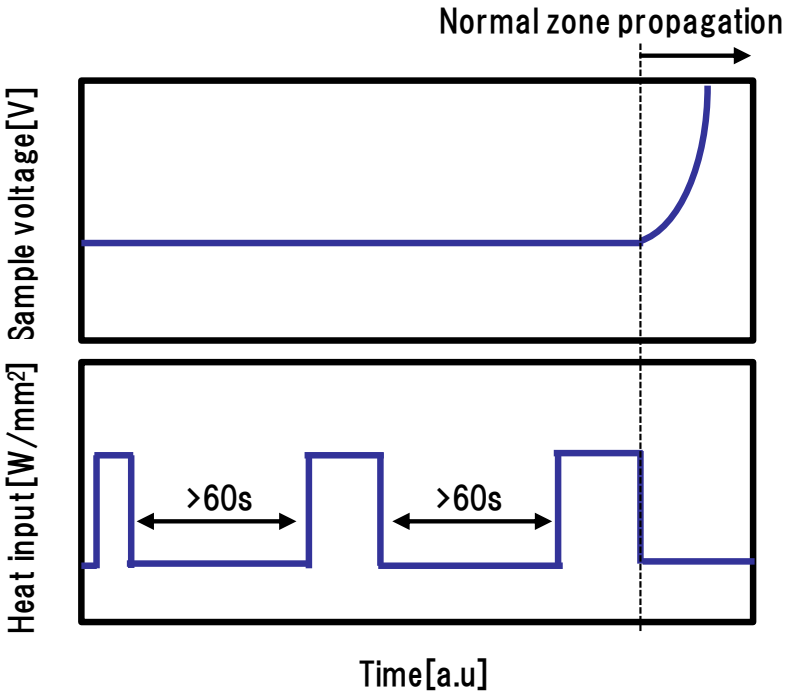

Fig. 4-20 Schematic diagram of the heater quench test. In this test, the amount of heat input was controlled with a resolution of 14 μJ by keeping the heater power at 0.14 W and controlling its duration in units of 0.1 ms.

5. Evaluation Result of The Quench Stability

In this chapter, the results of the heater quench test to evaluate the thermal stability of the superconducting coil with the helium-permeable structure are described. The results of three-point bending test to evaluate mechanical stability of the superconducting coils with the helium-permeable structure are also described.

5.1 Thermal Stability Evaluation by Heater

Table 5-1 shows the test conditions for the heater quench test. The test was performed by changing the energizing current to the test coil to 250 A, 200 A, and 150 A. Under each test condition, the current sharing temperature T_{cs} is 5.4 K, 5.7 K, 6.0 K. When the temperature of the superconducting wire rises to each current sharing temperature or higher by the heat input, the quench of the test coil is induced. The number of samples was 3 for each type of the test coil.

Fig. 5-1 shows typical measurement waveforms during the heater quench test. It is a measurement waveform under the test condition that the test coil with the helium-permeable structure was energized to 200 A in a magnetic field of 5.8 T. As described in Sections 4-4, we controlled the heat input with a resolution of 14 μJ by keeping the heater power at 0.14 W and controlling its duration in units of 0.1 ms. In this example, the superconducting-to-normal transition was not induced until the heat input duration was 79.5 ms. Then, the superconducting-to-normal transition was induced at the heat input duration of 79.6 ms, and a voltage waveform indicating that the normal zone propagation in the test coil was measured. In addition, in all the test coils, the start time of the superconducting-to-normal transition was not during heat input, but after about 3 ms to 10 ms from the end of heat input. Therefore, the amount of heat input seemed to be the minimum value to induce the superconducting-to-normal transition (hereafter referred to as “minimum heater energy for the quench”).

Fig. 5-2 shows the measurement results of minimum heater energy for the quench. All results are averages for three test coils. The standard deviation is indicated by error bars. There were significant differences beyond the error bar between the results of the two types of the test coils. The minimum heater energy for the quench of the test coils with the helium-permeable structure were 5.6 mJ to 22 mJ and about 2.3 to 3.1 times higher than those without the helium-permeable structure.

These results indicated that the helium permeable structure improved the

thermal stability of the superconducting coil. However, the differences of the minimum heater energy for the quench between both types of the test coils tended to decrease when the current of the test coil became larger. That is, the effect of the helium-permeable structure depended on the critical current margin and the current sharing temperature. We discuss the cause of this dependence in Section 6-1.

Table 5-1 Test conditions for the heater quench test

No.	Magnetic field [T]	Current of test coil [A]	Critical current margin [%]	Current sharing temperature T_{cs} [K]	Number of samples	Type of test coil
1	5.8	150	32.0	6.0	3	With the helium-permeable structure
2	5.8	200	42.6	5.7		
3	5.8	250	53.3	5.4		
4	5.8	150	32.0	6.0	3	Without the helium-permeable structure
5	5.8	200	42.6	5.7		
6	5.8	250	53.3	5.4		

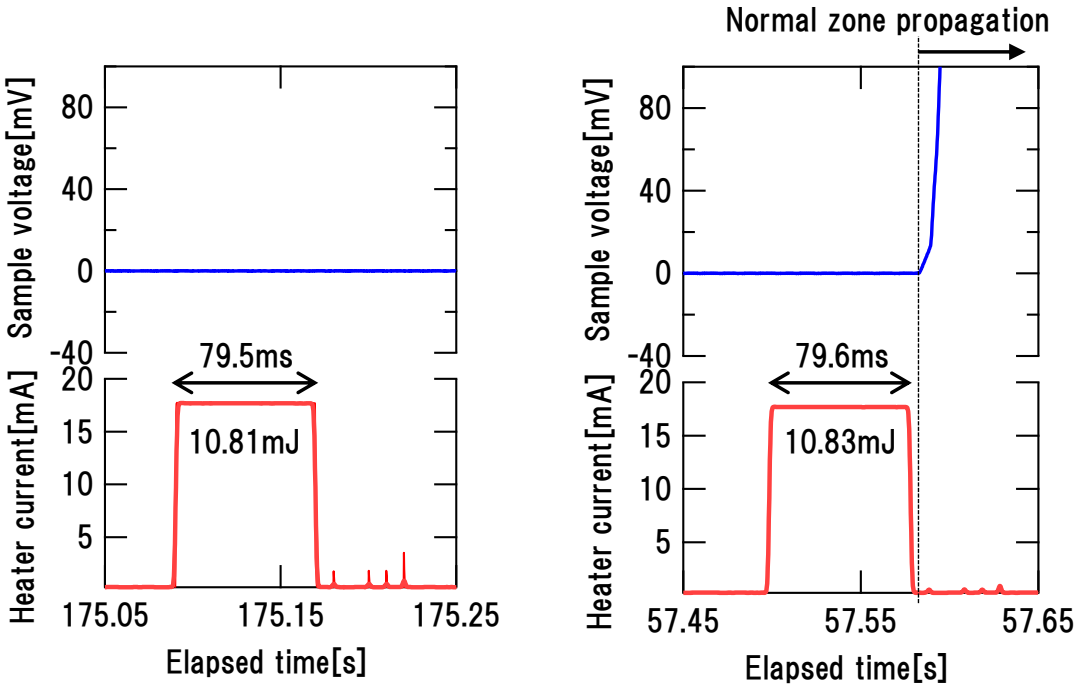

Fig. 5-1 Typical measurement waveforms during the heater quench test. The test coil with the helium-permeable structure was energized at 200 A in a magnetic field of 5.8 T.

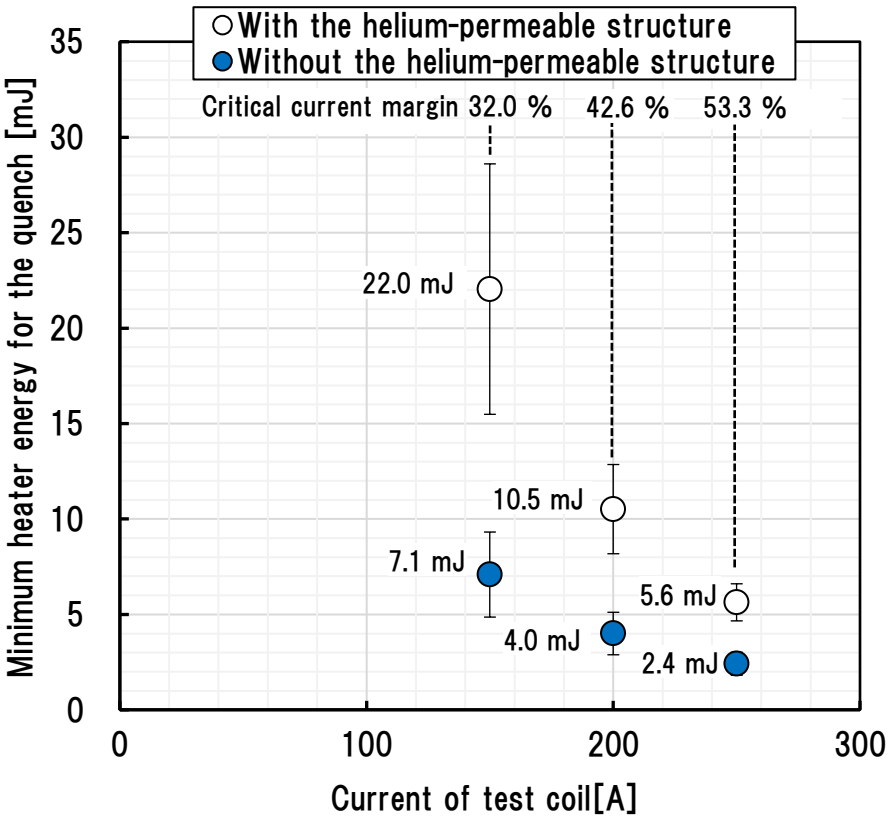

Fig. 5-2 Measurement results of minimum heater energy for the quench. All results are averages for three test coils. The standard deviation is indicated by error bars.

5.2 Mechanical Stability Evaluation by Three-point Bending Test

Table 5-2 shows the test conditions for the three-point bending test. In the previous section, the results show that the effect of the helium-permeable structure depended on the test coil current. Therefore, in the three-point bending test, the quench strains were evaluated while changing the test coil current to 250 A, 150A. Under each test condition, the critical current margin is 53.3 % and 32.0 %. The number of test coils was 3 or 4 for each test condition.

Fig. 5-3 shows a typical measurement waveform of the three-point bending test. It is a measurement waveform under the test condition that the test coil with the helium-permeable structure was energized to 150 A. The bending strain started to increase after the bending-load coil was energized, and the superconducting-to-normal transition occurred when the bending strain reached about 6000 με. Further, as shown in the enlarged display of Fig. 5-3, the voltage spike of the test coil was detected about 20 ms before the coil

voltage increased due to the superconducting-to-normal transition; therefore, mechanical disturbances triggered the coil quenches as intended.

Fig.5-4 shows evaluation results of the quench strains and the quench bending-load. In the case of the test coil current of 250 A as shown in Fig. 5-4 (a), the average quench strain of each test coil was almost the same regardless of the presence or absence of the helium-permeable structure, and they were consistent within the range of the error bar. On the other hand, in the case of the test coil current of 150 A as shown in Fig. 5-4 (b), the average quench strain of the test coil with the helium-permeable structure was about 1.6 times larger than that of the test coil without the helium-permeable structure.

Fig. 5-5 shows current dependence of the quench strains. With regard to the test coil with helium-permeable structure, additional tests were performed at 185 A to evaluate the current dependence in detail. In both test coils, the quench strains tended to increase as the coil current decreased. Then, in the region of 150 A or less (In other words, the critical current margin is 32.0 % or less. The sharing current temperature is 6.0 K or more.), the quench strain of the test coil with the helium-permeable structure increased significantly. On the other hand, there were almost no differences of the quench strains between both types of the test coils when the current of the test coil was 185 A or more.

These results indicate that the helium permeable structure improved not only thermal stability but also mechanical stability. However, the effect of the helium-permeable structure was expected only in the region under 150 A (In other words, the critical current margin is 32.0 % or less. The current sharing temperature is 6.0 K or more). The cause of this is also discussed in Section 6-1.

Table 5-2 Test conditions for three-point bending test

No.	Magnetic field [T]	Current of test coil [A]	Critical current margin [%]	Current sharing temperature T_{cs} [K]	Number of samples	Type of test coil
1	5.8	150	32.0	6.0	4	With the helium-permeable structure
2	5.8	250	53.3	5.4	3	
3	5.8	150	32.0	6.0	4	Without the helium-permeable structure
4	5.8	250	53.3	5.4	3	
5 (Additional)	5.8	185	39.4	5.8	4	With the helium-permeable structure

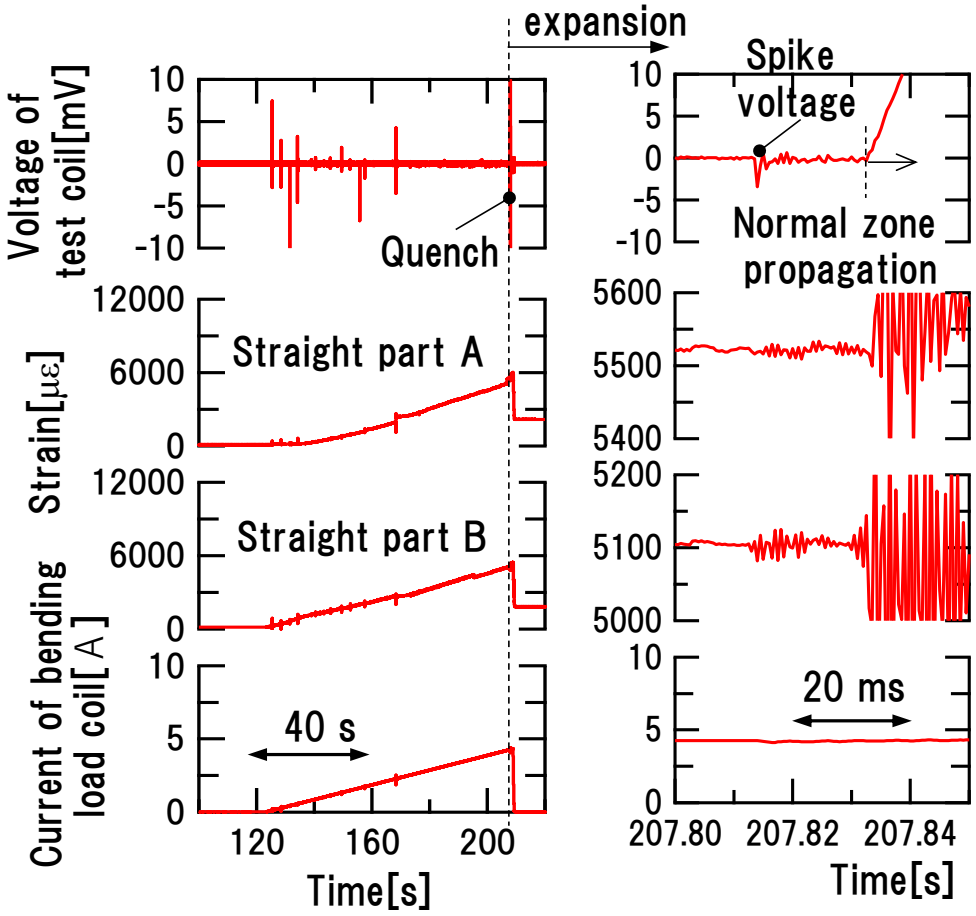

Fig. 5-3 Typical measurement waveform of the three-point bending test. The test coil with the helium-permeable structure was energized at 150 A in the magnetic field of 5.8 T.

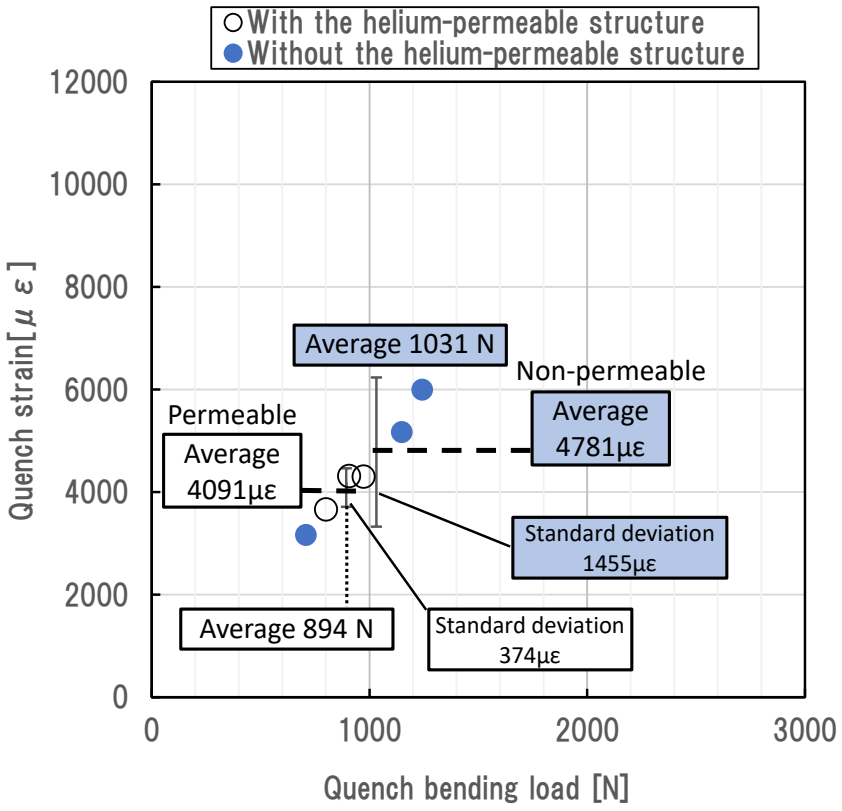

(a) Test coil current 250 A (Critical current margin 53.3 %, T_{cs} 5.4 K)

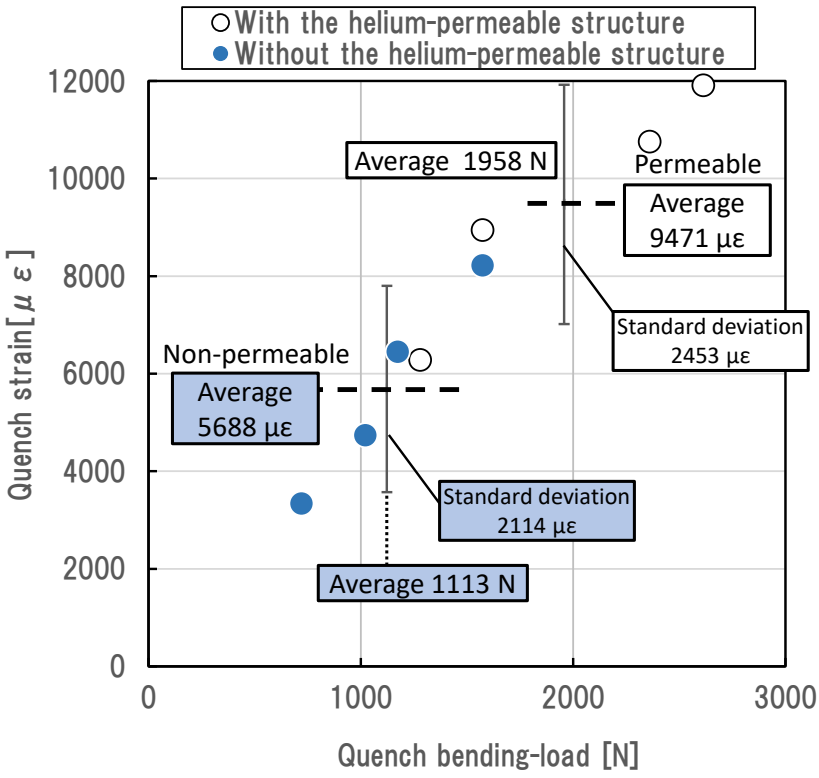

(b) Test coil current 150 A (Critical current margin 32.0 %, T_{cs} 6.0 K)

Fig. 5-4 Evaluation results of the quench strains and the quench bending-load.

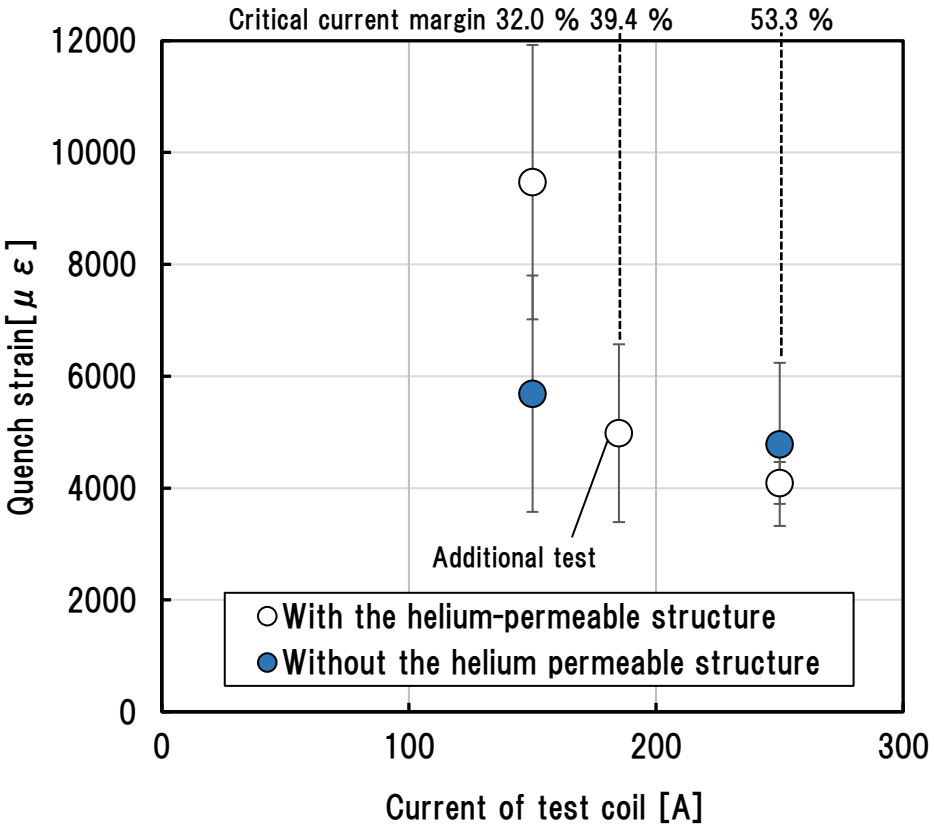

Fig. 5-5 Current dependence of the quench strain. Additional tests were performed at 185 A to evaluate the current dependence in detail. In the region of 150 A or less (The critical current margin is 32.0 % or less. The sharing current temperature is 6.0 K or more.), the quench strain of the test coil with the helium-permeable structure increased significantly.

6. Discussion

In Chapter 5, the helium permeable structure improved not only thermal stability but also mechanical stability. However, the effect of the helium permeable structure is expected only in the region under 150 A (In other words, the critical current margin is 32.0 % or less. The current sharing temperature is 6.0 K or more). In this chapter, such characteristics of the helium-permeable structure is discussed from mechanical and thermal point of view. The design guideline of the superconducting coil with the helium-permeable structure is also discussed.

6.1 Characteristics of Mechanical Disturbance Caused by The Helium-permeable Structure

The results of Section 3-4 indicated that the three-point bending test stand can not only evaluate the quench strains but also can analyze the characteristics of the mechanical disturbance generated in each test coil by analyzing the voltage spike. In this section, we analyze the voltage spike of the three-point bending test in Section 5-2 and discuss the characteristics of mechanical disturbance caused by the presence or absence of the helium-permeable structure.

Fig. 6-1 shows a typical example of the measured waveform during the three-point bending test performed in Section 5-2. In both case, strength of voltage spikes were almost the same, which were within ± 10 mV. The frequency of voltage spikes tended to be slightly lower in the test coil with the helium-permeable structure.

Fig. 6-2 shows the results of frequency analysis of voltage spike at the test coil current 250 A and 150 A. In each case, the detection threshold was ± 0.6 mV, which is about three times the noise level to prevent false detection. The helium-permeable infiltration structure did not significantly increase the frequency of mechanical disturbances in both cases. In the three-point bending test at a current of 150 A shown in Fig.6-6(a), the spike-frequency of the test coil with the helium-permeable structure was 4.7 counts/kN. The spike-frequency of the test coil without the helium-permeable structure was 9.7 counts/kN. The difference between them was only 5.0 counts/kN. In the three-point bending test at a current of 250 A shown in Fig.6-6(b), the spike-frequency of the test coil with the helium-permeable structure was 6.5 counts/kN. The spike-frequency of the test coil without the helium-permeable structure was 9.6 counts/kN. The difference between them

was only 3.1 counts/kN.

The frequency of the voltage spikes, which indicate that mechanical disturbance occurred in the coil winding, were almost the same regardless of the presence or absence of the helium-permeable structure. The presence of the helium-permeable structure did not cause a lot of mechanical disturbance. We consider that this is because the phenoxy resin applied as the self-bonding resin has three times larger fracture toughness than that of the epoxy resin. The higher fracture toughness restrained crack growth in the resin; therefore, the test coils with the helium-permeable structure seemed not to lose the quench stability.

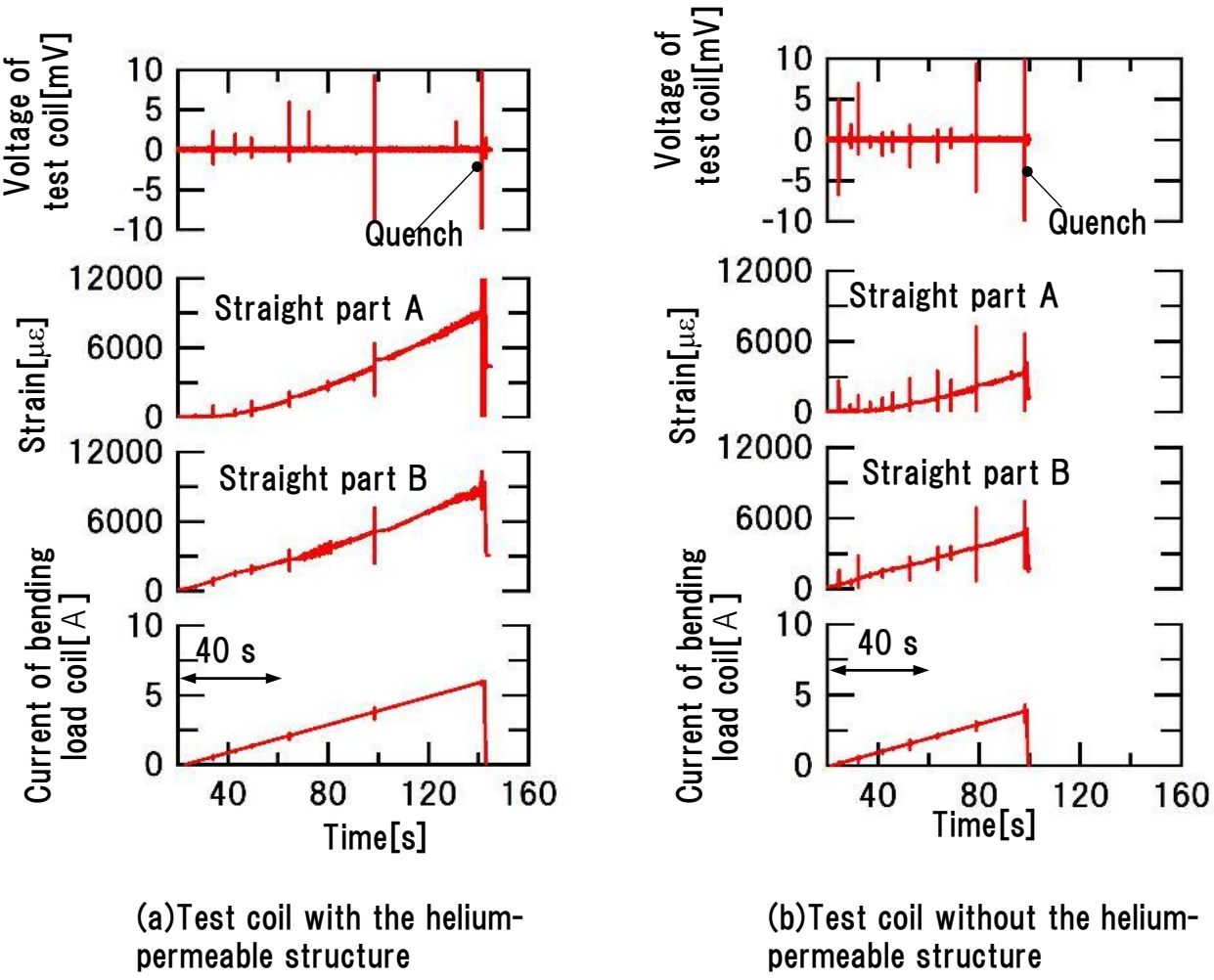

Fig. 6-1 Typical example of the measured waveform during the three-point bending test performed in Section 5-2. The frequency of voltage spikes of the test coil with the helium-permeable structure tended to be slightly lower.

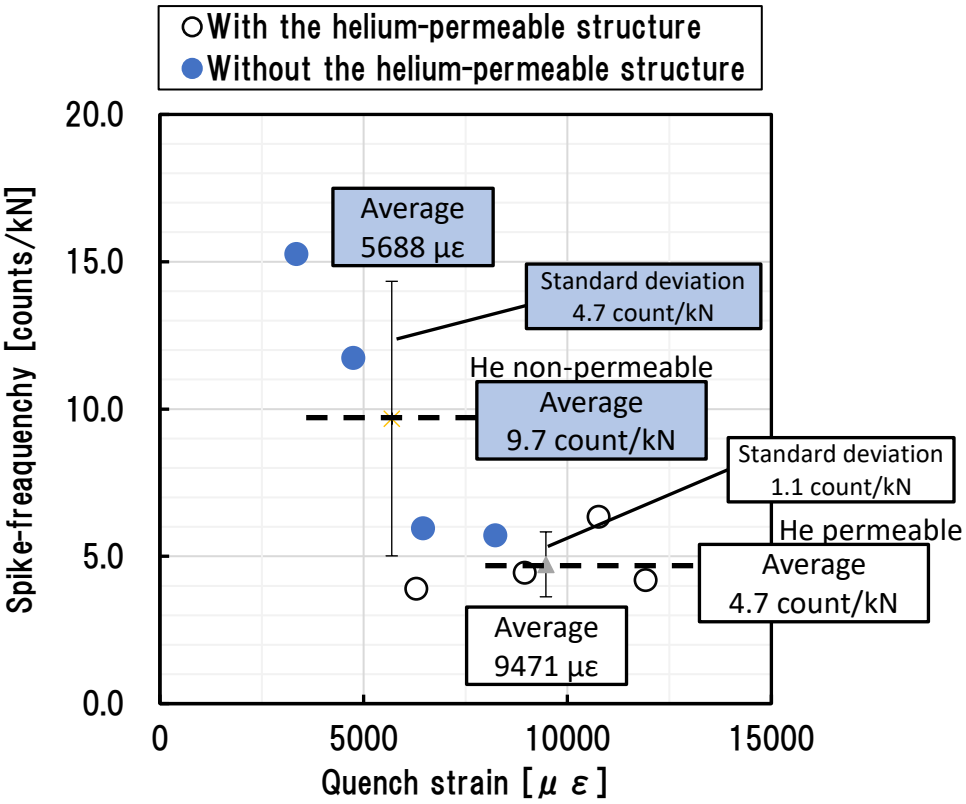

(a) Test coil current 150 A (Critical current margin 32.0 %, T_{cs} 6.0 K)

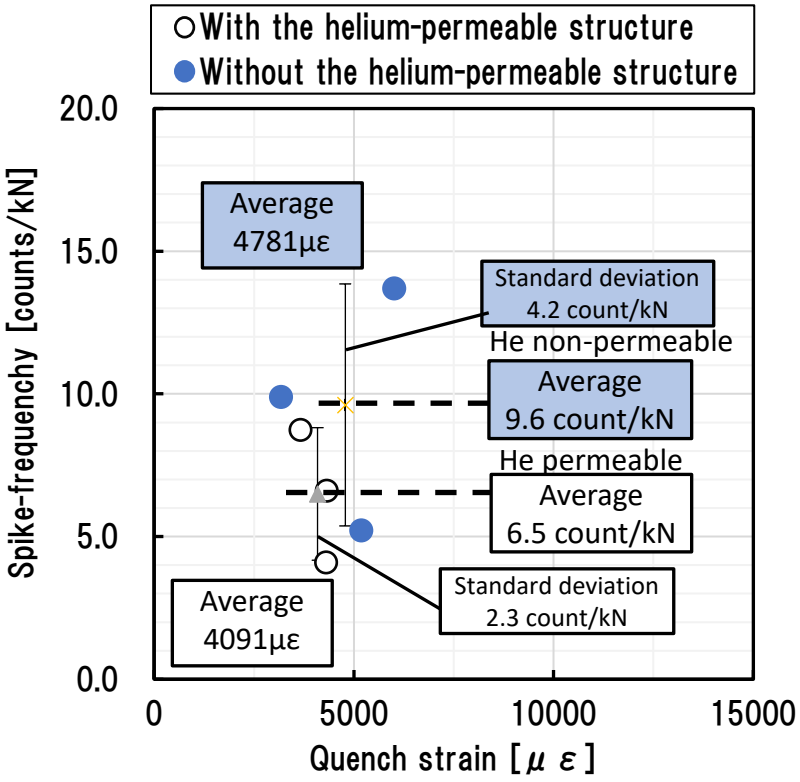

(b) Test coil current 250 A (Critical current margin 53.3 %, T_{cs} 5.4 K)

Fig. 6-2 Results of frequency analysis of voltage spikes. The detection threshold was ± 0.6 mV in each case.

6.2 Cooling Mechanism of the Helium-permeable Structure

The helium permeable structure improved not only thermal stability but also mechanical stability. However, the effect of the helium-permeable structure tended to decrease as the current sharing temperature decreases. In this section, we discuss the cooling mechanism of the helium-permeable structure by using transient thermal analysis.

Fig. 6-3 shows an analysis model used for transient thermal analysis. This is an axisymmetric model simulating a part of the coil winding. Physical properties such as thermal conductivity and specific heat of various members were referred to the literature values [55]. Since there is no physical property value for self-bonding resin, it was substituted with physical properties of the epoxy resin. By switching the physical properties of the area surrounded by three wires, it simulated the presence or absence of helium-permeable structure. To match the cross-sectional observation results of section 4-3, the proportion of the helium permeation structure is 2% of the coil cross-sectional area. Cooling by the helium-permeable structure was simulated by setting the pool boiling heat transfer correlations shown in Fig. 6-4 on the boundary surface of the resin and helium [70]. The heater was simulated by setting the heat source to the surface of the coil winding. The heater power is 0.08 W/mm^2 similar to the heater quench test of 5-1 section. The temperature of outer peripheral surface of the analysis model was fixed at 4.2 K, simulating cooling by the liquid helium.

Fig. 6-5 shows the analysis result of the coil temperature distribution when the heat input continues for 80 ms. This is the same condition as the case where the test coil with the helium-permeable structure (energized to 200 A) is quenched by the heater. The part shown in white in the figure is the helium-permeable structure. If there is a helium-permeable structure, the superconducting wires after the second layer are maintained at almost 4.2 K. It was found that the helium-permeable structure functions as a type of temperature fixed point and improved the quench stability.

Fig. 6-6 shows a change of the maximum temperature in the superconducting wire depending on the heat input. The current sharing temperature under each test condition are displayed as dashed lines on the graph for comparison. The analysis results show that the temperature rise is suppressed by the helium-permeable structure. The upper limit of the temperature rise is 5.9 K, which suggests that quench stability is improved by the effect of the helium-permeable structure under low current conditions where the current sharing temperature is 6.0 K or higher.

On the other hand, in the initial temperature rise up to 5.7 K, the analysis

results show that there is almost no difference regardless of the presence or absence of the helium-permeable structure. These results suggest that the effect of the helium-permeable structure is not expected under the condition of the high critical current margin where the current sharing temperature is 5.7 K or less. In addition, in the measured value of the minimum heater energy in Fig. 5.2, the difference between the presence and absence of the helium-permeable structure is smaller as the critical current margin is higher and the current sharing temperature is lower. These results show that the difference of the actual temperature rise between the presence and absence of the helium-permeable structure was small as well as the analysis results.

Incidentally, we consider that the actual temperature rise is delayed due to the heat propagation in the longitudinal direction of the wire. In order to accurately analyze the effect of the helium-permeable structure, three-dimensional thermal analysis will be required in the future.

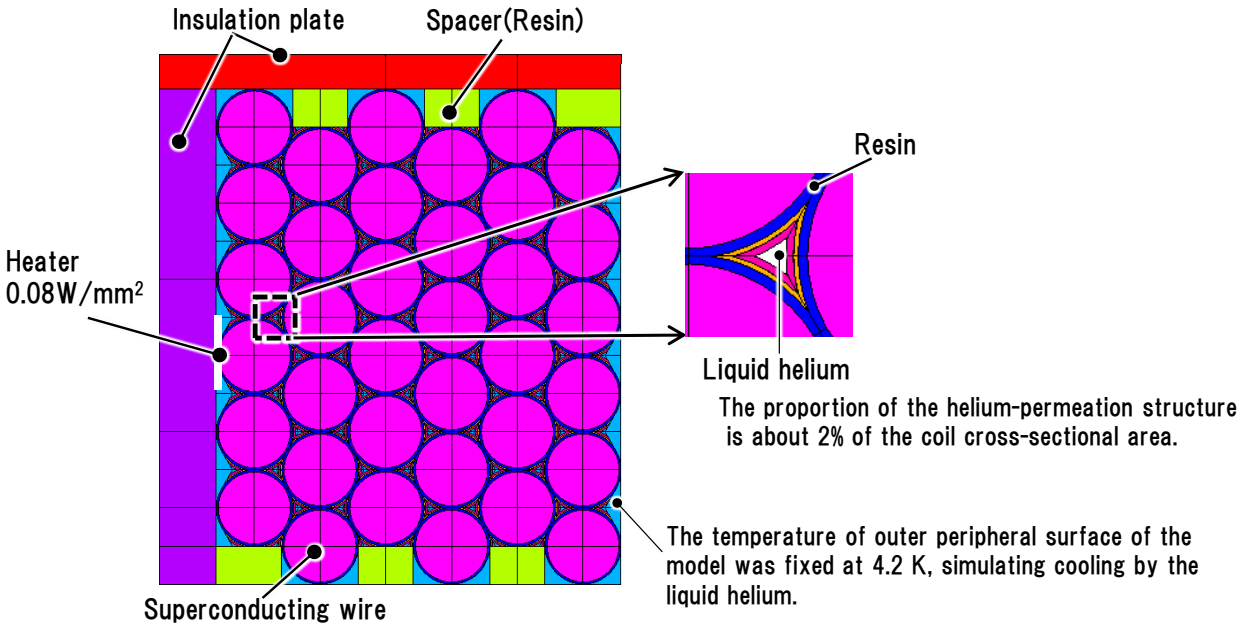

Fig. 6-3 The analysis model used for transient thermal analysis. The axisymmetric model simulates a part of the winding. Physical properties were referred to the literature values [55]. Since there is no physical property value for self-bonding resin, it was substituted with physical properties of the epoxy resin Cooling by the helium-permeable structure was simulated by setting the boiling heat transfer coefficient on the boundary surface of the resin and helium. The heater power is 0.08 W/mm^2 similar to the heater quench test of 5-1 section. The temperature of outer peripheral surface of the analysis model was fixed at 4.2 K, simulating cooling by the liquid helium.

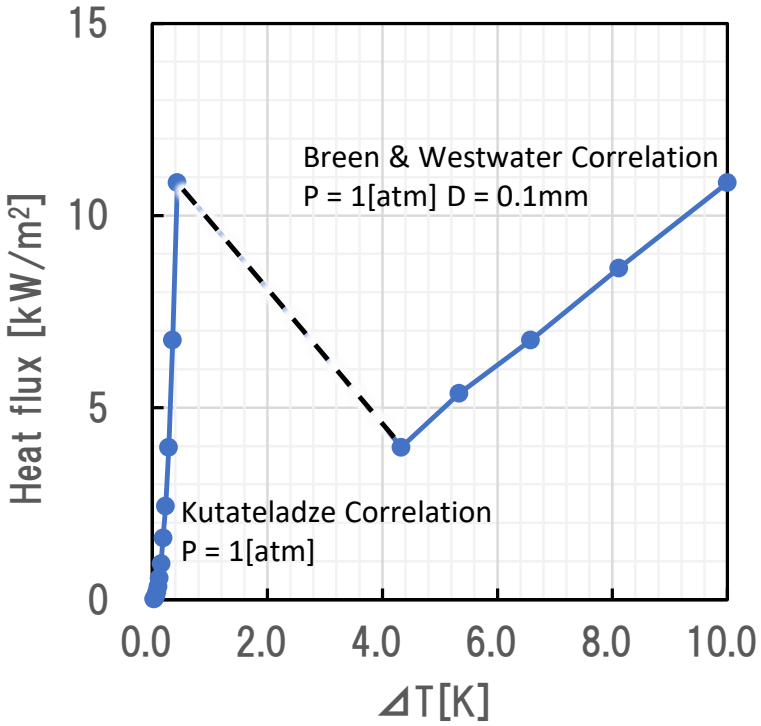

Fig. 6-4 Pool boiling heat transfer correlation for the liquid helium. Cooling by the liquid helium was simulated by setting this correlation on the boundary surface of the resin and helium [70].

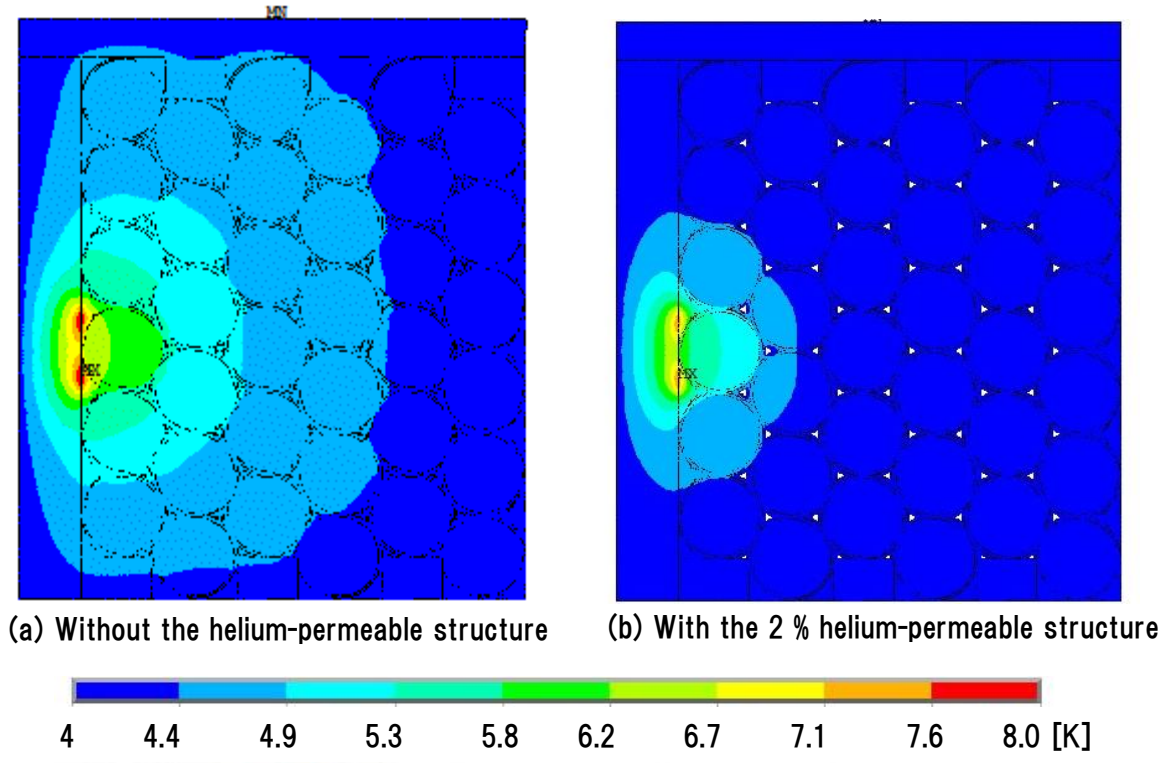

Fig. 6-5 Analysis result of the coil temperature distribution when the heat

input continues for 80 ms. (a)Without the helium-permeable structure. (b)With the helium-permeable structure.

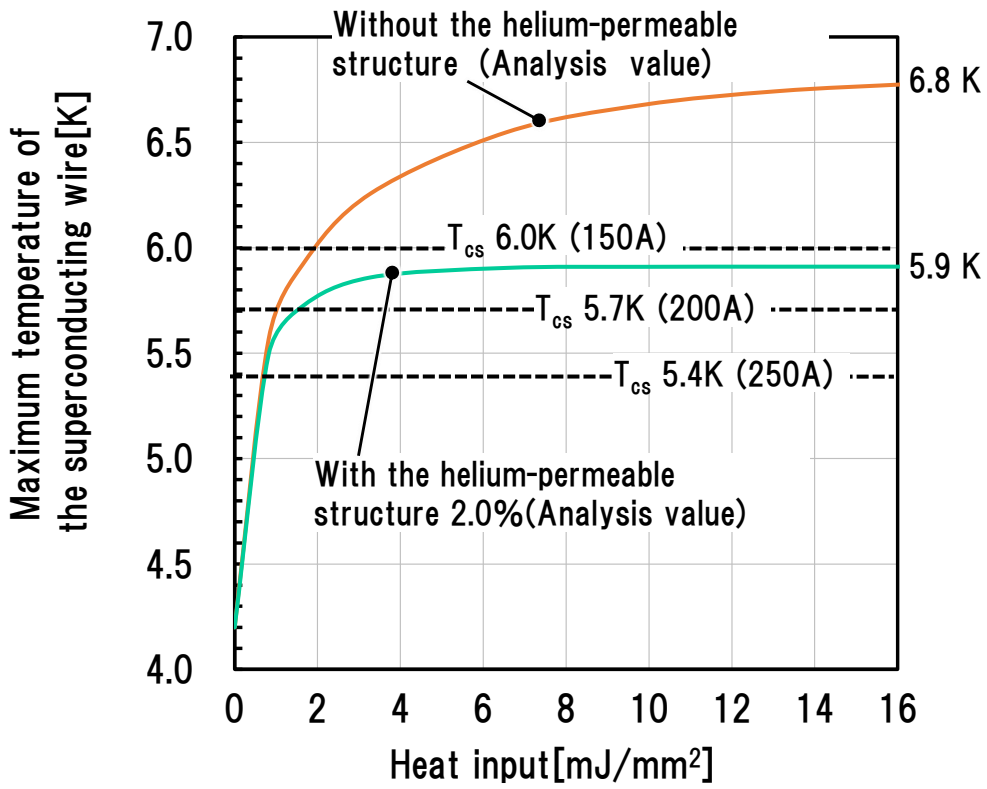

Fig. 6-6 Change of the maximum temperature in the superconducting wire depending on the heat input (Analysis result). The current sharing temperature under each test condition in Section 5-1 are displayed as dashed lines on the graph for comparison.

6.3 Design Guideline for Superconducting Coils with The Helium-permeable Structure

From the above results, we had three design guidelines of the superconducting coil with the helium-permeable structure as follows.

1)Expansion of the helium-permeable structure

Since the mechanical stability was not impaired even if the helium-permeable structure that occupies 2 % of the coil cross-sectional area was applied, expansion of the helium-permeable structure is expected to improve the quench stability.

For example, as shown in Section 4-2, the helium-permeable structure can be expanded to a cross-sectional area ratio of 6% by setting the molding pressure to 0.1 MPa. Then, the transient thermal analysis simulating the heater quench test is performed using the calculation model shown in Fig.6-7, and the effect of the expansion of the helium-permeable structure was calculated. Physical properties were referred to the literature values [50]. Fig. 6-8 shows a change of the maximum temperature in the superconducting wire depending on the heat input. When the helium permeable structure is expanded to a cross-sectional area ratio of 6 %, the upper limit of the temperature rise is reduced to 5.7 K equivalent to T_{cs} at the test coil current of 200 A as shown in Fig.6-8(a). Moreover, even in the initial temperature rise of 5.7K or less, the temperature suppression is about doubled as shown in Fig.6-8(b). By expanding the helium-permeable structure, it is possible to suppress the temperature rise of the superconducting wire, and further improvement of the quenching stability is expected.

Furthermore, past studies of the magnet for LHC revealed that MQE depends on the cooling perimeter of the superconducting wire [71,72]. As shown in Fig. 6-9, when the helium-permeable structure is expanded to a cross-sectional area ratio of 6 %, the cooling perimeter is expanded from 22 % to 47 %; therefore, further improvement of the quench stability is expected. It is a future task to manufacture a test coil with an expanded helium permeable structure and verify the improvement of quench stability.

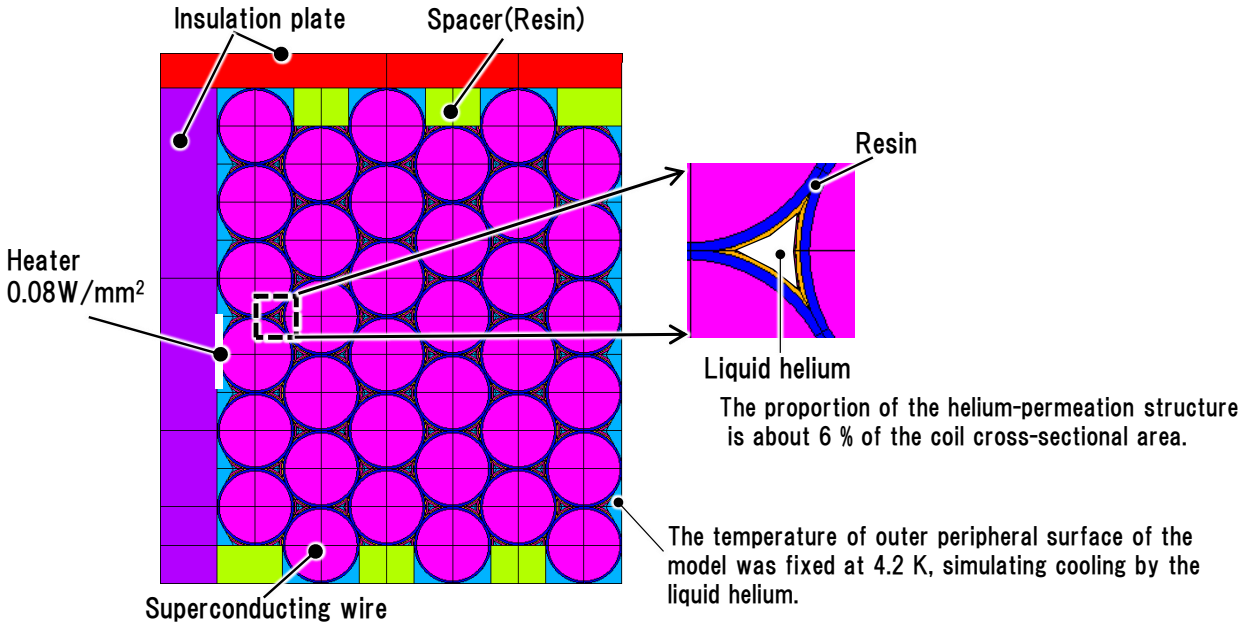

Fig. 6-7 Transient thermal analysis model when the helium-permeable structure is expanded to a cross-sectional area ratio of 6 %.

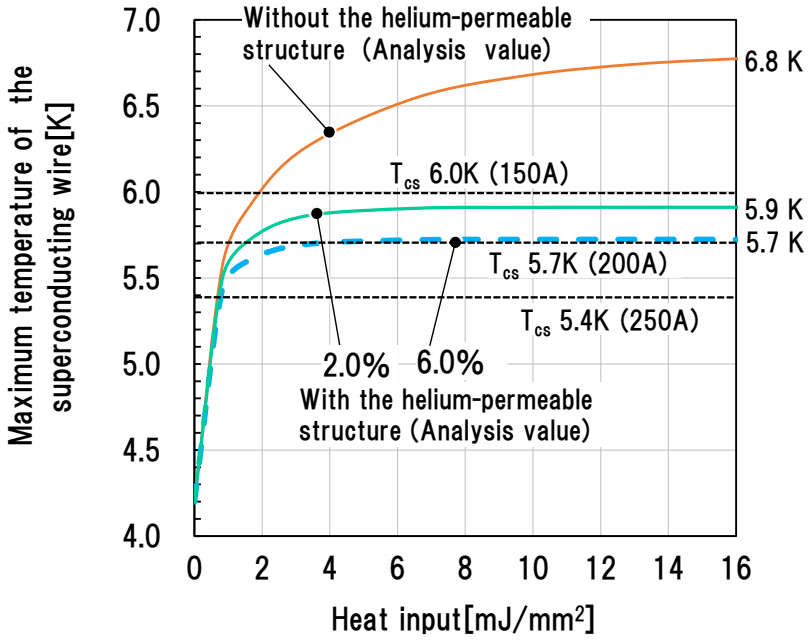

(a) the upper limit of the temperature rise

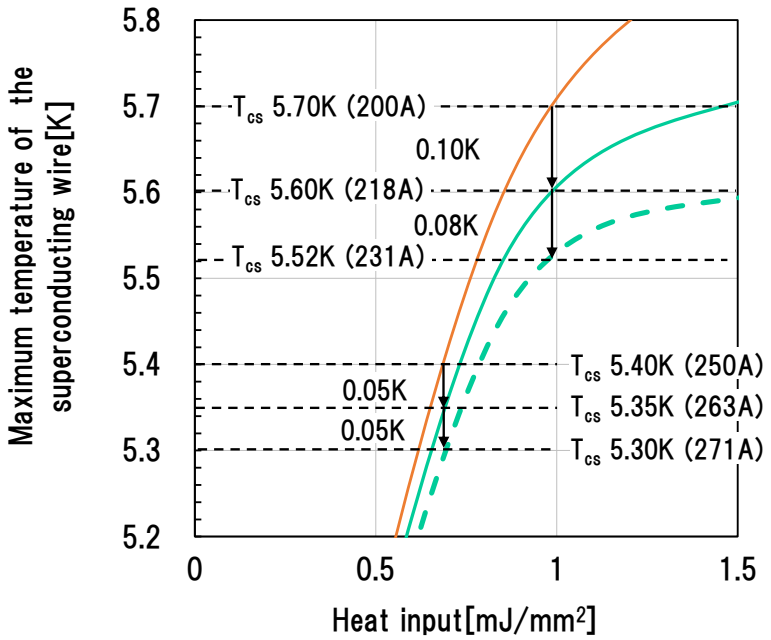

(b) initial temperature rise of 5.7K or less

Fig. 6-8 Change of the maximum temperature in the superconducting wire depending on the heat input (Analysis result). When the helium infiltration structure is expanded to a cross-sectional area ratio of 6 %, the upper limit of the temperature rise is reduced to 5.7 K.

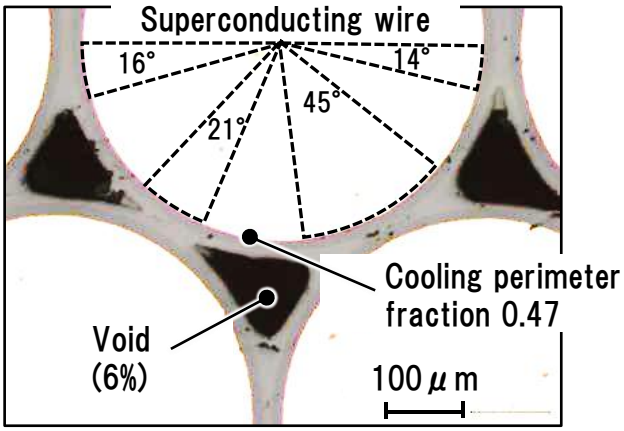

(a) Molding pressure 0.1MPa

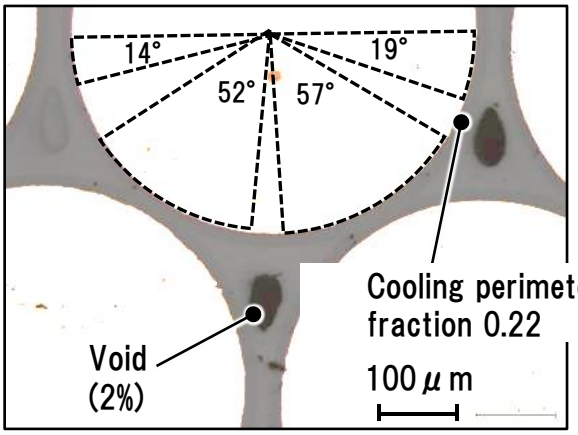

(b) Molding pressure 0.7MPa

Fig. 6-9 Comparison of cooling perimeter of the self-bonded coil. When the helium-permeable structure is expanded to a cross-sectional area ratio of 6%, the cooling perimeter is expanded from 22% to 47%; therefore, further improvement of the quench stability is expected.

2)Reduction of the number of the training quenches

From the results of the three-point bending test in Section 5-2, it was found that the quench stability was improved under the condition of the critical current margin of 32.0 % or less. These results suggested that the quench stability in the region of low critical current margin could be increased, and the number of training quenches could be reduced without expanding the helium-permeable structure. Fig.6-10 shows example of load lines of superconducting coils using the superconducting wire applied to the test coils in Chapter 4. If the rated current is designed to be 150 A as in coil designed II, the critical current margin is 32 % or less, and the effect of the helium-permeable structure can be expected in the entire excitation process. However, if the rated current is set low, a long superconducting wire is required to manufacture the coil, and the manufacturing cost increases. In the other hand, if the rated current is designed to be 250 A as in coil design I, the superconducting wire required for coil production can be shortened and manufacturing cost can be reduced, but the critical current margin increases to 53.3 %. However, from a different point of view, the critical current margin is 32 % or less up to the current of 195 A, which accounts for about 80 % of the excitation process, and the effect of helium-permeable structure can be expected. Therefore, it means that the number of training quenches can be reduced without expanding the helium-permeable structure in the current region of 195 A or less.

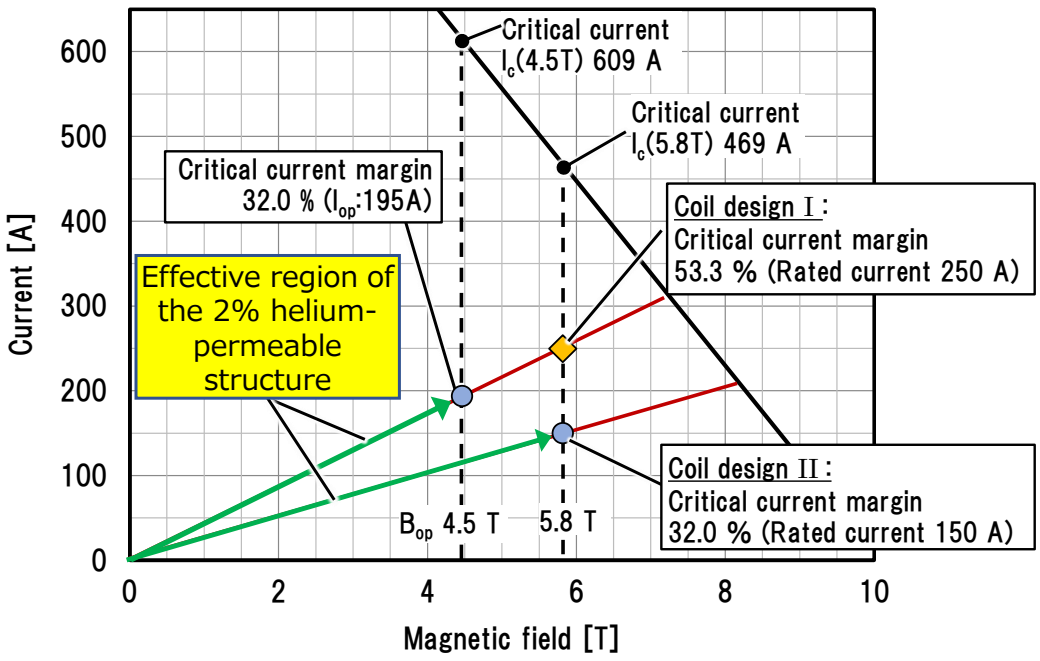

Fig. 6-10 Example of load lines of the magnet using the superconducting wire applied to the test coils. From the results of the three-point bending test in Section 5-2, it was found that the quench stability was improved under the condition of the critical current margin of 32.0 % or less. Even if the superconducting coil is designed with a rated current of 250 A and the critical current margin of 53.3 %, the critical current margin is 32.0 % at the coil current of 195 A. The number of training quenches in the region of low critical current margin can be reduced without expanding the helium-permeable structure.

3) Reinforcement of electromagnetic force support

The Young's modulus of the self-bonded coil tended to be lower than that of the prepreg- coil. If the Young's modulus is low, the amount of deformation of the coil winding will be large, so it may not be possible to generate a magnetic field with the desired accuracy with an MRI magnet or accelerator magnet that requires a precise magnetic field accuracy of several ppm to several hundred ppm. Therefore, when a self-bonded coil is applied, it is necessary to reinforce a support structure of the coils in order to suppress the deformation of the coil winding.

7. Conclusion

The coil windings using the monolithic superconducting wires can not have cooling channels due to structural constraints, but the superconducting coil molded with the self-bonded molding method can include voids which function as cooling channels in the coil winding ("Helium-permeable structure"). However, the larger helium-permeable structures could make the coil windings fragile and could lose the mechanical stability of superconducting coils. Therefore, we evaluated the quench stability of the helium-permeable structure in terms of both mechanical and thermal stability. Then, we clarified the design guideline for the superconducting coil with the helium-permeable structure. The results are as follows.

＜Development of the three-point bending test stand＞

In order to evaluating the effect of the helium-permeable structure in terms of both mechanical stability and thermal stability, we developed the three-point bending test stand working at a cryogenic temperature of 4.2 K within a magnet field. We obtained the following results in the verification test of the three-point bending test stand.

1) The three-point bending test stand operated correctly at the cryogenic temperature of 4.2 K within a magnetic field. The magnetic field could be generated at the position of the test coil as designed. The bending-load could be applied by the three-point bending test stand as designed.

2) The racetrack-shaped test coils were quenched by the three-point bending test. The three-point bending test stand could evaluate the mechanical stability of the superconducting coil with the reproducibility for multiple samples.

3) The average quench strain of the self-bonded molding coils was about 2.5 times higher than the prepreg molding coils. The voltage spike frequency, which indicate that mechanical disturbance occurred in the coil winding, were higher in the prepreg molding coil and were about 20 times that of the self-bonded molding coil. Therefore, we considered the self-bonded molding method is suitable as the molding method for the superconducting coil with the helium-permeable structure.

＜Evaluation of the quench stability of the helium-permeable structure＞

In order to evaluate the effect of the helium-permeable structure on the quench stability, we made the two types of test coils: (a)test coil with the helium-permeable structure and (b)test coil without the helium-permeable structure. Then, we compared the quench strains and the minimum heater energy for the quench between them. The test coils were energized from 150 A to 250 A in the magnetic field of 5.8 T, and the critical current margin was from 32.0 % to 53.3 %. Since the critical current margin of superconducting coils using commercially available superconducting wires is designed to be 55% or less to ensure sufficient quench stability [36], the three-point bending test to evaluate the effect of the helium-permeable structure can be performed under practical load condition. We obtained the following results.

1)The minimum heater energy for the quench of the test coils with the helium-permeable structure were about 2.3 to 3.1 times higher than those without the helium-permeable structure. These results indicated that the helium permeable structure improved the thermal stability of the superconducting coil. However, the differences of the minimum heater energy for the quench between both types of the test coils tended to decrease when the current of the test coil became larger, and the current sharing temperature became smaller.

2)The quench strains of the test coils with the helium-permeable structure were about 1.6 times larger compared to the test coils without the helium-permeable structure when the current of the test coils was 150 A (the critical current margin 32.0 %). On the other hand, there were almost no differences of the quench strains between both types of the test coils when the current of the test coil was 185 A or more (the critical current margin 39.4 % or more). Although the quench strains depended on the critical current margin, the helium permeable structure had the effect to improve the mechanical stability of the superconducting coils.

3)The cooling mechanism of helium-permeable structure was investigated by a transient thermal analysis of the coil windings. It was found that the helium-permeable structure functions as a type of temperature fixed point and enhances thermal stability. However, it was also found that there is almost no difference in the initial temperature rise from 4.2 K to 5.7 K regardless of the presence or absence of the helium-permeable structure. In other words, the effect of the helium-permeable structure is not expected under the condition of the high critical current margin where the current

sharing temperature is 5.7 K or less.

＜The design guidelines for the superconducting coils with a helium-permeable structure＞

From the above results, we had three design guidelines of the superconducting coil with the helium-permeable structure as follows.

1)Expansion of the helium-permeable structure is expected to improve the quench stability since the mechanical stability was not impaired even if the helium-permeable structure that occupies 2 % of the coil cross-sectional area was applied. Furthermore, past studies revealed that MQE (Minimum Quench Energy) depends on the cooling perimeter of the superconducting wire. For example, in the test coil of this thesis, when the helium-permeable structure is expanded to a cross-sectional area ratio of 6 %, the c cooling perimeter is expanded from 22 % to 47 %, and further improvement of the quench stability is expected.

2) The number of training quenches can be reduced under the condition of low critical current margin without expanding the helium permeation structure, since the quench stability was improved under the critical current margin of 32.0 % or less in the three-point bending test.

3) The Young's modulus of the self-bonded coil tended to be lower than that of the prepreg- coil. Therefore, when a self-bonded coil is applied, it is necessary to reinforce a support structure according to the magnitude of the electromagnetic force in order to suppress the deformation of the coil winding.

8. Bibliography

[1] M. Fujita, "The coil design of the superconducting MRI magnet," in *IEEE Transactions on Magnetics*, vol. 24, no. 6, pp. 2907-2909, Nov. 1988, doi: 10.1109/20.92284

[2] Q. Wang *et al.*, "High Magnetic Field Superconducting Magnet for 400 MHz Nuclear Magnetic Resonance Spectrometer," in *IEEE Transactions on Applied Superconductivity*, vol. 21, no. 3, pp. 2072-2075, June 2011, doi: 10.1109/TASC.2010.2090854.

[3] M. A. Green and E. Willen, "Superconducting dipoles and quadrupoles for a 2 TeV muon collider," in *IEEE Transactions on Applied Superconductivity*, vol. 7, no. 2, pp. 743-746, June 1997, doi: 10.1109/77.614610.

[4] Y. Iwata,* K. Noda,et al., "Design of a superconducting rotating gantry for heavy-ion therapy", in PHYSICAL REVIEW SPECIAL TOPICS - ACCELERATORS AND BEAMS 15, 044701 (2012)

[5] K. Sawada, "Outlook of the Superconducting Maglev," in *Proceedings of the IEEE*, vol. 97, no. 11, pp. 1881-1885, Nov. 2009, doi: 10.1109/JPROC.2009.2030246.

[6] Wada H and Ikehira H 2007 *J. Cryo. Soc. Jpn* 42 180

[7] Tachikawa K 2004 *J. Cryog. Soc. Japan* 39 377

[8] 小林慎一・中島隆芳・山崎浩平・佐藤謙一：「高温超電導材料Ⅲ—ビスマス系酸化物高温超電導線—」, 低温工学, Vol. 47, No. 7, pp. 422-429 (2012)

[9] T. Kiyoshi *et al.*, "Bi-2223 Innermost Coil for 1.03 GHz NMR Magnet," in *IEEE Transactions on Applied Superconductivity*, vol. 21, no. 3, pp. 2110-2113, June 2011, doi: 10.1109/TASC.2010.2082475.

[10] R. Heller *et al.*, "Electrical, Mechanical and Thermal Characterization of Bi-2223/AgAu Material for Use in HTS Current Leads for W7-X," in *IEEE Transactions on Applied Superconductivity*, vol. 18, no. 2, pp. 1443-1446, June 2008, doi: 10.1109/TASC.2008.920567.

[11] J. Bascuñán, P. Michael, S. Hahn, T. Lecrevisse and Y. Iwasa, "Construction and Test Results of Coil 2 of a Three-Coil 800-MHz REBCO Insert for the 1.3-GHz High-Resolution NMR Magnet," in *IEEE Transactions on Applied Superconductivity*, vol. 27, no. 4, pp. 1-4, June 2017, Art no. 4300504, doi: 10.1109/TASC.2016.2641341.A

[12] Y. Shiohara, K. Nakaoka, T. Izumi and T. Kato: J. Japan Inst. Met. Mater. **80**(2016) 406-419.

[13] H. Tanaka, T. Suzuki, M. Kodama, Y. Ichiki, T. Haba and K. Okamoto, "Tensile and Bending Stress Tolerance on Round MgB2 Wire Made By In Situ PIT Process," in *IEEE Transactions on Applied Superconductivity*, vol. 28, no. 4, pp. 1-5, June 2018, Art no. 8400605, doi: 10.1109/TASC.2018.2797978.A

[14] C. E. Bruzek *et al.*, "Cable Conductor Design for the High-Power MgB2 DC Superconducting Cable Project of BEST PATHS," in *IEEE Transactions on Applied Superconductivity*, vol. 27, no. 4, pp. 1-5, June 2017, Art no. 4801405, doi: 10.1109/TASC.2016.2641338.A

[15] H. S. Kim *et al.*, "Demonstration of a Conduction Cooled React and Wind MgB2 Coil Segment for MRI Applications," in *IEEE Transactions on Applied Superconductivity*, vol. 26, no. 4, pp. 1-5, June 2016, Art no. 4400305, doi: 10.1109/TASC.2015.2514063.

[16] Manabu Aoki et al.," Development of fast on/off MgB_2 magnet", AP2-5-INV, abstract of The 33rd International Symposium on Superconductivity
[17] K. Tachikawa："Metallic superconductors [3]", TEION KOGAKU **45** (2010) 88-98 (in Japanese)
[18] Hideshige Moriyama,et al., "Examinations on Impregnating Epoxy Resins Used for Superconducting Coils" T. IEE Japan, Vol. 111-B, No. 9,'91
[19] V. E. Keilin *et al.*, "Considerable stability increase in superconducting windings doped with extremely high specific heat substances," in *IEEE Transactions on Applied Superconductivity*, vol. 15, no. 2, pp. 1629-1632, June 2005, doi: 10.1109/TASC.2005.849211. A
[20] S. Chouhan *et al.*, "The Superconducting Horizontal Bend Magnet for the Jefferson Lab's 11 GeV/c Super High Momentum Spectrometer," in *IEEE Transactions on Applied Superconductivity*, vol. 20, no. 3, pp. 226-229, June 2010, doi: 10.1109/TASC.2009.2038715. A
[21] Hitoshi Takahashi ,et al., "DEVELOPMENT OF NEW RADIATION-RESISTANT MAGNETS USING CYANATE ESTER RESIN", Proceedings of the 17th Annual Meeting of Particle Accelerator Society of Japan
[22] Moriyama H., Mitsui H., Ohmori J., Murai S., Nishijima S., Okada T. (1996) Mechanical and Thermal Properties of Self-Bonded Superconducting Winding. In: Kittel P. (eds) Advances in Cryogenic Engineering. A Cryogenic Engineering Conference Publication, vol 41. Springer, Boston, MA. https://doi.org/10.1007/978-1-4613-0373-2_61
[23] A. F. Lietzke *et al.*, "Quench antenna and fast-motion investigations during training of a 7 T dipole," in *IEEE Transactions on Applied Superconductivity*, vol. 5, no. 2, pp. 1012-1015, June 1995, doi: 10.1109/77.402722.
[24] JIMGA,ヘリウム生産・販売実績 5 年推移
https://www.jimga.or.jp/files/page/statistics/regularly/TRU_he_2015-19.pdf
[25] APS Helium Report;
https://www.aps.org/policy/reports/popa-reports/helium-crisis.cfm
[26] L. Dresner, "Quench energies of potted magnets," in *IEEE Transactions on Magnetics*, vol. 21, no. 2, pp. 392-395, March 1985, doi: 10.1109/TMAG.1985.1063724.
[27] M. V. Wilson "Superconducting Magnets", Monographs on Cryogenics, Clarendon Press, Oxford (1983) p. 76.
[28] K. Seo, M. Morita, S. Nakamura, T. Yamada and Y. Jizo, "Minimum quench energy measurement for superconducting wires," in *IEEE Transactions on Magnetics*, vol. 32, no. 4, pp. 3089-3093, July 1996, doi: 10.1109/20.511529.
[29] M. Breschi *et al.*, "Minimum Quench Energy and Early Quench Development in NbTi Superconducting Strands," in *IEEE Transactions on Applied Superconductivity*, vol. 17, no. 2, pp. 2702-2705, June 2007, doi: 10.1109/TASC.2007.898373.
[30] Kimio Yamada, Manabu Aoki, Yuji Matsui,Measurement of minimum quench energy in a superconducting winding using a YAG laser,Cryogenics,Volume 48, Issues 11–12,2008,Pages 518-520,ISSN 0011-2275,https://doi.org/10.1016/j.cryogenics.2008.08.001.
[31] M.I. Yunus, Y. Iwasa, J.E.C. Williams,A.c. loss induced quenching in multicoil adiabatic superconducting magnets,Cryogenics,Volume 35, Issue 2,1995,Pages 93-100,ISSN 0011-2275,

[32] E.S.Bobrov,J.E.C.Williams,andY.Iwasa:[Experimental and theoretical investigation of mechanical disturbances in epoxy-impregnated superconducting coil.2.Shear-stress-induced epoxy fracture as the principal source of premature quenches and training-theoretical analysis],Cryogenics 1985 vol25
[33] Y,Iwasa,"Case studies in superconducting magnets : design and operational issues Second edition", pp. 128
[34] Stephen Myers, Herwig Schopper, (2020) "Particle Physics Reference Library Volume 3: Accelerators and Colliders",pp.359, Springer, https://doi.org/10.1007/978-3-030-34245-6
[35] Zlobin A.V., Schoerling D. (2019) "Superconducting Magnets for Accelerators. In: Schoerling D., Zlobin A. (eds) Nb3Sn Accelerator Magnets. Particle Acceleration and Detection", pp.10,Springer, Cham. https://doi.org/10.1007/978-3-030-16118-7_1
[36] T. Satow, "Optimum conditions of stabilizer ratio and critical current margin for maximizing the current density of a tightly-wound superconducting magnet," in IEEE Transactions on Applied Superconductivity, vol. 3, no. 1, pp. 539-542, March 1993, doi: 10.1109/77.233761.
[37] A.Yamamoto," Superconducting Magnets for ILC Detectors" ,the 9th ACFA ILC Physics & Detector Workshop & ILC GDE Meeting,2007
[38] E. Todesco and P. Ferracin, "Limits to High Field Magnets for Particle Accelerators," in IEEE Transactions on Applied Superconductivity, vol. 22, no. 3, pp. 4003106-4003106, June 2012, Art no. 4003106, doi: 10.1109/TASC.2011.2181143.
[39] R. Herzog, M. Lewandowska, M. Bagnasco, M. Calvi, C. Marinucci and P. Bruzzone, "Helium Flow and Temperature Distribution in a Heated Dual-Channel CICC Sample for ITER," in *IEEE Transactions on Applied Superconductivity*, vol. 19, no. 3, pp. 1488-1491, June 2009, doi: 10.1109/TASC.2009.2018751.
[40] N. Kimura, A. Yamamoto, T. Shintomi, A. Terashima, V. Kovachev and M. Murakami, "Heat transfer characteristics of Rutherford-type superconducting cables in pressurized He II," in *IEEE Transactions on Applied Superconductivity*, vol. 9, no. 2, pp. 1097-1100, June 1999, doi: 10.1109/77.783489. P. F. Dahl *et al.*, "Superconducting Magnet Models for Isabelle," in *IEEE Transactions on Nuclear Science*, vol. 20, no. 3, pp. 688-692, June 1973, doi: 10.1109/TNS.1973.4327216.
[41] N. Banno and N. Amemiya, "Numerical analysis of AC loss in high T/sub c/ twisted tape carrying AC transport current in external AC magnetic field. Effect of twisting on loss reduction," in *IEEE Transactions on Applied Superconductivity*, vol. 9, no. 2, pp. 2561-2564, June 1999, doi: 10.1109/77.785009.
[42] H. Kasahara *et al.*, "Development of 100 kVA AC superconducting coil using NbTi cables with a CuSi alloy matrix," in *IEEE Transactions on Magnetics*, vol. 32, no. 4, pp. 2751-2755, July 1996, doi: 10.1109/20.511444. A
[43] A. Ishiyama, S. B. Kim and T. Takahashi, "Permissible disturbance energies in filled and unfilled high-performance superconducting magnets," in *IEEE Transactions on Magnetics*, vol. 30, no. 4, pp. 2483-2486, July 1994, doi: 10.1109/20.305781. A

[44] 宇佐美三郎，江島英博，鈴木隆之，浅野克彦：「エポキシ樹脂の低温における微小欠陥強度とクリープ変形」，低温工学 34 (1999) 105-116
[45] Green M.A., Coyle D.E., Miller P.B., Wenzel W.F. (1979) Vacuum Impregnation with Epoxy of Large Superconducting Magnet Structures. In: Clark A.F., Reed R.P., Hartwig G. (eds) Nonmetallic Materials and Composites at Low Temperatures. Cryogenic Materials Series. Springer, Boston, MA. https://doi.org/10.1007/978-1-4615-7522-1_28
[46] S. Nishijima, et al, "Study of Disturbances in Superconducting Magnets by Acoustic Emission Method", *IEEE Trans. Magn.*, vol. 21, no. 2, pp. 388–391, Mar. 1985.
[47] T. Takao and O. Tsukamoto, "Stability against the frictional motion of conductor in superconducting windings," in *IEEE Transactions on Magnetics*, vol. 27, no. 2, pp. 2147-2150, March 1991, doi: 10.1109/20.133637.
[48] M. Aoki, K. Yamada, Y. Matsui, T. Nakayama and M. Abe: "Measurement of sudden displacements in superconducting coils using search-coils", TEION KOGAKU **44** (2009) 427-432 (in Japanese)
[49] R. Ando, M. Aoki, T. Seki, K. Shibata and M. Abe, "An Experimental Study on the Superconducting Coil Behaviors Using Electromagnetic Pulse Signals During Ramping," in *IEEE Transactions on Applied Superconductivity*, vol. 22, no. 3, pp. 9000804-9000804, June 2012, Art no. 9000804, doi: 10.1109/TASC.2011.2177950.
[50] T. A. Painter, I. R. Dixon and W. Denis Markiewicz, "Voltage spike and magnet quench behavior in the NHMFL 900 MHz bucket test," in *IEEE Transactions on Applied Superconductivity*, vol. 14, no. 2, pp. 1613-1616, June 2004, doi: 10.1109/TASC.2004.831011.
[51] T. Ogitsu, K. Tsuchiya and A. Devred, "Investigation of wire motion in superconducting magnets," in *IEEE Transactions on Magnetics*, vol. 27, no. 2, pp. 2132-2135, March 1991, doi: 10.1109/20.133633.
[52] T. Ogitsu, et al, "Quench Antenna for Superconducting Particle Accelerator Magnets.", *IEEE Trans. Appl. Superconduc.*, vol. 30, no. 4, pp. 2273–2276, Jul. 1994.
[53] S. Jongeleen, et al, "Quench Localization and Current Redestribution after Quench in Superconducting Dipole Magnets Wound with Rutherford-Type Cables", *IEEE Trans. Appl. Superconduc.*, vol. 7, no. 2, pp. 179-182, Jun. 1997.
[54] M. Aoki and Y. Matsui, "Locating a Mechanical Disturbance Source in a Superconducting Coil Using Pickup Coils on a Diaphragm," in *IEEE Transactions on Applied Superconductivity*, vol. 28, no. 2, pp. 1-5, March 2018, Art no. 4900405, doi: 10.1109/TASC.2017.2781183.
[55] 超電導・低温工学ハンドブック，社団法人　低温工学協会　編，pp. 1067,1084-1096.
[56] N. Amemiya, K. Ryu, T. Kikuchi and O. Tsukamoto, "Influence of current re-distribution and thermal diffusion among strands on stability of superconducting cables against local disturbances," in *IEEE Transactions on Magnetics*, vol. 30, no. 4, pp. 2281-2284, July 1994, doi: 10.1109/20.305730.
[57] N. Amemiya, H. Yonekawa, N. Tsuchioka and O. Tsukamoto, "Experimental study on current re-distribution and stability of multi-strand superconducting cables," in *IEEE Transactions on Applied Superconductivity*, vol. 7, no. 2, pp. 942-945, June 1997, doi: 10.1109/77.614660.

[58] 植村益次：日本複合材料学会誌 7(2) , 74-81(1981).
[59] T. C. Cosmus and M. Parizh, "Advances in Whole-Body MRI Magnets," in *IEEE Transactions on Applied Superconductivity*, vol. 21, no. 3, pp. 2104-2109, June 2011, doi: 10.1109/TASC.2010.2084981.A
[60] H.IWAI, et al., “Issues of three-point and 4-Point Modes in Flexural Testing Methods for Advanced Composite Material”, 日本複合材料学会誌,18,2(1992),60-6
[61] JIS K7171
[62] Y. -. N. Cheng, R. W. Brown, M. R. Thompson, T. P. Eagan and S. M. Shvartsman, "A comparison of two design methods for MRI magnets," in *IEEE Transactions on Applied Superconductivity*, vol. 14, no. 3, pp. 2008-2014, Sept. 2004, doi: 10.1109/TASC.2004.831507.
[63] Y,Iwasa,”Case studies in superconducting magnets：design and operational issues”, pp. 212-213
[64] Y,Iwasa,”Case studies in superconducting magnets：design and operational issues”, pp 268
[65] T.Ueki,K. Nojima, K. Asano, S. Nishijima, and T. Okada, “Toughness of epoxy resin systems for cryogenic use,” Adv. Cryogenic Eng. (Material),vol. 44, pp. 277–283, 1998.
[66] T.Ueki, S. Nishijima, and Y. Izumi, “Designing of epoxy resin systems for cryogenic use,” Cryogenics, vol. 45, pp. 141–148,2005.
[67] W.L.L LENDERS,”THE ORTHOCYCLIC METHOD OF COIL WINDING”,Philips Technical Review,Volume 23, 1961/62,No.12, pp. 365-404.
[68] スリーボンドテクニカルレビュー：[接着化学序説<その２>],1983 年 4 月.
[69] JIS K 6850
[70] 信貴、平井藍訳：低温工学ハンドブック、内田老鶴圃新社(1982)　P559
[71] P. Bauer*, J. Donnier, L. Oberli, “Tip heater for Minimum Quench Energy Measurements on Superconducting Strand”, LHC Project Report 248, 7 October 1998.
[72] Y. Iwamoto *et al.*, "Quench stability against beam-loss in superconducting magnets at the 50 GeV proton beam line for the J-PARC neutrino experiment," in *IEEE Transactions on Applied Superconductivity*, vol. 14, no. 2, pp. 592-595, June 2004, doi: 10.1109/TASC.2004.829983.

9. Appendix A

Achievement

A.1 Peer-reviewed Journal

1)M. Aoki, R. Nakagawa, A. Miyazoe, R. Ando, I. Masami and K. Sasaki, "Evaluation of Strain Dependence of Superconducting Magnet Quenches by Using a Three-Point Bending Test Stand," in *IEEE Transactions on Applied Superconductivity*, vol. 28, no. 4, pp. 1-4, June 2018, Art no. 4702904, doi: 10.1109/TASC.2018.2817338.

A.2 International Conference

1) Manabu Aoki 3LP4-13 Evaluation of Strain Tolerance to the Superconducting Magnet Quenching by the three-point Bending Test Stand, he 13th biennial European Conference on Applied Superconductivity, EUCAS 2017

2) Manabu Aoki, 2P-p46 “Evaluation of Quench Tolerance of the Superconducting Magnet using three-point Bending Test Stand”,1st Asian ICMC and CSSJ 50th Anniversary Conference, 2016

3) Manabu Aoki, 9P-48 “Evaluation of Quench Energy of the Superconducting Coil with Liquid Helium Permeable Structure”,10th ACASC/2nd Asian-ICMC/CSSJ Joint Conference, 2019

10. Appendix B

B.1 Drawing of the three-point bending test stand

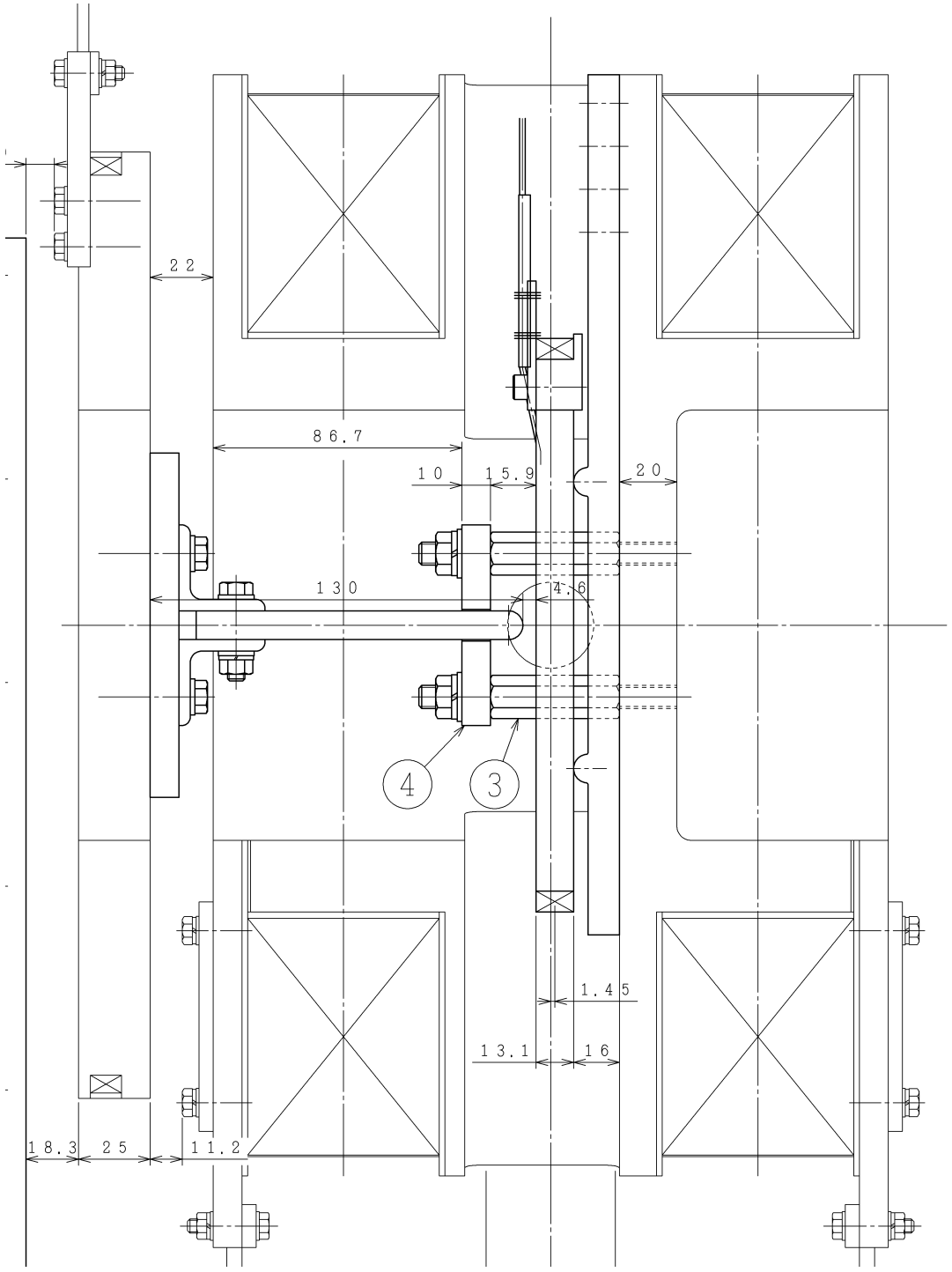

Fig.B-1 Cross-sectional drawing of the three-point bending test stand

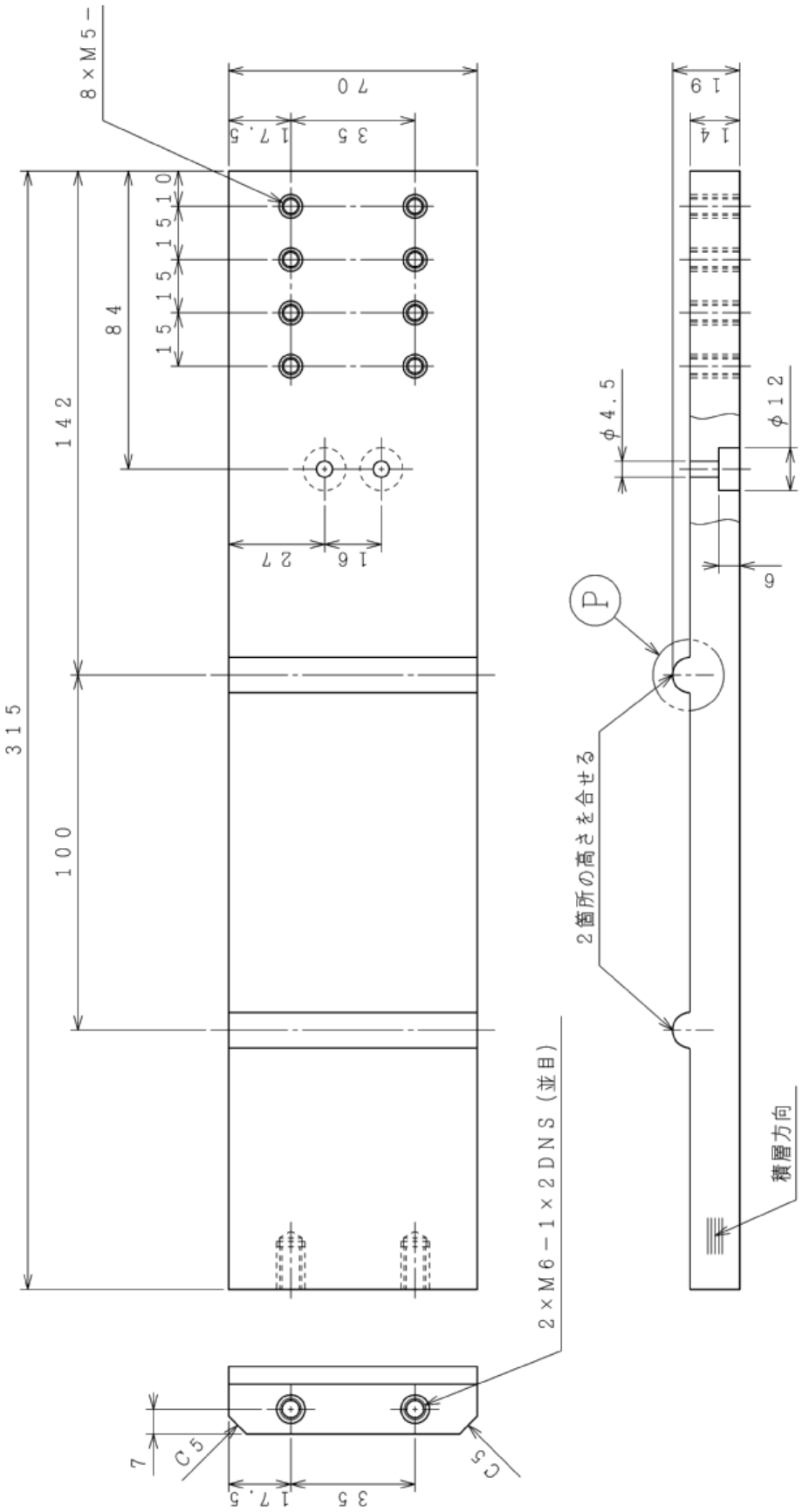

Fig.B-2 Drawing of sample holder

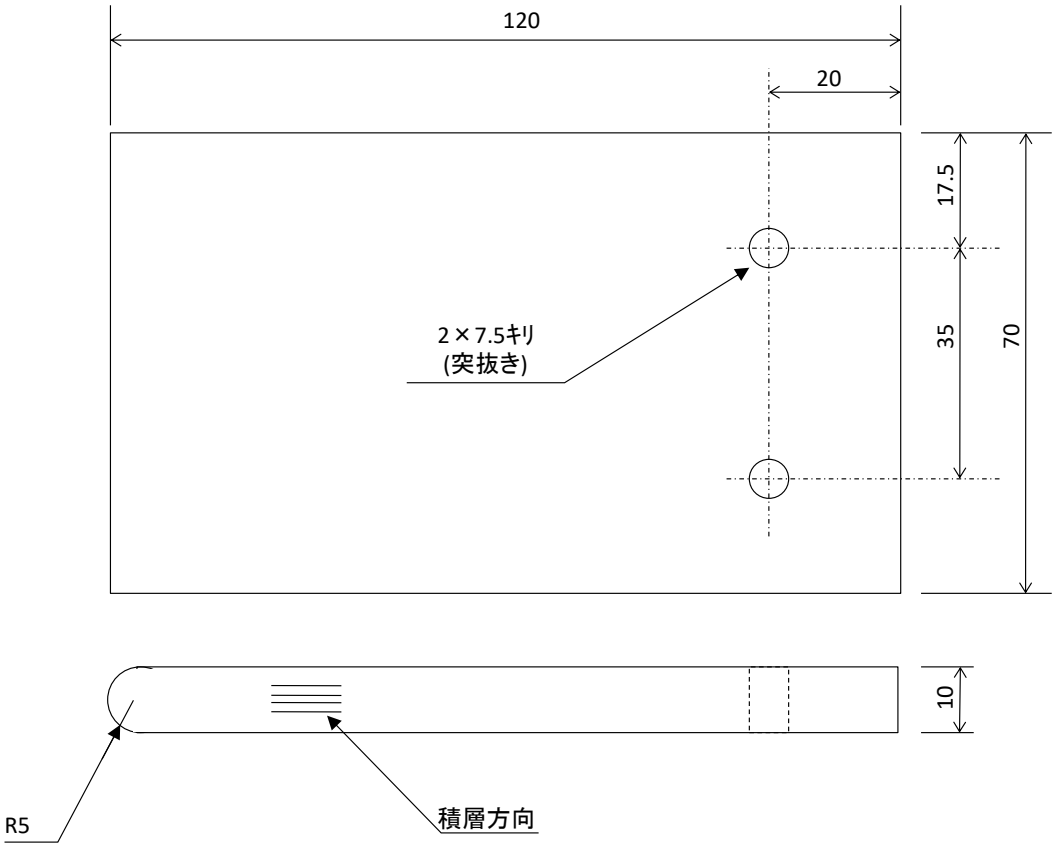

Fig.B-3 Drawing of the FRP plate to bend the test coil